**Supporting Experimental Information for**

# Magnesium-Catalysed Nitrile Hydroboration

Catherine Weetman, Mathew D. Anker, Merle Arrowsmith, Michael S. Hill,* Gabriele Kociok-Köhn, David J. Liptrot and Mary F. Mahon

*Department of Chemistry, University of Bath, Claverton Down, Bath, BA2 7AY, UK*

# Experimental Data

## General Experimental Procedures

All manipulations were carried out using standard Schlenk line and glovebox techniques under an inert atmosphere of argon. NMR experiments were conducted in Youngs tap NMR tubes made up and sealed in a Glovebox. NMR spectra were collected on a Bruker AV300 spectrometer operating at 300.2 MHz ($^{1}$H), 75.5 MHz ($^{13}$C), 96.3 MHz ($^{11}$B). The spectra were referenced relative to residual solvent resonances or an external $BF_3.OEt_2$ standard ($^{11}$B). Solvents (Toluene, THF, hexane) were dried by passage through a commercially available (Innovative Technologies) solvent purification system, under nitrogen and stored in ampoules over molecular sieves. $C_6D_6$ and $d_8$-toluene were purchased from Fluorochem Ltd. and dried over molten potassium before distilling under nitrogen and storing over molecular sieves. Di-*n*-butylmagnesium (1.0 M solution in n-heptane) and pinacolborane were purchased from Sigma-Aldrich Ltd. and used without further purification. [HC{(Me)CN(2,6-$^{i}Pr_2C_6H_3$)}$_2$Mg*n*Bu] was synthesised by a literature procedure.[1]

## Stoichiometric Reactions

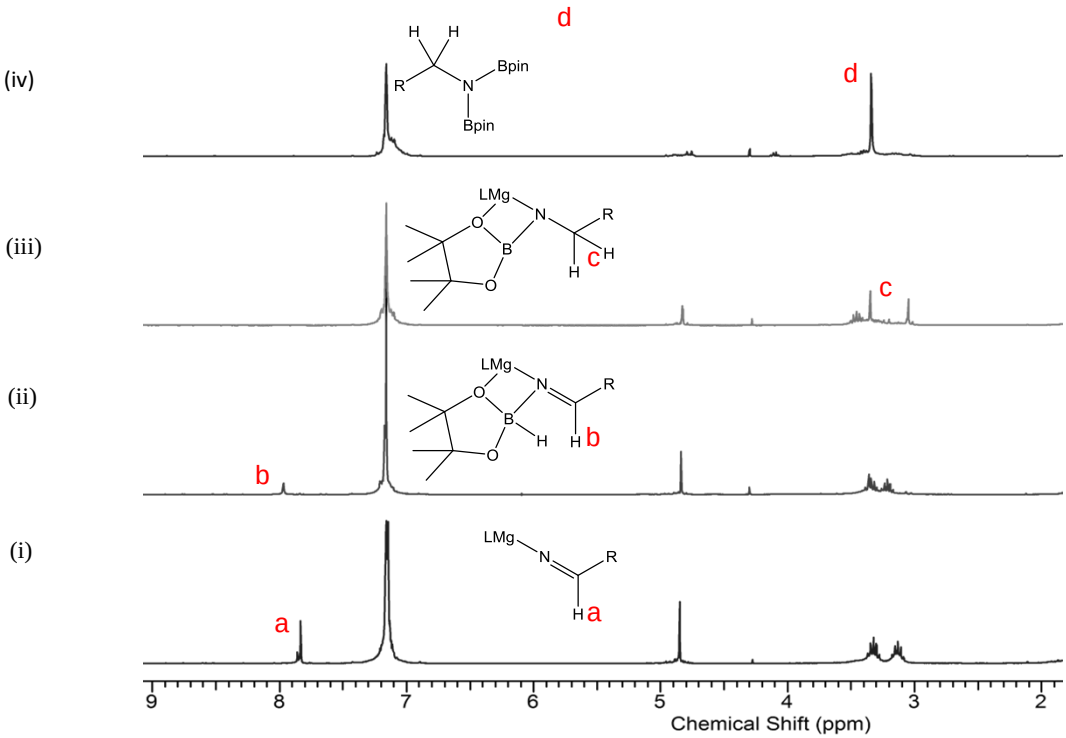


**Scheme S1: S**tacked $^{1}$H NMR spectra in $C_6D_6$ recorded during the stoichiometric reduction of *t*-BuCN with HBpin. (i) Magnesium aldimide formation after addition of HBpin and *t*-BuCN to **V**; (ii) Magnesium aldimidoborate formation on addition of a further equivalent of HBpin; (iii) Intramolecular hydride transfer with formation of magnesium borylamide; (iv) Bis(boryl)amine formation after addition of a further equivalent of HBpin.

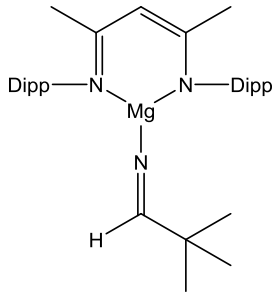


**NMR Scale:** LM**g**Bu (**V)** (0.04 mmol, 20 mg) was dissolved in 0.5 ml of $C_6D_6$ along with HBpin (0.04 mmol, 5.8 μL). This was left at room temperature for 5 minutes to form LMgH in situ before adding $^t$BuCN (0.04 mmol, 4.4 μL). This was heated at 60 $^o$C overnight to yield the insertion product, LMgNCH$^t$Bu. $^1$H NMR ($C_6D_6$, 300 MHz): 7.83 (1H, s, N=C*H*), 7.21 – 7.11 (6H, m, Ar-*H*), 4.85 (1H, s, NC($CH_3$)C*H*), 3.32 (2H, sept, $J_{HH}$ = 6 Hz, C*H*($CH_3$)$_2$), 3.13 (2H, sept, $J_{HH}$ = 6 Hz, C*H*($CH_3$)$_2$), 1.66 (6H, s, NC(C*H*$_3$)CH), 1.43 (6H, d, $J_{HH}$ = 9 Hz, CH(C*H*$_3$)$_2$), 1.23 (6H, d, $J_{HH}$ = 9 Hz, CH(C*H*$_3$)$_2$), 1.20 (6H, d, $J_{HH}$ = 9 Hz, CH(C*H*$_3$)$_2$), 1.12 (6H, d, $J_{HH}$ = 9 Hz, CH(C*H*$_3$)$_2$), 1.03 (9H, s, C(C*H*$_3$)$_3$. $^{13}$C{$^1$H} NMR ($C_6D_6$, 75 MHz): 174.5 (N=*C*H), 170.5 (N*C*($CH_3$)), 147.0 (*ipso-C*-Ar), 142.8 (*ortho-C*-Ar), 142.5 (*ortho-C*-Ar), 126.2 (*para-C*-Ar), 124.6 (*meta-C*-Ar), 96.1 (NC($CH_3$)*C*H), 37.5 (N=CH*C*($CH_3$)$_3$), 29.2 (*C*H($CH_3$)$_2$), 27.2, 27.1, 26.1, 25.7, 25.0, 24.8.

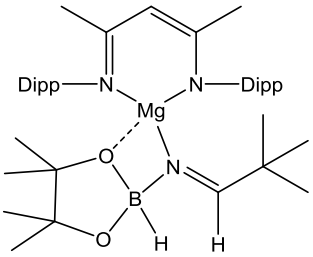


**Compound 4: NMR Scale:** To the previous solution additional HBpin (0.04 mmol, 5.8 μL) was added and left overnight at room temperature to yield the borate intermediate. $^1$H NMR ($C_6D_6$, 300 MHz): 7.97 (1H, s, N=C*H*), 7.21 – 7.10 (6H, m, Ar-*H*), 4.84 (1H, s, NC($CH_3$)C*H*), 3.34 (2H, sept, $J_{HH}$ = 6 Hz, C*H*($CH_3$)$_2$, 3.21 (2H, sept, $J_{HH}$ = 6 Hz, C*H*($CH_3$)$_2$), 1.63 (6H, s, NC(C*H*$_3$)CH), 1.40 (6H, d, $J_{HH}$ = 9 Hz, CH(C*H*$_3$)$_2$), 1.37 (6H, d, $J_{HH}$ = 9 Hz, CH(C*H*$_3$)$_2$), 1.23 (6H, d, $J_{HH}$ = 9 Hz, CH(C*H*$_3$)$_2$), 1.21 (6H, d, $J_{HH}$ = 9 Hz, CH(C*H*$_3$)$_2$), 1.07 (12H, s, OC(C*H*$_3$)$_2$), 1.00 (9H, s, C(C*H*$_3$)$_3$). $^{13}$C{$^1$H} NMR ($C_6D_6$, 75 MHz): 178.4 (N=*C*H), 170.5 (N*C*($CH_3$)), 145.7 (*ipso-C*-Ar), 143.3 (*ortho-C*-Ar), 142.6 (*ortho-C*-Ar), 126.1 (*para-C*-Ar), 124.7 (*meta-C*-Ar), 124.4 (*meta-C*-Ar), 96.0 (NC($CH_3$)*C*H), 83.0 (O*C*($CH_3$)$_2$), 82.6 (O*C*($CH_3$)$_2$), 37.8 (N=CH*C*($CH_3$)$_3$), 29.17 (*C*H($CH_3$)$_2$), 28.4 (*C*H($CH_3$)$_2$), 27.5, 27.2, 26.1, 25.9, 25.3 (OC(*C*H$_3$)$_2$), 25.1. $^{11}$B NMR ($C_6D_6$, 96 MHz): 8.5 (d, $J_{HB}$ = 105.6 Hz, N*B*H).

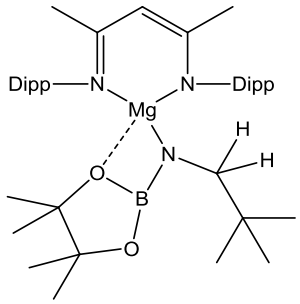


**NMR Scale:** Previous NMR sample was allowed to stand at room temperature for 48 hrs. $^{1}$H NMR ($C_6D_6$, 300 MHz): 7.21 – 7.10 (6H, m, Ar-*H*), 4.83 (1H, s, NC($CH_3$)C*H*), 3.46 (2H, sept, $J_{HH}$ = 6 Hz, C*H*($CH_3$)$_2$), 3.35 (2H, s, NC$H_2$), 3.31 (2H, sept, $J_{HH}$ = 6 Hz, C*H*($CH_3$)$_2$), 1.64 (6H, s, NC(C$H_3$)CH), 1.39 (12H, d, $J_{HH}$ = 6 Hz, CH(C$H_3$)$_2$), 1.26 (12H, d, $J_{HH}$ = 6 Hz, CH(C$H_3$)$_2$), 1.06 (24H, s, OC(C$H_3$)$_2$). $^{13}$C{$^{1}$H} NMR ($C_6D_6$, 75 MHz): 170.6 (N*C*($CH_3$)CH), 145.8 (*ipso-C*-Ar), 143.1 (*ortho-C*-Ar), 125.8 (*para-C*-Ar), 124.4 (*meta-C*-Ar), 95.8 (NC($CH_3$)*C*H), 83.1 (O*C*($CH_3$)$_2$), 82.6 (O*C*($CH_3$)$_2$), 58.5 (N*C*$H_2$), 34.3 (NC$H_2$*C*($CH_3$)$_3$), 28.6, 28.4, 27.2, 26.2, 25.9, 25.3, 25.1, 14.7 (C(*C*$H_3$)$_3$). $^{11}$B NMR ($C_6D_6$, 96 MHz): 7.05 (d, $J_{HB}$ = 105.6 Hz, N*B*H).

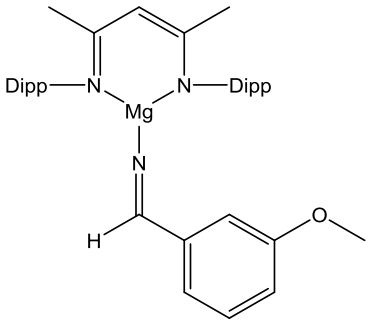


**Compound 2: NMR Scale:** LM**g**Bu (**V**) (0.06 mmol, 30 mg) was dissolved in 0.5 ml of $C_6D_6$ along with HBpin (0.06 mmol, 8.4 μL). This was left at room temperature for 5 minutes to form LMgH in situ before adding (3-MeO)PhCN (0.06 mmol, 7.3 μL). This was heated at 60 $^{o}$C overnight to yield the insertion product, LMgNCHPh(3-MeO). $^{1}$H NMR ($C_6D_6$, 300 MHz): 8.63 (1H, s, NC*H*), 7.56 – 6.80 (10H, m, Ar-*H*), 4.89 (1H, s, NC($CH_3$)C*H*), 3.42 (3H, s, OC$H_3$), 3.29 (4H, m, C*H*($CH_3$)$_2$), 1.68 (6H, s, NC(C$H_3$)CH), 1.42 (6H, d, $J_{HH}$ = 6Hz, CH(C$H_3$)$_2$), 1.24 (6H, d, $J_{HH}$ = 6Hz, CH(C$H_3$)$_2$), 0.97 (6H, d, $J_{HH}$ = 6Hz, CH(C$H_3$)$_2$), 0.90 (6H, d, $J_{HH}$ = 6Hz, CH(C$H_3$)$_2$). $^{13}$C{$^{1}$H} NMR ($C_6D_6$, 75 MHz): 172.5 (N=*C*H), 170.4 (N*C*($CH_3$)CH), 165.0, 160.9, 147.7, 145.2, 144.1, 142.9, 139.4, 130.3, 126.2, 124.8, 95.2 (NC($CH_3$)*C*H), 55.6 (O*C*$H_3$), 32.3 (*C*H($CH_3$)$_2$), 29.6, 28.7, 28.2, 27.2, 24.7, 23.4.

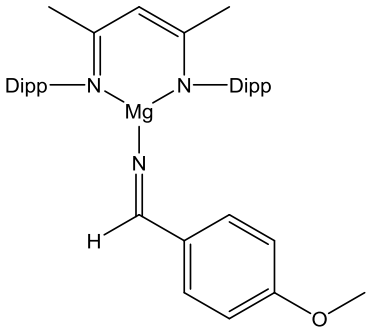


**Compound 3: NMR Scale:** LM**g**Bu (**V)** (0.06 mmol, 30 mg) was dissolved in 0.5 ml of $C_6D_6$ along with HBpin (0.06 mmol, 8.4 µL). This was left at room temperature for 5 minutes to form LMgH in situ before adding (4-MeO)PhCN (0.06 mmol, 8.0 mg). This was heated at 60 $^{o}$C overnight to yield the insertion product, LMgNCHPh(4-MeO). $^{1}$H NMR ($C_6D_6$, 300 MHz): 8.58 (1H, s, NC*H*), 7.80 – 6.81 (10H, m, Ar-*H*), 4.87 (1H, s, NC($CH_3$)C*H*), , 3.66 (4H, m, C*H*($CH_3$)$_2$), 2.99 (3H, s, OC$H_3$) 1.73 (6H, s, NC(C$H_3$)CH), 1.47 (6H, d, $J_{HH}$ = 6Hz, CH(C$H_3$)$_2$), 1.32 (6H, d, $J_{HH}$ = 6Hz, CH(C$H_3$)$_2$), 0.91 (6H, d, $J_{HH}$ = 6Hz, CH(C$H_3$)$_2$), 0.89 (6H, d, $J_{HH}$ = 6Hz, CH(C$H_3$)$_2$). $^{13}$C{$^{1}$H} NMR ($C_6D_6$, 75 MHz): 171.7 (N=*C*H), 169.6 (N*C*($CH_3$)CH), 162.3, 147.7, 146.7, 144.1, 142.9, 135.0, 126.2, 124.2, 94.7 (NC($CH_3$)*C*H), 55.3 (O*C*$H_3$), 32.3 (*C*H($CH_3$)$_2$), 29.8, 28.8, 27.2, 26.1, 25.8, 24.9, 24.6, 23.4.

## Catalytic reactions

**NMR scale:** 10 mg (0.02 mmol, ie. 10 mol%) of LMgBu was dissolved in 0.5 ml of $C_6D_6$, 60.9 µL (0.42 mmol) of pinacolborane was then added followed by 0.2 mmol of nitrile. This mixture was then transferred to a sealed Youngs tap NMR tube and the reaction was kept in an oil bath at 60 $^oC$. These were regularly monitored by $^1H$ and $^{11}B$ NMR spectroscopy until complete conversion was observed.

**Scale up:** In a Schlenk flask 50mg (0.1 mmol, ie. 10 mol%) of LMgBu was dissolved in 5ml of toluene, 304.7 µL (2.1 mmol) of pinacolborane was then added followed by 1 mmol of nitrile. This mixture was then transferred to an oil bath at 60$^oC$, for the observed NMR reaction time. Toluene was then removed *in vacuo* and the remaining solid was redissolved in the minimum volume of hexane and left to crystallize in the freezer overnight.

***N-{B(OCMe$_2$)$_2$}* -propan-1-amine**

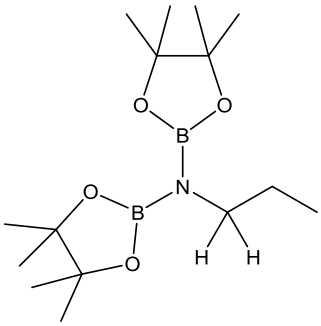

**NMR scale:** 14.3 µL of propionitrile. $^1H$ NMR ($C_6D_6$, 300 MHz): 3.42 (2H, t, $J_{HH}$ = 6 Hz, NC$H_2$), 1.75 (2H, m, $J_{HH}$ = 6 Hz, C$H_2$CH$_3$), 1.07 (24H, s, OCC$H_3$), 0.96 (3H, $J_{HH}$ = 9 Hz, CH$_2$C$H_3$). $^{13}C\{^1H\}$ NMR (75.5 MHz, $C_6D_6$, 298 K): 82.6 (O*C*(CH$_3$)$_2$), 46.5 (N*C*H$_2$), 27.2 (CH$_2$*C*H$_2$CH$_3$), 25.1 (OC(*C*H$_3$)$_2$), 11.9 (CH$_2$*C*H$_3$). $^{11}B$ NMR (96.3 MHz, $C_6D_6$, 298 K): 29.5 N*B*. **Scale up:** 71.3 µL of propionitrile, 60 $^oC$ for 1 hr. Isolated as yellow crystals (228 mg, 70% yield). Elemental analysis: calcd. (found) for $C_{15}H_{31}B_2NO_4$: C 57.92 (57.68); H 10.05 (10.14); N 4.50 (4.40).

***N-{B(OCMe$_2$)$_2$}* - 2-methylpropan-1-amine**

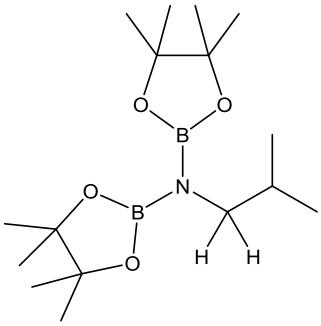

**NMR scale:** 18.0 µL of isobutyronitrile, 60 $^oC$ for 1 hr. $^1H$ NMR (300 MHz, $C_6D_6$, 298 K): 3.28 (2H, d, $J_{HH}$ = 6 Hz, NC$H_2$), 2.05 (1H, m, $J_{HH}$ = 6 Hz, C*H*(CH$_3$)$_2$), 1.07 (24H, s, OC(C$H_3$)$_2$), 1.01 (6H, d, $J_{HH}$ = 6 Hz, CH(C$H_3$)$_2$). $^{13}C\{^1H\}$ NMR (75.5 MHz, $C_6D_6$, 298 K): 82.6 (O*C*(CH$_3$)$_2$), 52.1 (N*C*H$_2$), 31.6 (*C*H(CH$_3$)$_2$), 25.1 (OC(*C*H$_3$)$_2$), 20.7 (CH(*C*H$_3$)$_2$). $^{11}B$ NMR (96.3 MHz, $C_6D_6$, 298 K): 29.6 N*B*. **Scale up:** 89.8 µL of isobutyronitrile. Isolated as a yellow oil (313 mg, 96% yield). An accurate microanalysis could not be obtained for this compound.

***N-{B(OCMe$_2$)$_2$}* - 2,2-dimethylpropan-1-amine**

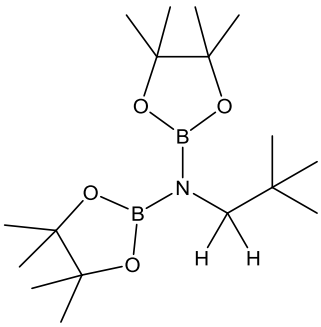

**NMR scale:** 22.1 µL trimethylacetonitrile, 60 $^{o}$C for 5.5 hr. $^{1}$H NMR (300 MHz, $C_6D_6$, 298 K): 3.30 (2H, s, NC*H*$_2$), 1.08 (24H, s, OC(C*H*$_3$)$_2$), 1.03 (9H, s, C(C*H*$_3$)$_3$). $^{13}$C{$^{1}$H} NMR (75.5 MHz, $C_6D_6$, 298 K): 82.6 (O*C*(CH$_3$)$_2$), 55.3 (N*C*H$_2$), 34.0 (*C*(CH$_3$)$_3$), 28.4 (C(*C*H$_3$)$_3$), 25.1 (OC(*C*H$_3$)$_2$)). $^{11}$B NMR (96.3MHz, $C_6D_6$, 298 K) δB(ppm): 29.5 N*B*. **Scale up:** 110.5 µL of trimethylacetonitrile. Isolated as colorless crystals (181 mg, 54% yield). Elemental analysis: calcd. (found) for $C_{17}H_{35}B_2NO_4$: C 60.22 (60.11); H 10.40 (10.55); N 4.13 (3.95).

***N-{B(OCMe$_2$)$_2$}* – cyclohexylmethanamine**

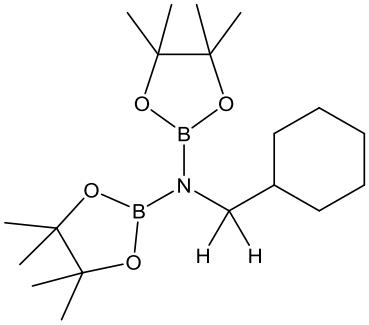

**NMR scale:** 23.8 µL cyclohexanitrile, 60 $^{o}$C for 1 hr. $^{1}$H NMR (300 MHz, $C_6D_6$, 298 K): 3.31 (2H, d, $J_{HH}$ = 6 Hz, NC*H*$_2$), 1.92 (2H, m, NCH$_2$C*H*) 1.70 – 1.20 (10H, m, Cy-*H*), 1.07 (24H, s, OCC*H*$_3$). $^{13}$C{$^{1}$H} NMR (75.5MHz, $C_6D_6$, 298 K): 82.6 (O*C*(CH$_3$)$_2$), 50.8 (N*C*H$_2$), 41.3 (NCH$_2$*C*H), 31.5 (Cy-*C*), 27.6 (Cy-*C*), 27.0 (Cy-*C*), 25.1 (OC(*C*H$_3$)$_2$). $^{11}$B NMR (96.3 MHz, $C_6D_6$, 298 K): 29.7 N*B*. **Scale up:** 118.8 µL of cyclohexanitrile, 60 $^{o}$C for 1 hr. Isolated as colorless crystals (265 mg, 75% yield). An accurate microanalysis could not be obtained for this compound.

***N-{B(OCMe$_2$)$_2$}* – phenylmethanamine**

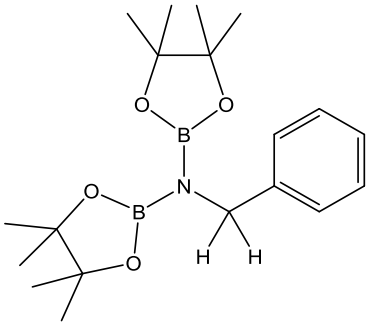

**NMR scale:** 19.5 µL benzonitrile, 60 $^{o}$C for 12 hr. $^{1}$H NMR (300 MHz, $C_6D_6$, 298 K): 7.57 (2H, m, *o*-H), 7.25 (2H, m, *m-H*), 7.11 (1H, m, *p-H*), 4.60 (2H, s, NC$H_2$), 1.02 (24H, s, OC(C$H_3$)$_2$). $^{13}$C{$^{1}$H} NMR (75.5 MHz, $C_6D_6$, 298 K): 144.1 (*o-C*), 128.4 (*p*-C), 127.0 (*m-C*), 82.9 O*C*(CH$_3$)$_2$, 48.2 (N*C*H$_2$), 25.1 (OC(*C*H$_3$)$_2$). $^{11}$B NMR (96.3 MHz, $C_6D_6$, 298 K): 29.5 N*B*. **Scale up:** 103.12 µL of Benzonitrile, 60 $^{o}$C for 15 hrs. Isolated as colorless crystals (202 mg, 56% yield). Elemental analysis: calcd. (found) for $C_{19}H_{31}B_2NO_4$: C 63.55 (63.38); H 8.70 (8.82); N 3.90 (4.00).

***N-{B(OCMe$_2$)$_2$}* - *o*-tolylmethanamine**

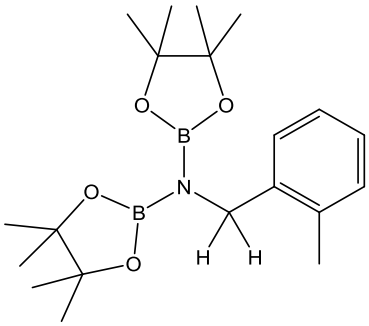

**NMR scale:** 23.7 µL o-tolunitrile, 60 $^{o}$C for 15 hr. $^{1}$H NMR (300 MHz, $C_6D_6$, 298 K): 7.64 (1H, d, $J_{HH}$ = 6 Hz, *o-H*), 7.24 (1H, m, *p*-H), 7.08 (1H, m, *m-H*), 7.00 (1H, m, *m-H*), 4.60 (2H, s, NC$H_2$), 2.12 (3H, s, *o*-C$H_3$), 1.03 (24H, s, OC(C$H_3$)$_2$). $^{13}$C{$^{1}$H} NMR (75.5 MHz, $C_6D_6$, 298 K): 141.5 (*o-C*), 135.7 (*o-C*CH$_3$), 130.5 (*p-C*), 126.3 (*m-C*), 125.9 (*m-C*HC(CH$_3$), 82.9 (O*C*(CH$_3$)$_2$), 45.8 (N*C*H$_2$), 25.0 (OC(*C*H$_3$)$_2$), 19.4 (*o-C*H$_3$). $^{11}$B NMR (96.3 MHz, $C_6D_6$, 298 K): 29.8 N*B*. **Scale up:** 118.5 µL of *o*-tolunitrile, 60 $^{o}$C for 15 hrs. Isolated as colorless crystals (275 mg, 73% yield). Elemental Analysis for $C_{20}H_{33}B_2NO_4$: Calculated (found): C 64.38 (64.45); H 8.92 (8.85); N 3.75 (3.63).

***N-{B(OCMe$_2$)$_2$}* - *m*-tolylmethanamine**

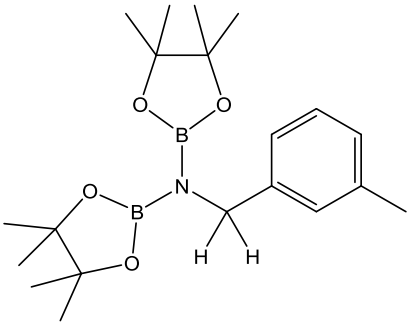

**NMR scale:** 22.0 µL m-tolunitrile, 60 $^{o}$C for 15 hr. $^{1}$H NMR (300 MHz, $C_6D_6$, 298 K): 7.43 (1H, d, $J_{HH}$ = 6 Hz, *o-H*), 7.38 (1H, s, *o-H*), 7.20 (1H, m, *p-H*), 6.95 (1H, m, *m-H*), 4.60 (2H, s, NC$H_2$), 2.19 (3H, s, *m*-C$H_3$), 1.04 (24H, s, OC(C$H_3$)$_2$). $^{13}$C{$^{1}$H} NMR (75.5 MHz, $C_6D_6$, 298 K): 144.0 (*o-C*), 137.8 (*o-C*HC(CH$_3$)), 129.3 (*p-C*), 128.7 (*i*-C) 127.7 (*m-C*CH$_3$), 125.4 (*m-C*), 82.9 (O*C*(CH$_3$)$_2$), 48.2 (N*C*H$_2$), 25.1 (OC(*C*H$_3$)$_2$), 21.9 (Ar*C*H$_3$). $^{11}$B NMR (96.3 MHz, $C_6D_6$, 298 K): 29.9 N*B*. **Scale up:** 120.0 µL of *m*-tolunitrile, 60 $^{o}$C for 15 hrs. Isolated colorless crystals (305 mg, 81% yield). An accurate microanalysis could not be obtained for this compound.

***N-{B(OCMe$_2$)$_2$}* - *3*-(fluoro)phenylmethanamine**

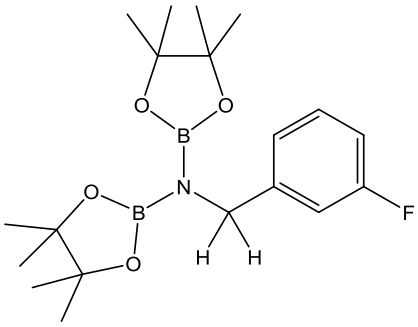

**NMR scale:** 21.4 µL 3-(fluoro)benzonitrile, 60 $^{o}$C for 14 hr. $^{1}$H NMR (300 MHz, $C_6D_6$, 298 K): 7.40 (1H, m, *o*-C*H*), 7.25 (1H, d, $J_{HH}$ = 7.3 Hz, *o*-C*H*), 7.00 (2H, m, *m*-C*H*, *p*-C*H*), 4.51 (2H, s, NC$H_2$), 1.02 (24H, s, OC(C$H_3$)$_2$). $^{13}$C{$^{1}$H} NMR (75.5 MHz, $C_6D_6$, 298 K): 130.2 (*o-C*), 128.7 (*o-C*), 128.5 (*p-C*), 128.5 (*m-C*), 128.3 (*m-C*), 83.1 (O*C*(CH$_3$)$_2$), 47.8 (N*C*H$_2$), 25.0 (OC(*C*H$_3$)$_2$). $^{11}$B NMR (96.3 MHz, $C_6D_6$, 298 K): 29.5 N*B*. **Scale up:** 106.9 µL of 3-(fluoro)benzonitrile, 60 $^{o}$C for 14 hrs. Isolated pale yellow crystals (215 mg, 59% yield). Elemental analysis: calcd. (found) for $C_{19}H_{30}B_2FNO_4$: C 60.52 (60.55); H 8.02 (7.93); N 3.71 (3.85).

***N-{B(OCMe$_2$)$_2$} - 3*-(methoxy)phenylmethanamine**

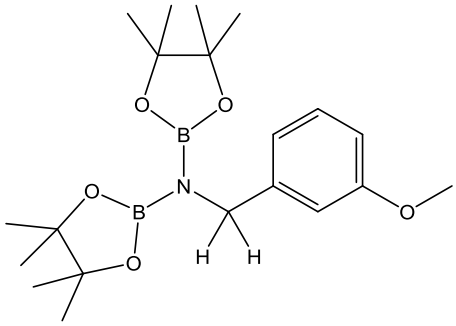

**NMR scale:** 24.5 µL 3-(methoxy)benzonitrile, 60 $^{o}$C for 15 hr. $^{1}$H NMR (300 MHz, $C_6D_6$, 298 K): 7.26 (1H, m, *o*-C*H*), 7.25 (1H, m, *o*-C*H*), 6.78 (1H, m, *p*-C*H*), 6.64 (1H, m, *m*-C*H*), 4.64 (2H, s, NC$H_2$), 3.41 (3H, s, OC$H_3$), 1.05 (24H, s, OC(C$H_3$)$_2$). $^{13}$C{$^{1}$H} NMR (75.5 MHz, $C_6D_6$, 298 K): 129.7 (*o-C*), 128.7 (*o-C*), 128.5 (*p-C*), 128.3 (*m-C*, 82.9 (O*C*(CH$_3$)$_2$), 55.0 (O*C*H$_3$), 48.3 (N*C*H$_2$), 25.1 (OC(*C*H$_3$)$_2$). $^{11}$B NMR (96.3 MHz, $C_6D_6$, 298 K): 30.0 N*B*. **Scale up:** 122.3 µL of 3-(methoxy)benzonitrile, 60 $^{o}$C for 15 hrs. Isolated as pale yellow crystals (308 mg, 81% yield). An accurate microanalysis could not be obtained for this compound.

***N-{B(OCMe$_2$)$_2$} - p*-tolylmethanamine**

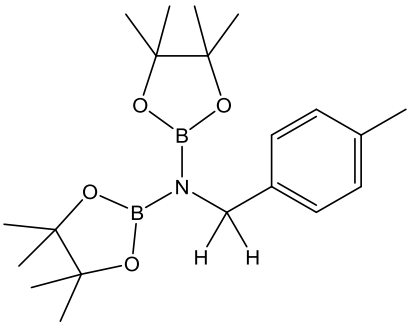

**NMR scale:** 23.9 µL *p*-tolunitrile, 60 $^{o}$C for 13 hr. $^{1}$H NMR (300 MHz, $C_6D_6$, 298 K): 7.50 (2H, d, $J_{HH}$ = 9 Hz, *o-H*), 7.06 (2H, d, $J_{HH}$ = 9 Hz, *m-H*), 4.58 (2H, s, NC$H_2$), 2.15 (3H, s, *p*-C$H_3$), 1.04 (24H, s, OC(C$H_3$)$_2$). $^{13}$C{$^{1}$H} NMR (75.5 MHz, $C_6D_6$, 298 K): 141.2 (*o-C*), 136.1 (*p-C*), 129.4 (*i-C*), 128.5 (*m-C*), 82.9 (O*C*(CH$_3$)$_2$), 47.9 (N*C*H$_2$), 25.1 (OC(*C*H$_3$)$_2$), 21.5 (*p-C*H$_3$). $^{11}$B NMR (96.3 MHz, $C_6D_6$, 298 K): 29.7 N*B*. **Scale up:** 119.4 µL of *p*-tolunitrile, 60 $^{o}$C for 15 hrs. Isolated as colorless crystals (270 mg, 72% yield). Elemental analysis: calcd. (found) for $C_{20}H_{33}B_2NO_4$: C 64.38 (64.20); H 8.92 (8.80); N 3.75 (3.87).

***N-{B(OCMe$_2$)$_2$} – 4-*(fluoro)phenylmethanamine**

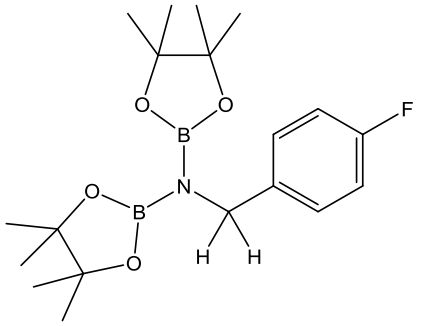


**NMR scale:** 21.9 µL 4-(fluoro)benzonitrile, 60 $^{o}$C for 12 hr. $^{1}$H NMR (300 MHz, $C_6D_6$, 298 K): 7.40 (2H, m, *o-H*), 6.88 (2H, t, $J_{HH}$ = 9 Hz, *m*-H), 4.45 (2H, s, NC$H_2$), 1.02 (24H, s, OC(C$H_3$)$_2$). $^{13}$C{$^{1}$H} NMR (75.5 MHz, $C_6D_6$, 298 K): 164.2 (*p-C*), 139.9 (*o-C*), 130.1 (*i-C*), 115.5 (*m-C*), 82.9 (O*C*(CH$_3$)$_2$), 47.5 (N*C*H$_2$), 25.1 (OC(*C*H$_3$)$_2$). $^{11}$B NMR (96.3 MHz, $C_6D_6$, 298 K): 29.7 N*B*. $^{19}$F NMR (376.5 MHz, $C_6D_6$, 298 K) δF (ppm): -116.89 4-*F*. **Scale up:** 109.4 µL of 4-(fluoro)benzonitrile, 60 $^{o}$C for 15 hrs. Isolated as colorless crystals (230 mg, 61% yield). Elemental analysis: calcd. (found) for $C_{19}H_{30}B_2FNO_4$: C 60.52 (60.55); H 8.02 (7.93); N 3.74 (3.83).

***N-{B(OCMe$_2$)$_2$} – 4-*(Chloro)phenylmethanamine**

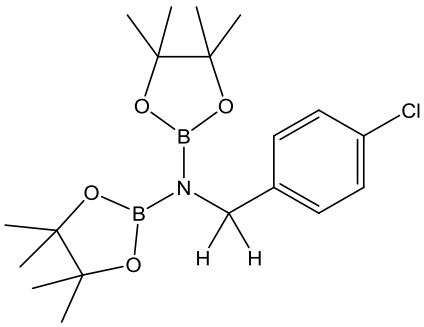


**NMR scale:** 27.5 mg 4-(chloro)benzonitrile, 60 $^{o}$C for 12 hr. $^{1}$H NMR (300 MHz, $C_6D_6$, 298 K): 7.36 (2H, d, $J_{HH}$ = 7.3 Hz, *o*-C*H*), 7.20 (2H, d, $J_{HH}$ = 7.3 Hz, *m*-C*H*), 4.46 (2H, s, NC$H_2$), 1.02 (24H, s, OC(C$H_3$)$_2$). $^{13}$C{$^{1}$H} NMR (75.5 MHz, $C_6D_6$, 298 K): 129.9 (*o-C*), 128.9 (*p-C*), 128.7 (*m-C*), 83.0 (O*C*(CH$_3$)$_2$), 47.5 (NCH$_2$), 25.1 (OC(*C*H$_3$)$_2$). $^{11}$B NMR (96.3 MHz, $C_6D_6$, 298 K): 29.0 (N*B*). **Scale up:** 137.6 mg of 4-(chloro)benzonitrile, 60 $^{o}$C for 12 hrs. Isolated as pale yellow crystals (231 mg, 59% yield). Elemental analysis: calcd. (found) for $C_{19}H_{30}B_2ClNO_4$: C 57.99 (57.47); H 7.68 (7.40); N 3.56 (3.52).

***N-{B(OCMe$_2$)$_2$} – 4*-(trifluoromethyl)phenylmethanamine**

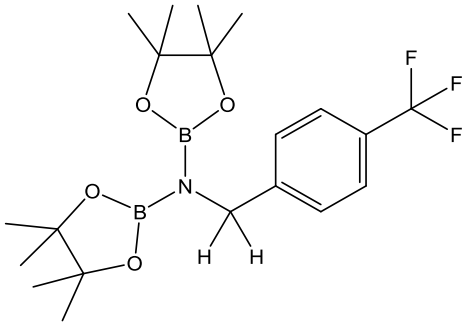

**NMR scale:** 26.8 μL 4-(trifluoromethyl)benzonitrile, 60 $^{o}$C for 12.5 hr. $^{1}$H NMR (300 MHz, $C_6D_6$, 298 K): 7.41 (4H, s, Ar-*H*), 4.46 (2H, s, NC*H*$_2$), 1.01 (24H, s, OC(C*H*$_3$)$_2$). $^{13}$C{$^{1}$H} NMR (75.5 MHz, $C_6D_6$, 298 K): 148.1 (*o*-*C*), 128.5 (*p*-C), 125.6 (*m*-*C*), 83.1 (O*C*(CH$_3$)$_2$), 47.8 (N*C*H$_2$), 25.0 (OC(*C*H$_3$)$_2$). $^{11}$B NMR (96.3 MHz, $C_6D_6$, 298 K): 29.6 N*B*. $^{19}$F NMR (376.5 MHz, $C_6D_6$, 298 K) δF (ppm): -61.94 C*F*$_3$. **Scale up:** 133.9 μL of 4-(trifluoromethyl)benzonitrile, 60 $^{o}$C for 15 hrs. Isolated as colorless crystals (325 mg, 76% yield). An accurate microanalysis could not be obtained for this compound.

***N-{B(OCMe$_2$)$_2$} – 4*-(methoxy)phenylmethanamine**

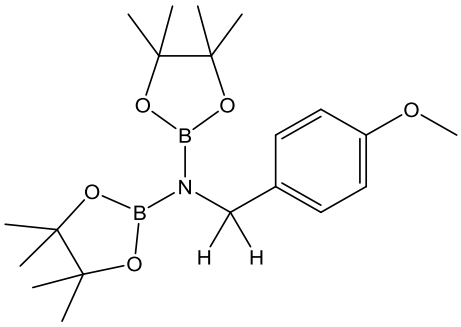

**NMR scale:** 26.6 mg 4-methoxybenzonitrile, 60 $^{o}$C for 13.5 hr. $^{1}$H NMR (300 MHz, $C_6D_6$, 298 K): 7.53 (2H, d, $J_{HH}$ = 6 Hz, *o*-*H*), 6.85 (2H, d, $J_{HH}$ = 9 Hz, *m*-*H*), 4.54 (2H, s, NC*H*$_2$), 3.36 (3H, s, OC*H*$_3$), 1.04 (24H, s, OC(C*H*$_3$)$_2$). $^{13}$C{$^{1}$H} NMR (75.5 MHz, $C_6D_6$, 298 K): 159.3 (*p*-*C*), 136.4 (*o*-*C*), 129.8 (*i*-*C*), 114.2 (*m*-*C*), 82.9 (O*C*(CH$_3$)$_2$), 55.1 (O*C*H$_3$), 47.6 (N*C*H$_2$), 25.1 (OC(*C*H$_3$)$_2$). $^{11}$B NMR (96.3 MHz, $C_6D_6$, 298 K): 29.7 N*B*. **Scale up:** 133.2 mg of 4-methoxybenzonitrile, 60 $^{o}$C for 15 hrs. Isolated as colorless crystals (225 mg, 58% yield). Elemental analysis: calcd. (found) for $C_{20}H_{33}B_2NO_4$: C 61.74 (61.60); H 8.55 (8.50); N 3.60 (3.50).

***N-{B(OCMe$_2$)$_2$}* – diphenylacetoamine**

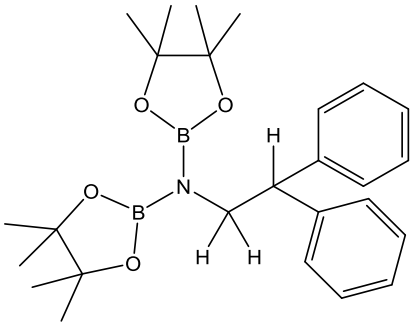


**NMR scale:** 38.6 mg diphenylacetonitrile, 60 $^{o}$C for 30 hr. $^{1}$H NMR (300 MHz, $C_6D_6$, 298 K): 7.43 (4H, d, $J_{HH}$ = 6 Hz, *o-H* ), 7.05 (4H, m, *m-H*), 6.94 (2H, m, *p-H*), 4.65 (1H, t, $J_{HH}$ = 6 Hz, $NCH_2CH$), 4.10 (2H, d, $J_{HH}$ = 9 Hz, $NCH_2CH$), 1.02 (24H, s, $C(CH_3)_2$). $^{13}C\{^{1}H\}$ NMR (75.5 MHz, $C_6D_6$, 298 K): 144.28 (*ipso-C*), 129.62 (*o-C*), 128.87 (*p-C*), 126.71 (*m-C*), 82.70 ($C(CH_3)_2$), 54.44 ($NCH_2CH$), 49.55 ($NCH_2CH$), 25.07 ($C(CH_3)_2$). $^{11}$B NMR (96.3 MHz, $C_6D_6$, 298 K): 29.6 N*B*. **Scale up:** 133.2 mg of diphenylacetonitrile, 60 $^{o}$C for 30 hrs. Isolated as colorless crystals (199 mg, 43% yield). An accurate microanalysis could not be obtained for this compound.

## $^{1}$H and $^{13}$C{$^{1}$H} NMR spectra

### *N-{B(OCMe$_2$)$_2$}* -propan-1-amine

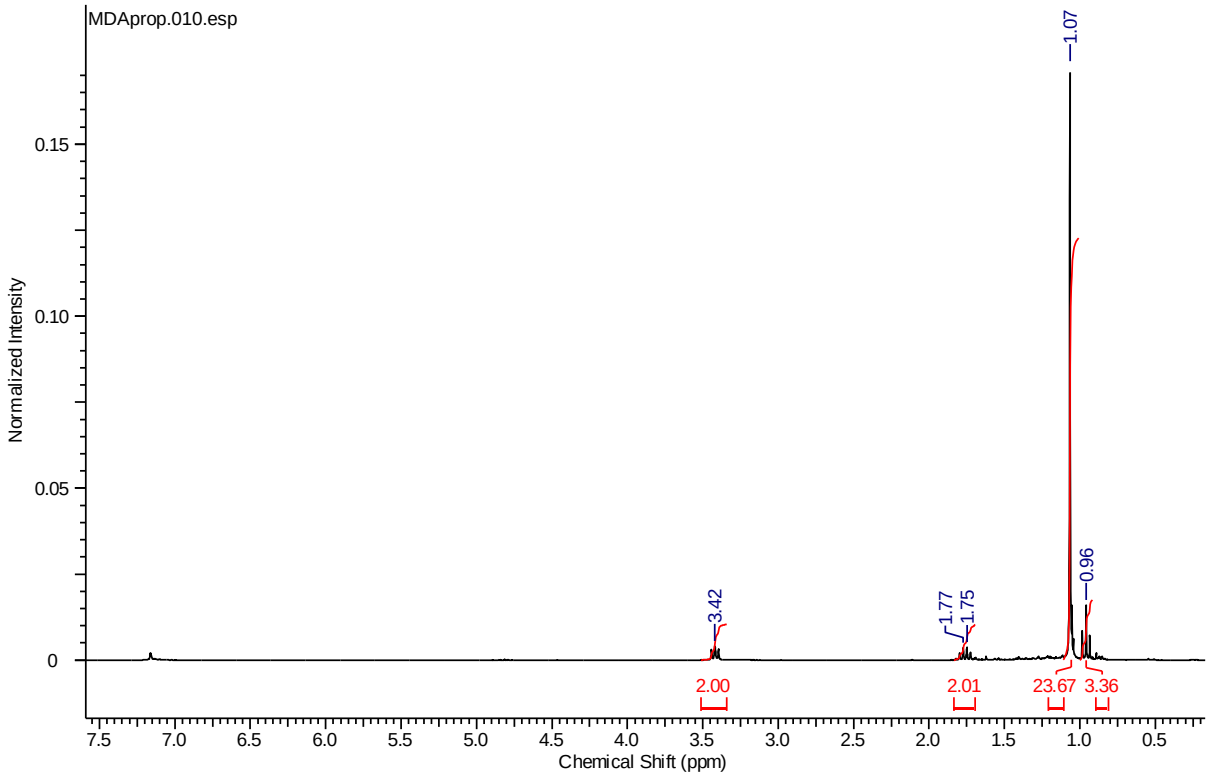


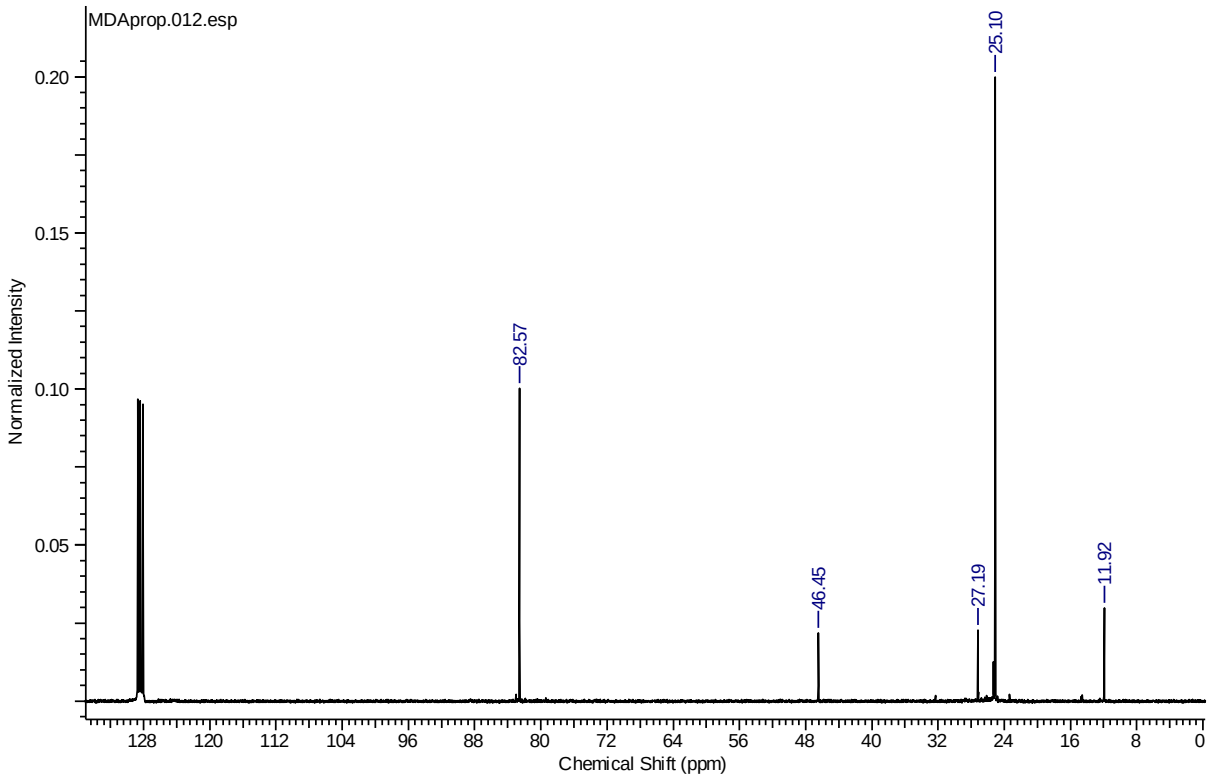

***N*-{*B*(*OCMe*$_2$)$_2$}** - **2-methylpropan-1-amine**

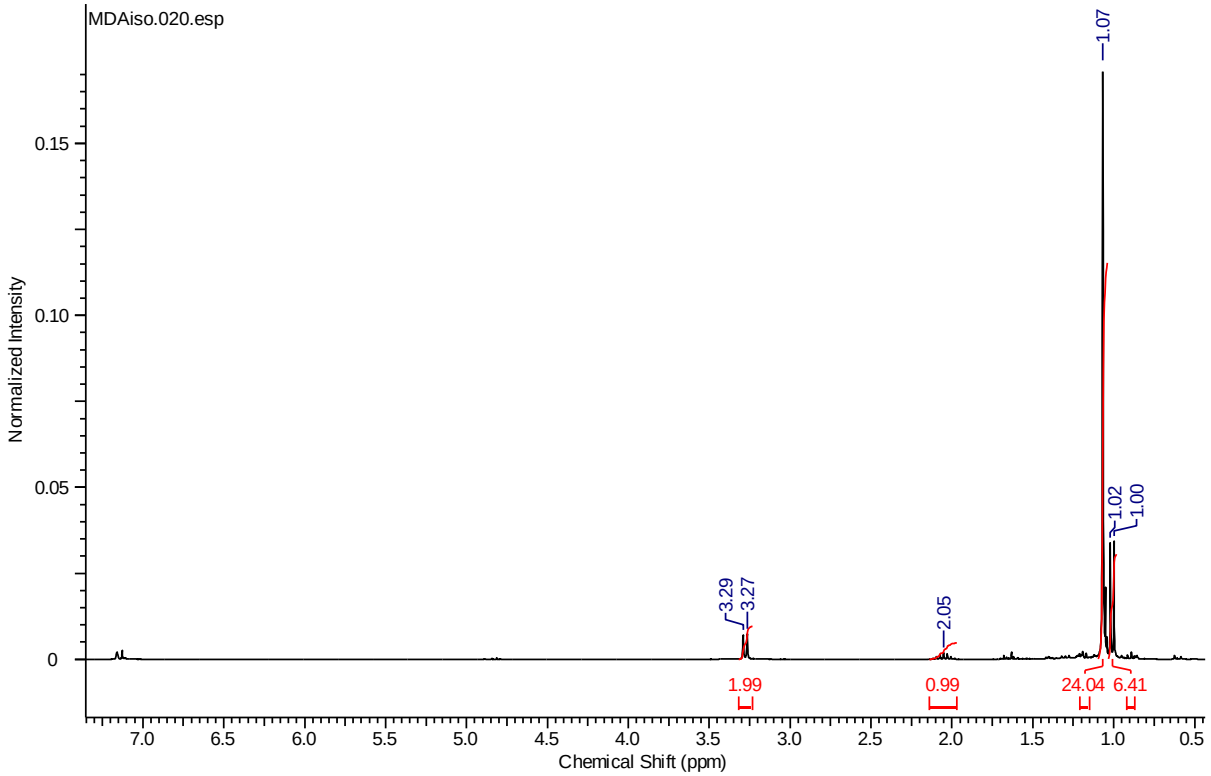


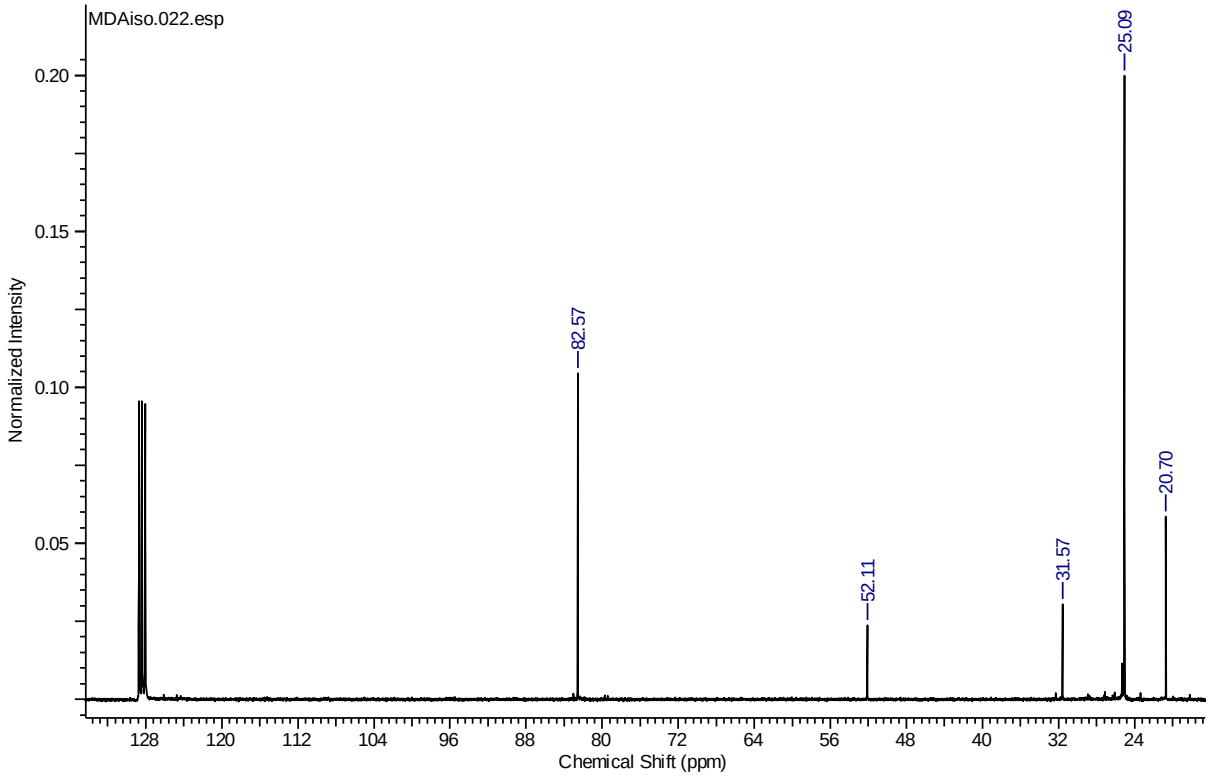

***N*-{*B*(*OCMe*$_2$)$_2$}** - **2,2-dimethylpropan-1-amine**

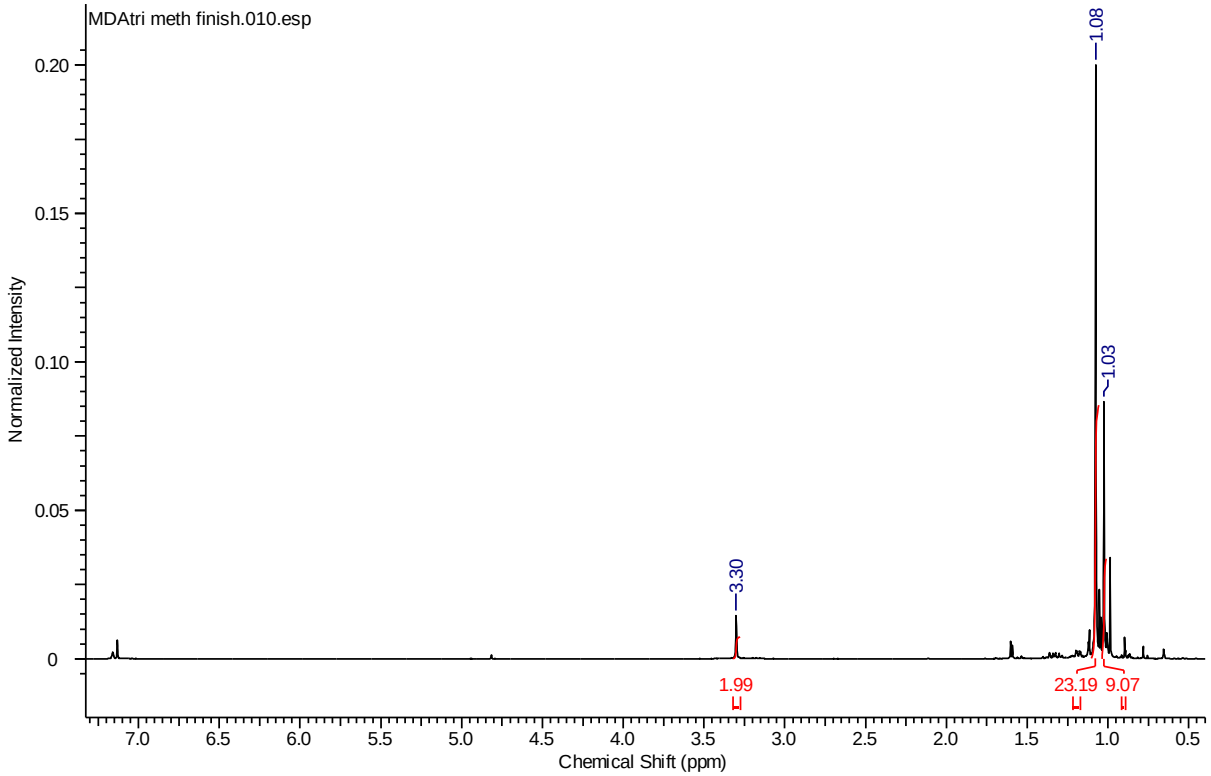


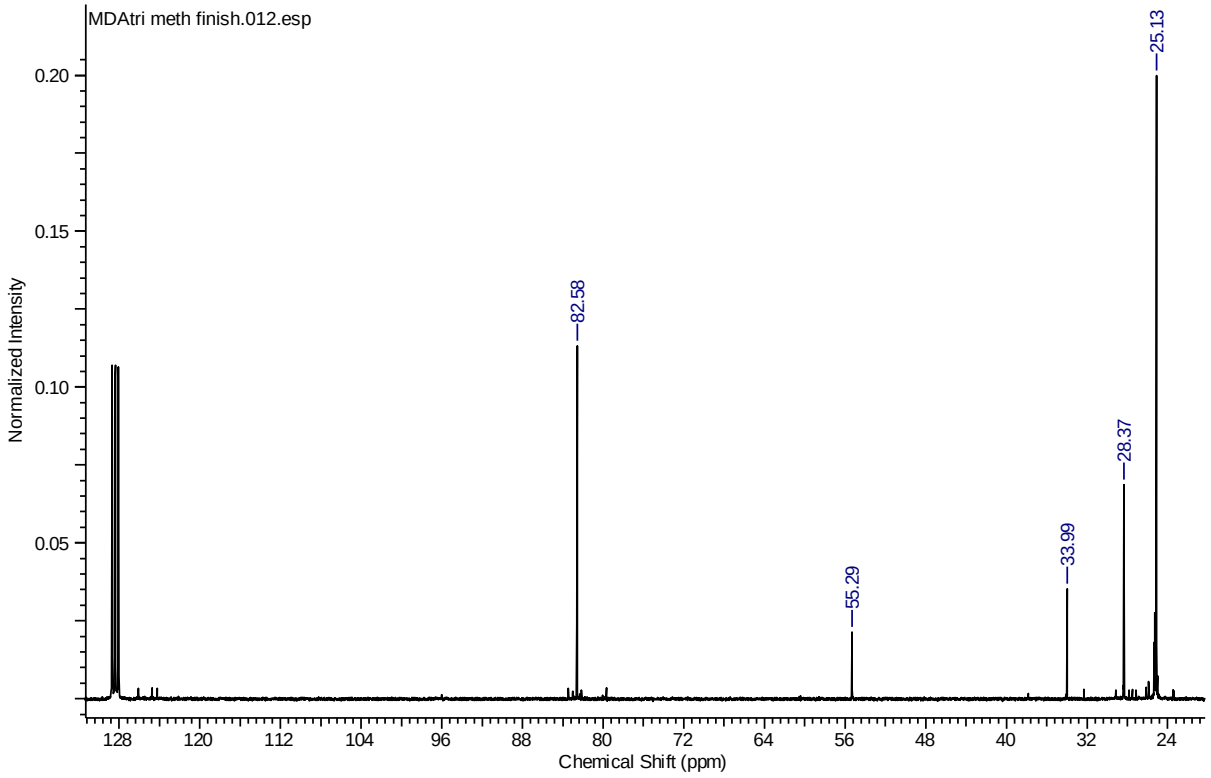

***N*-{B(OCMe$_2$)$_2$} – cyclohexylmethanamine**

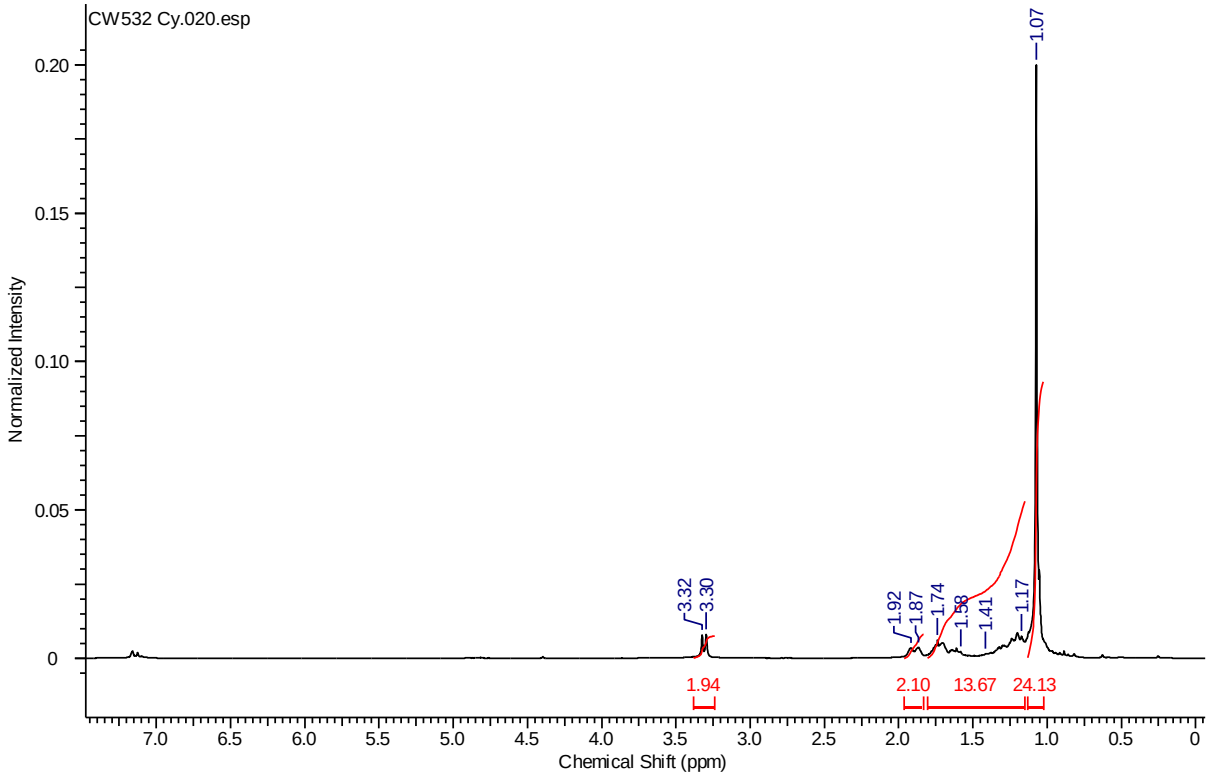


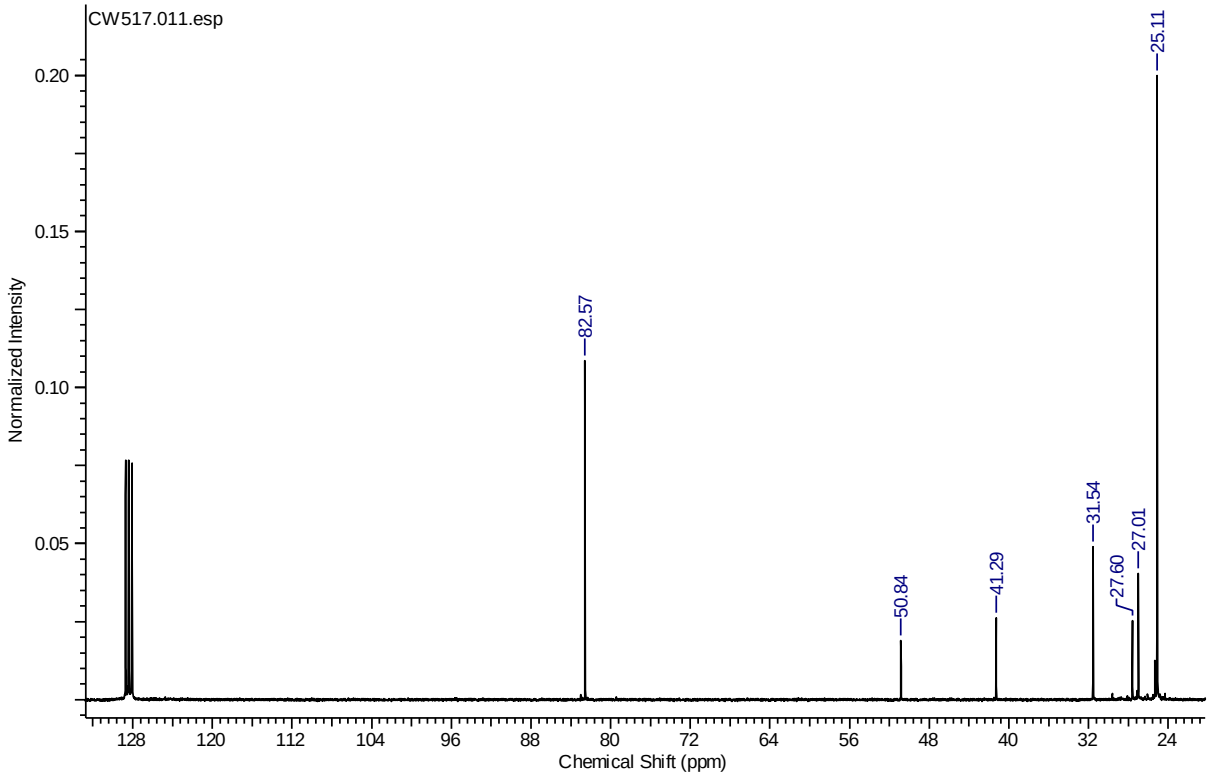

***N*-{*B*(*OCMe*$_2$)$_2$}** – **phenylmethanamine**

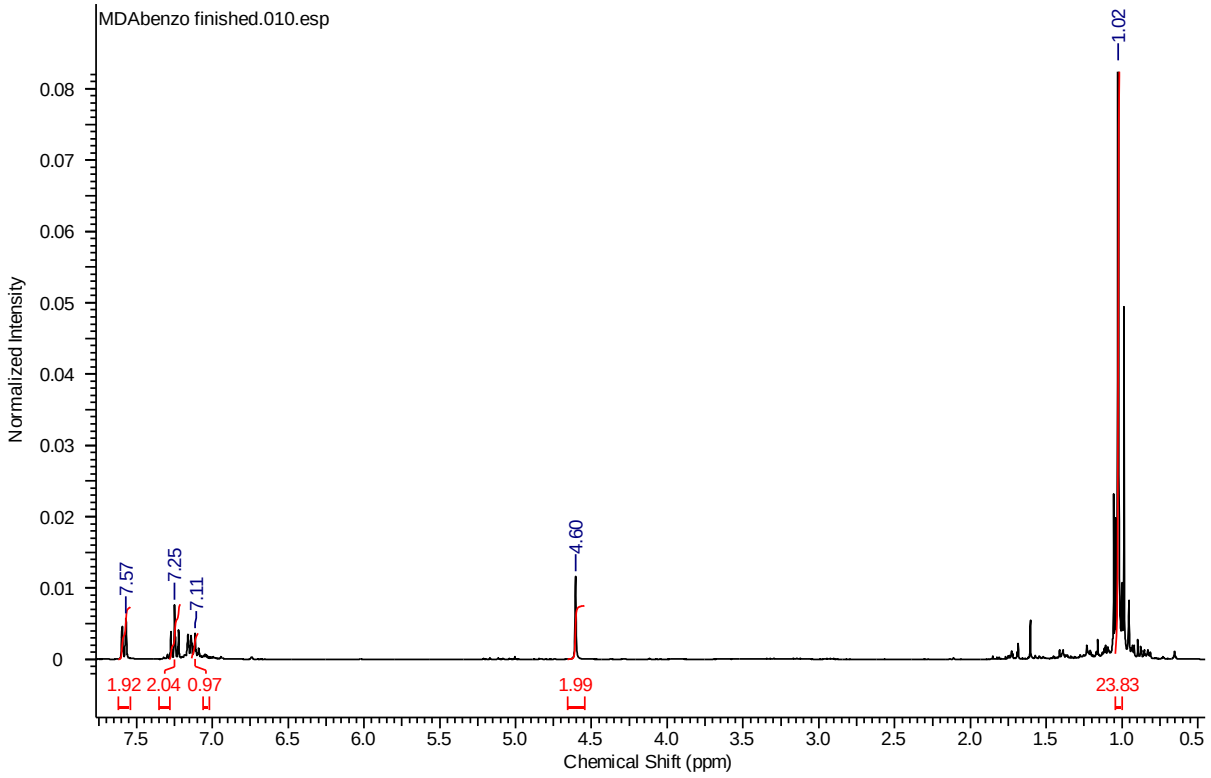


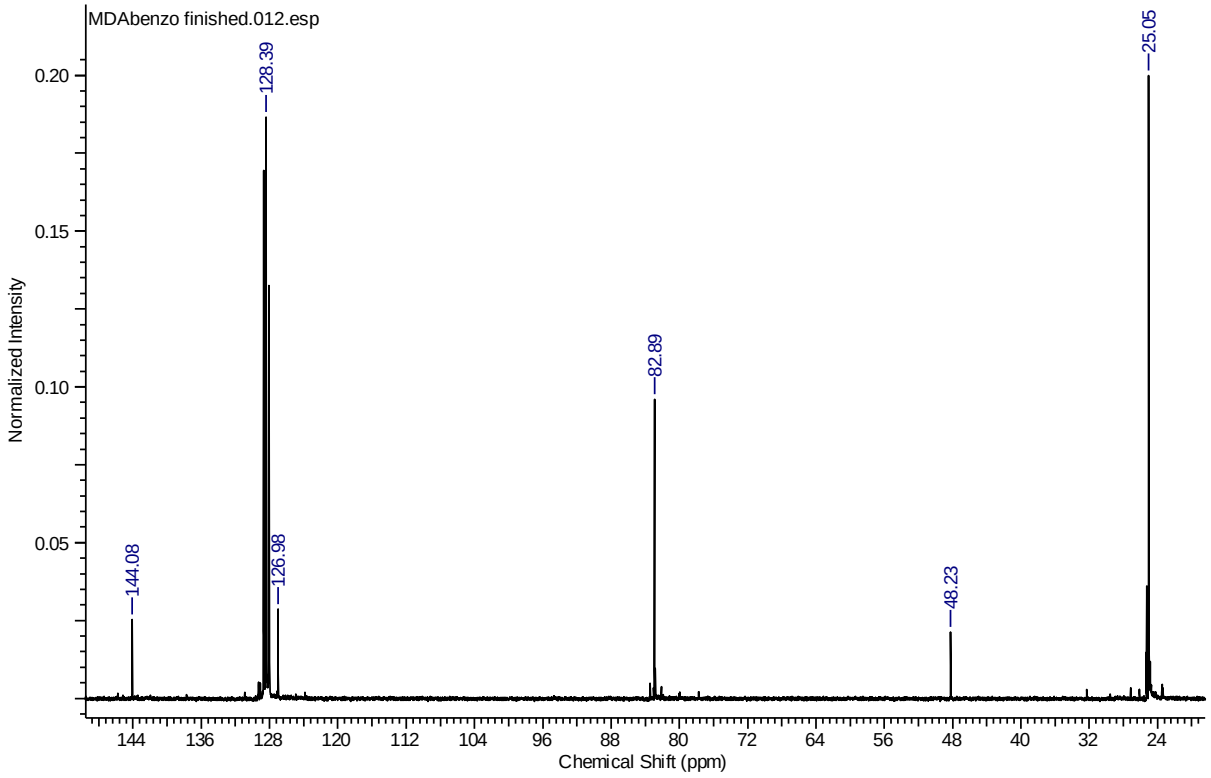

***N*-{*B*(*OCMe*$_2$)$_2$} - *o*-tolylmethanamine**

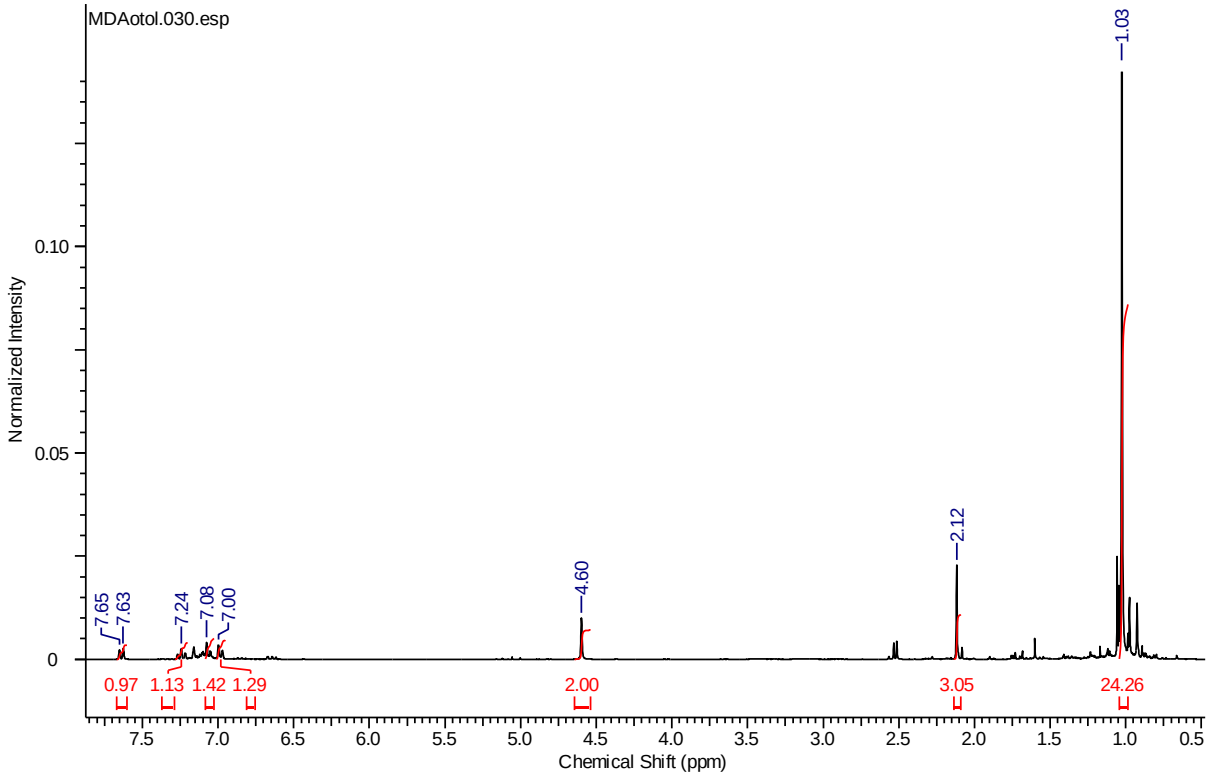


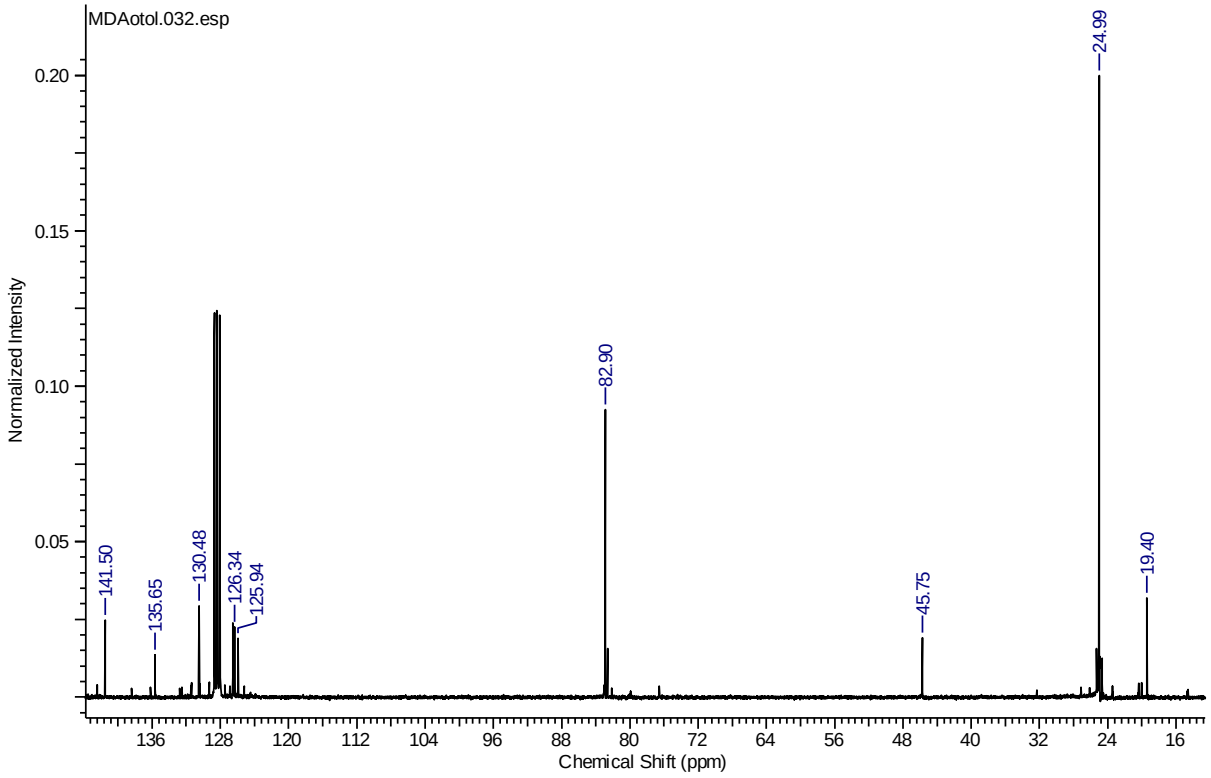

***N*-{B(OCMe$_2$)$_2$} - *m*-tolylmethanamine**

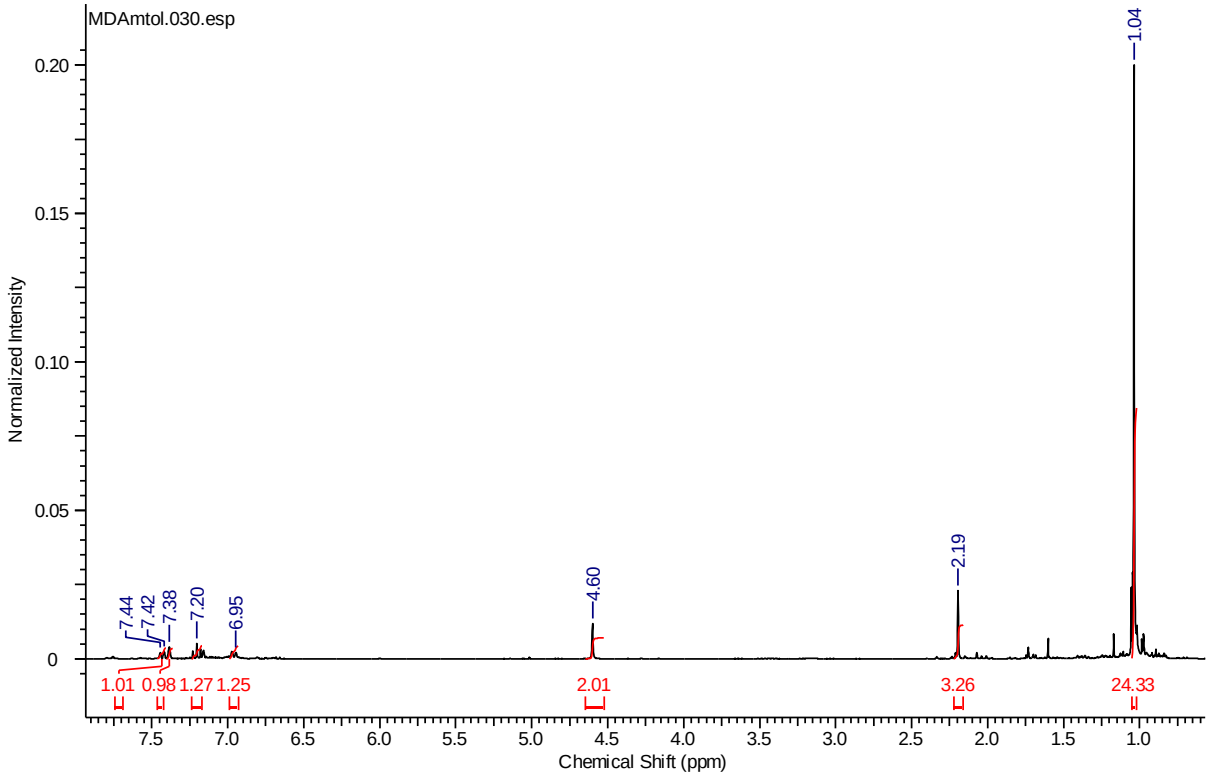


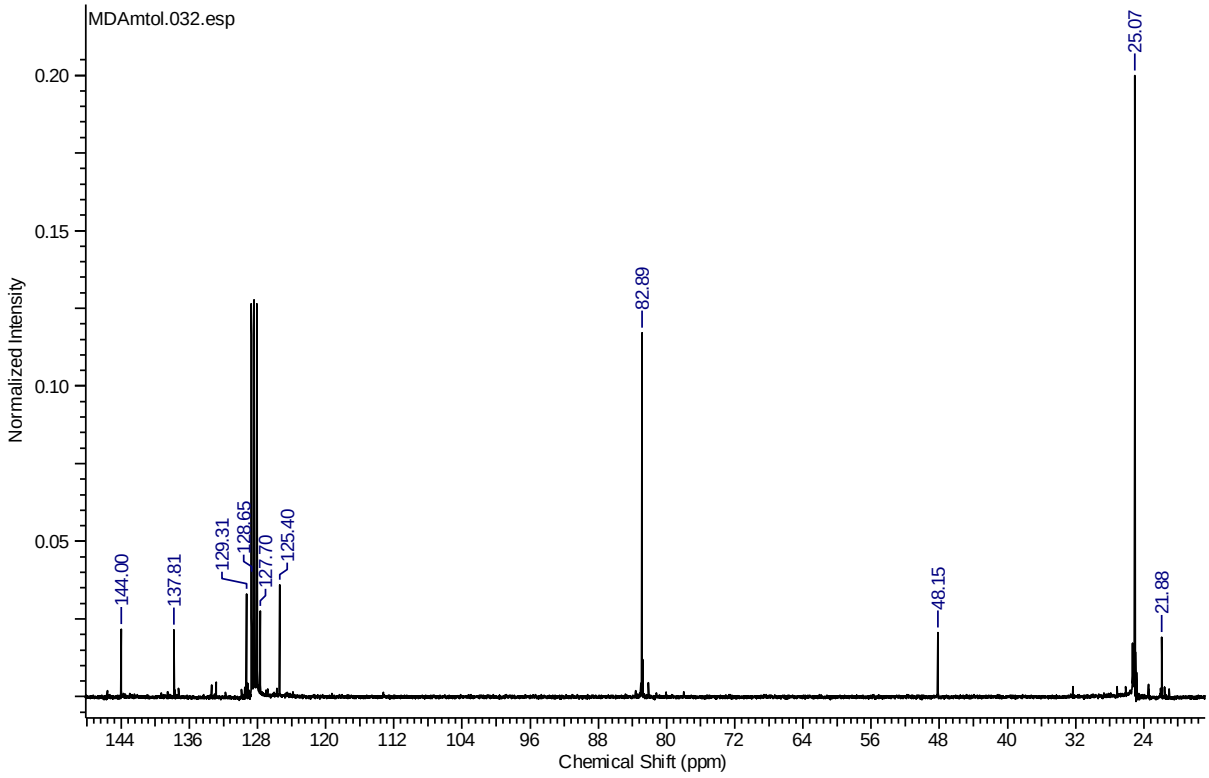

***N*-{*B*(*OCMe*$_2$)$_2$}-*p*-tolylmethanamine**

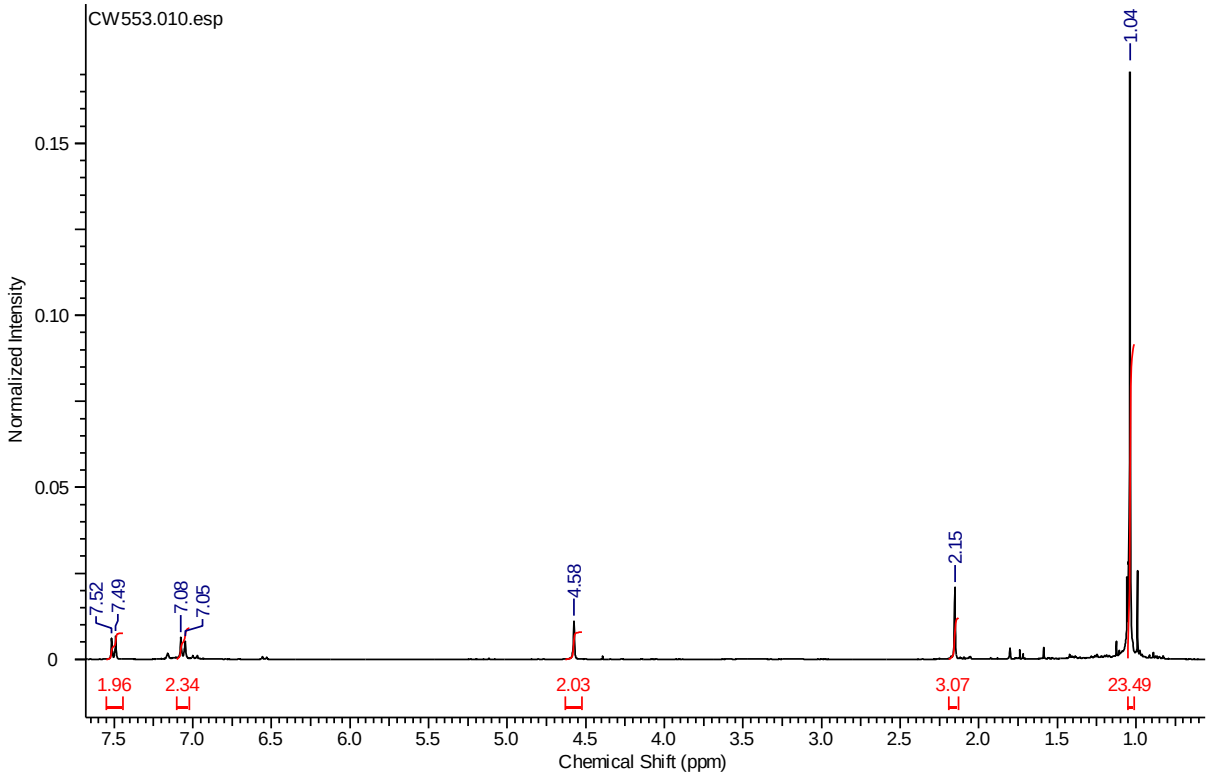


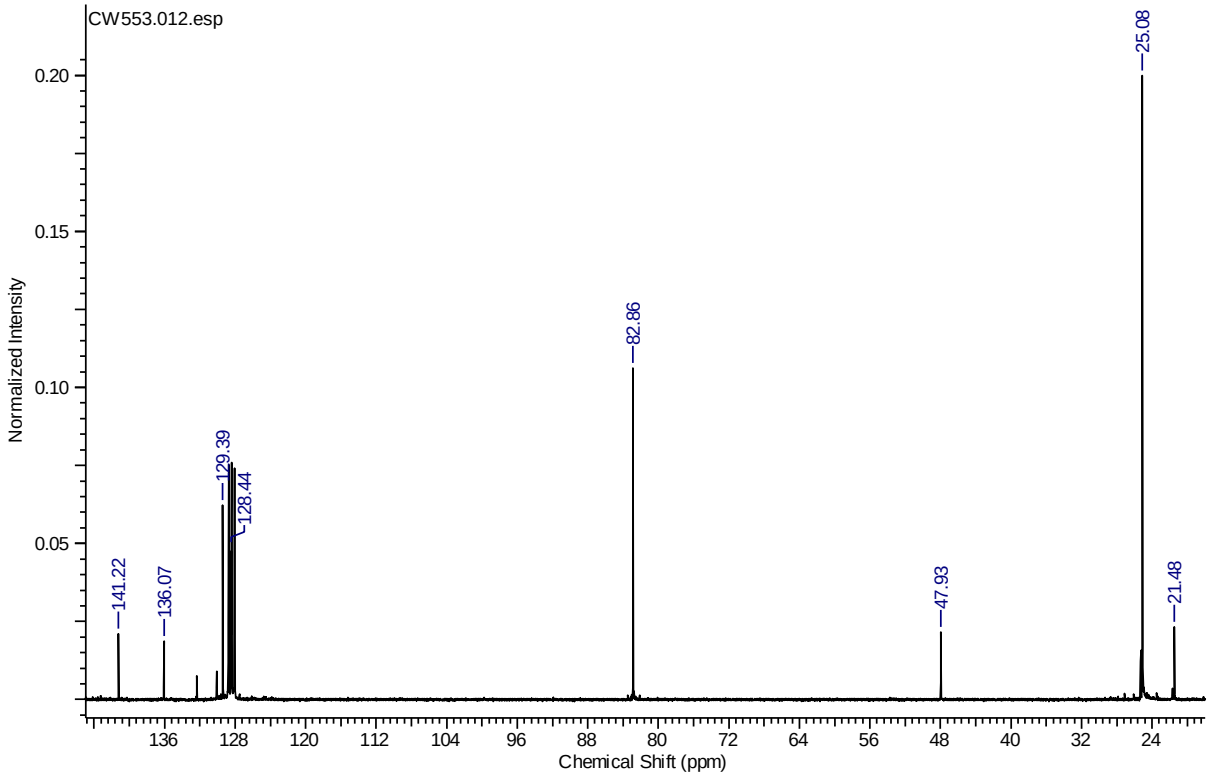

***N*-{*B*(*OCMe*$_2$)$_2$}-4-fluorophenylmethanamine**

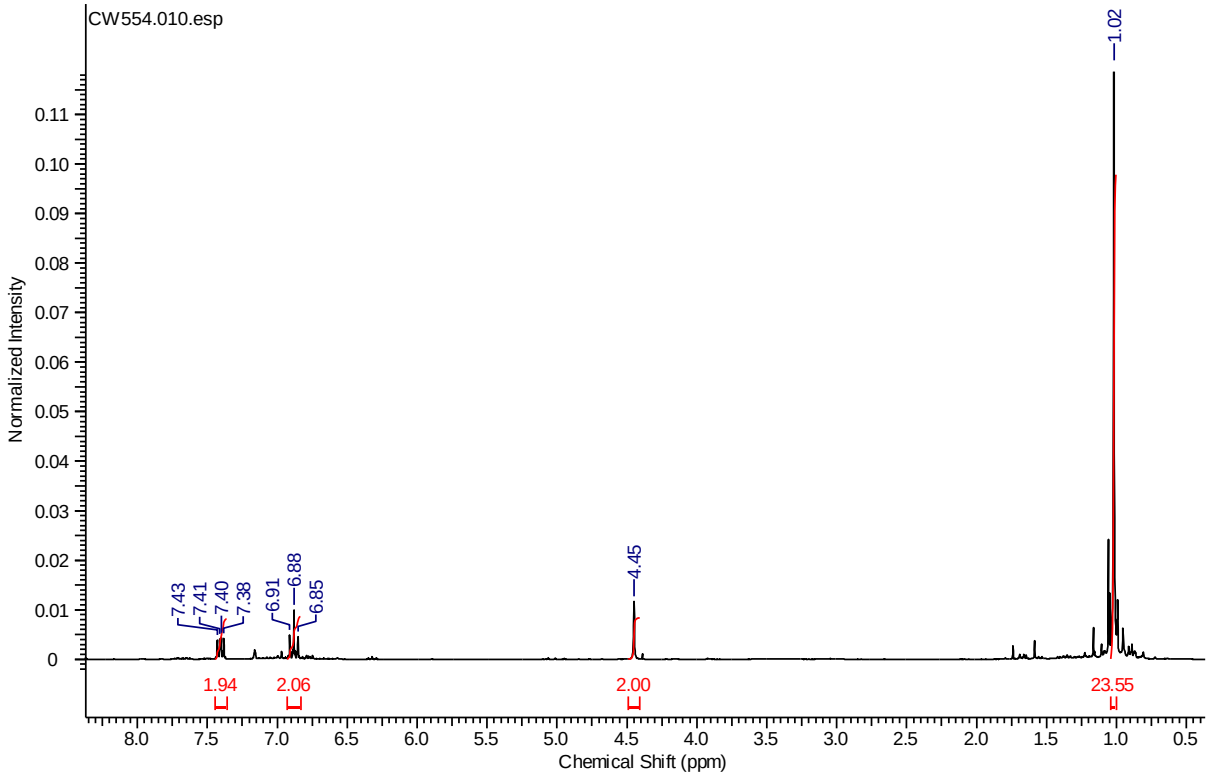


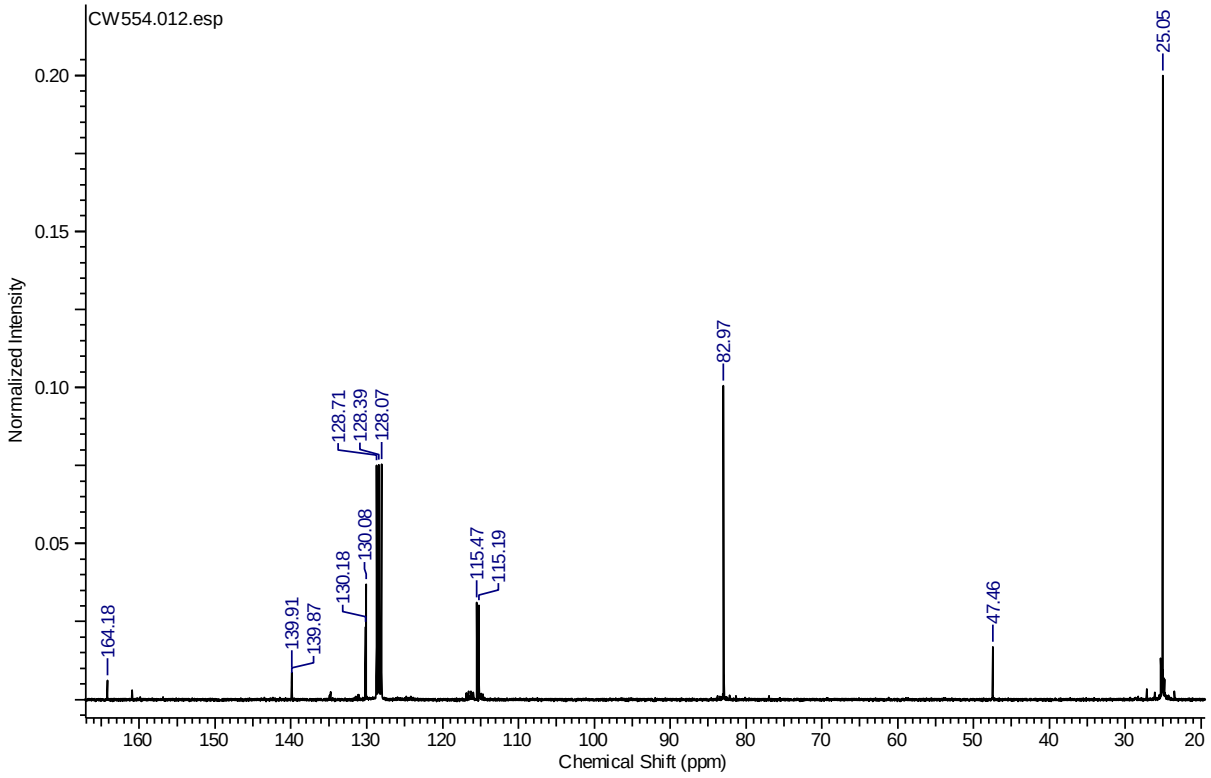

***N*-{*B*(*OCMe*$_2$)$_2$}-4-(trifluoromethyl)phenylmethanamine**

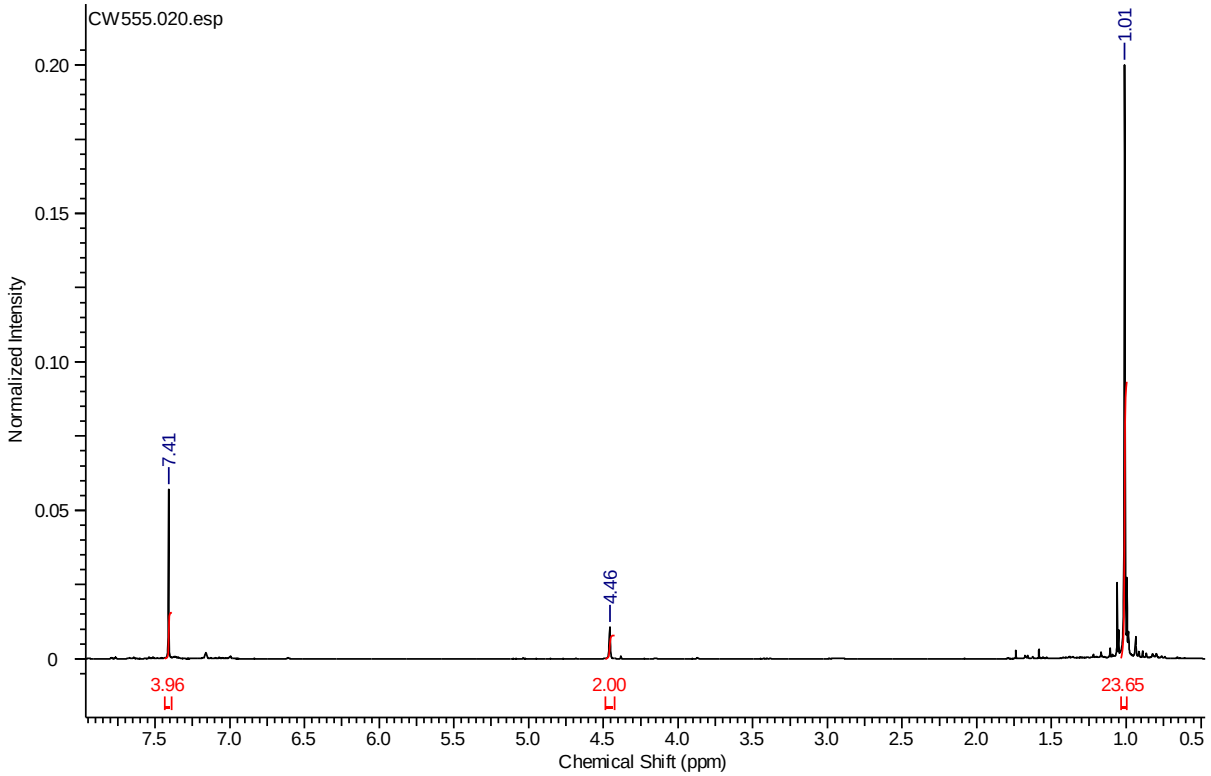


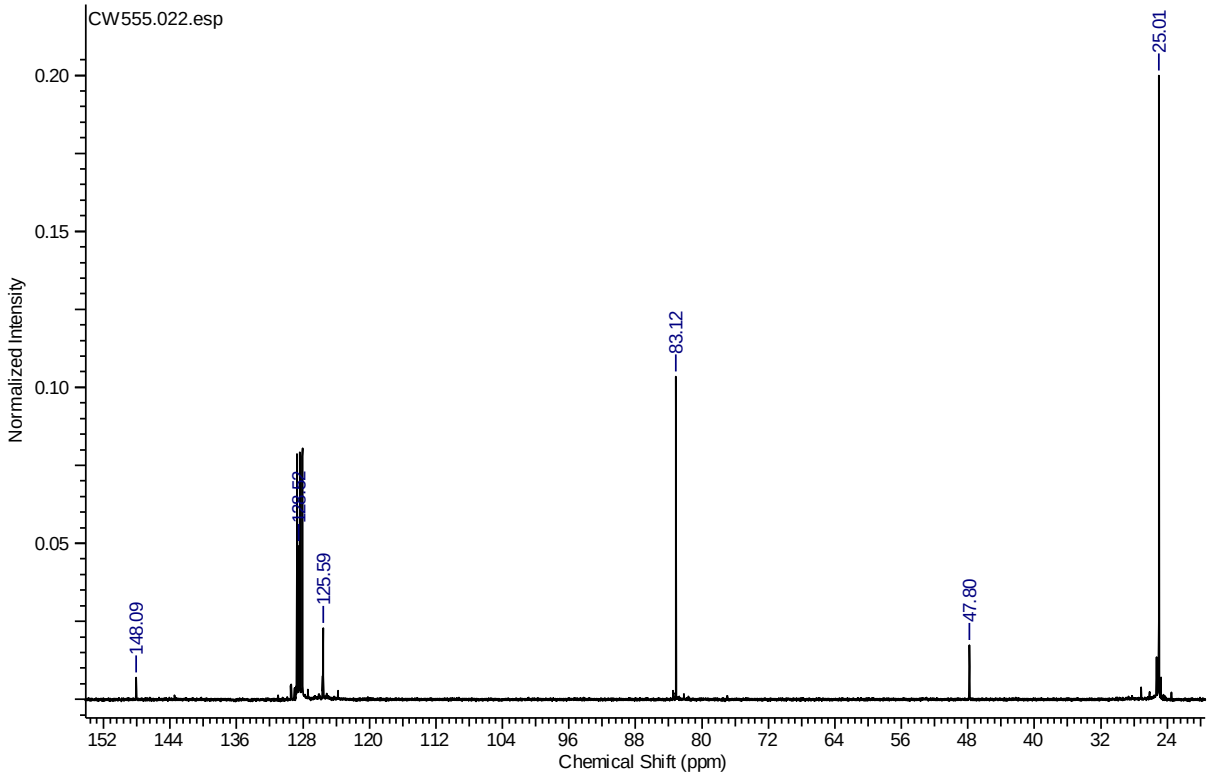

***N*-{*B*(*OCMe*$_2$)$_2$} – *4*-(Methoxy)phenylmethanamine**

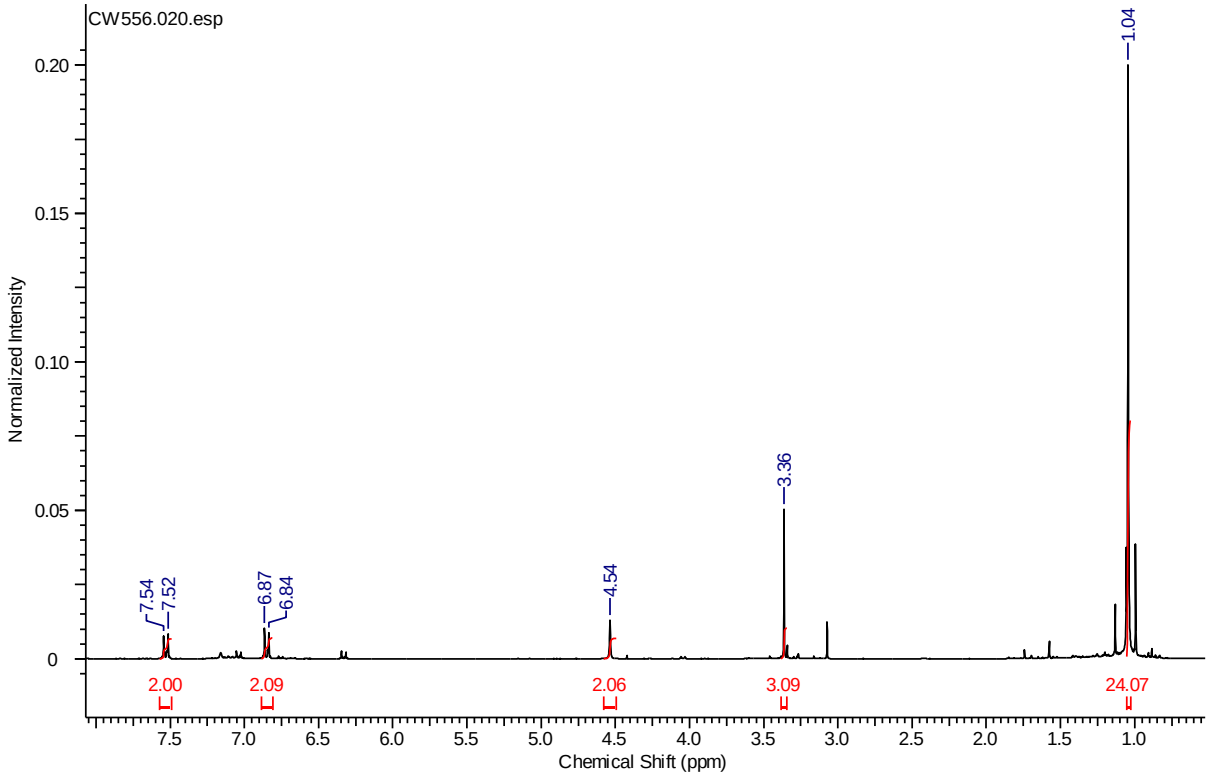


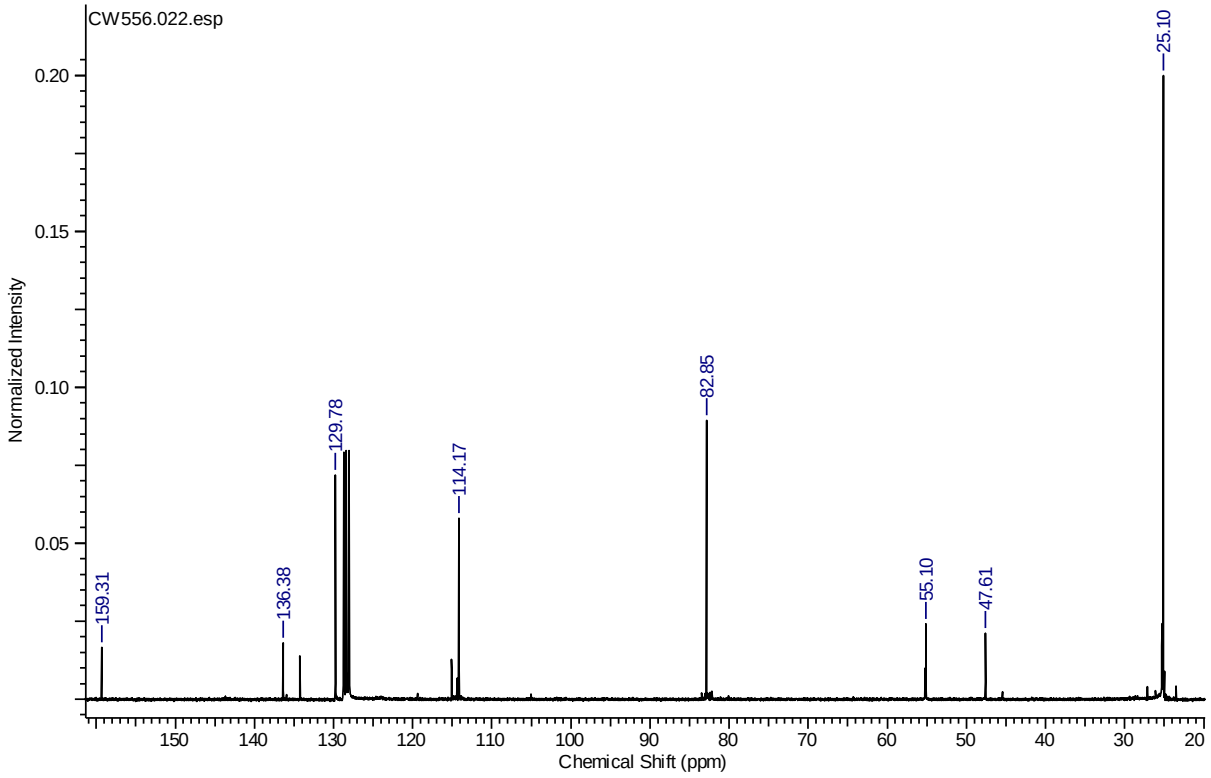

***N*-{*B*(*OCMe*$_2$)$_2$}** – **diphenylacetoamine**

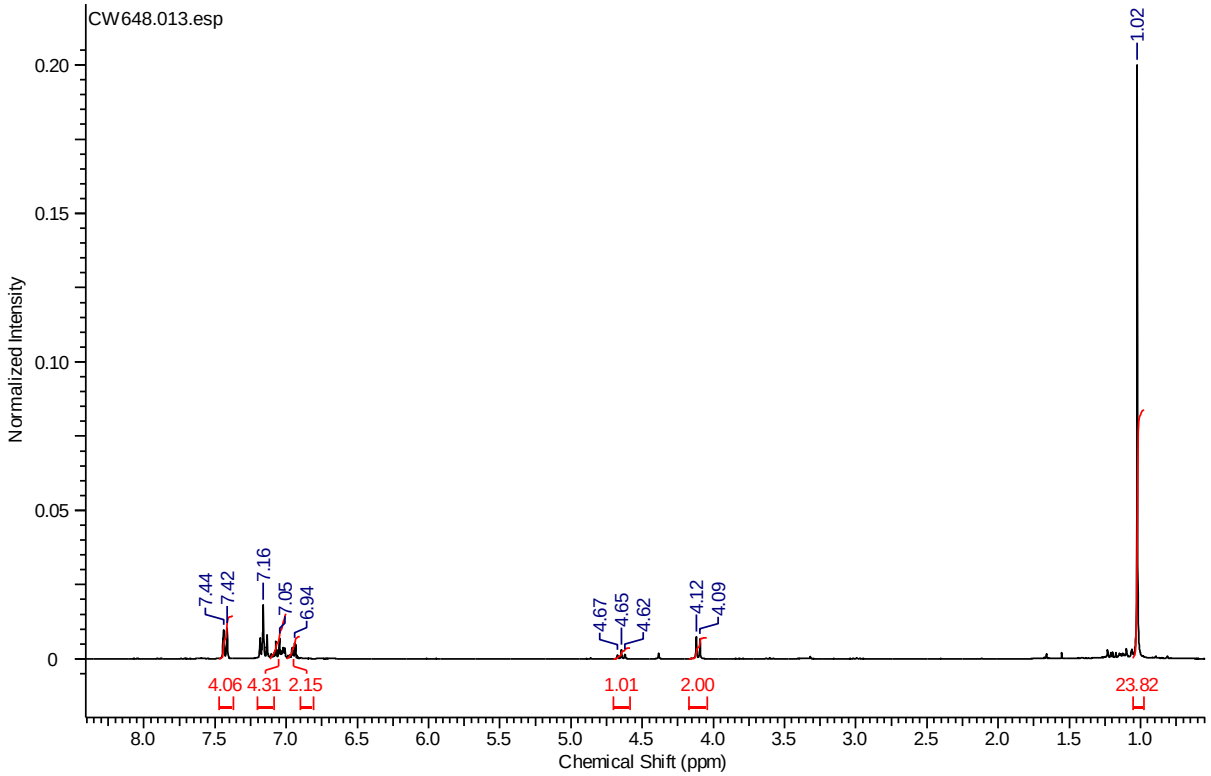


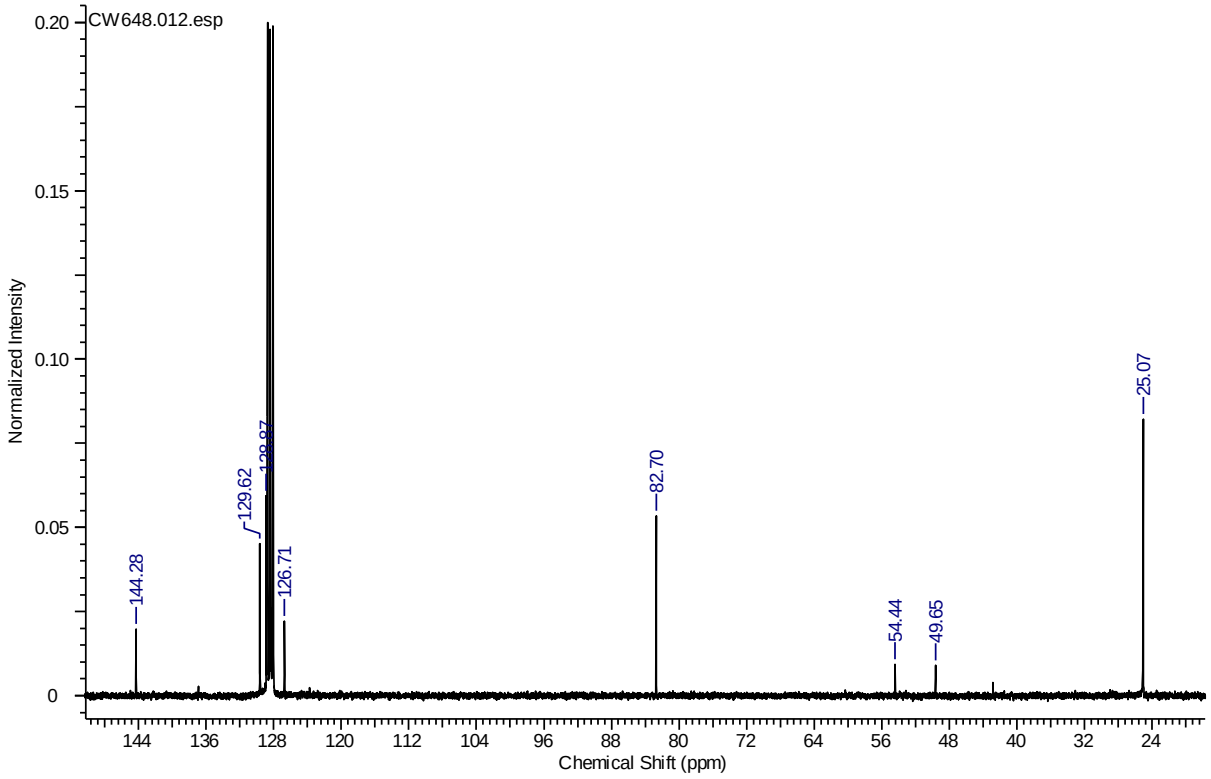

**X-ray Structural Analyses**

Diffraction data for compounds **1** – **5** were collected on a Nonius Kappa CCD with a low temperature device at 150 K, utilizing Mo-Kα radiation monochromated with graphite (λ = 0.71070 Å). Processing utilized the Nonius software,[2] with structure solution and refinement using XSeed[3] or WINGX-1.70[4] suite of programs throughout and visualized utilizing ORTEP 3.[5] The asymmetric unit of **2** comprises half of a dimer which straddles a crystallographic inversion center. Compound **5** co-crystallized with one molecule of toluene and a molecule of hexane which was half occupied. All bond lengths in the hexane molecule have been restrained. The phenyl group in the toluene molecule has been refined using constraints.

**References**


1. A. P. Dove, V. C. Gibson, P. Hormnirun, E. L. Marshall, J. A. Segal, A. J. P. White and D. J. Williams, *Dalton. Trans.* 2003, 3088.

2. DENZO-SCALEPACK Z. Otwinowski and W. Minor, " Processing of X-ray Diffraction Data Collected in Oscillation Mode ", Methods in Enzymology, Volume 276: Macromolecular Crystallography, part A, p.307-326, 1997,C.W. Carter, Jr. & R. M. Sweet, Eds., Academic Press.

3. G. M. Sheldrick, *SHELXL97-2, Program for Crystal Structure Refinement*, Universität Göttingen, Göttingen, Germany, 1998.

4. L. J. Barbour, *X-Seed - A Software Tool for Supramolecular Crystallography*, *J. Supramol. Chem.* 2001, **1**, 189.

5. C. Barnes, *J. Appl. Cryst*. 1997, **30**, 568.

## Kinetic Experiments

All NMR Data were recorded on a Bruker AV400 NMR operating at 400.13 MHz ($^1$H) and were recorded at 323 K unless stated otherwise. All data were processed using ACD/Labs group spectra common integral analysis software.

In a glovebox a stock solution of the precatalyst was made to the relevant concentration, 0.5 mL of the catalyst solution was transferred to a Youngs tap NMR tube followed by addition of the relevant quantity of HBpin, followed by the chosen substrate. The tube was sealed, removed from the glovebox, immediately frozen with liquid nitrogen and thawed just prior to loading into the NMR spectrometer which had been preheated to a chosen temperature (if required). $^1$H NMR spectra were recorded at regular intervals. Reaction kinetics were monitored using the intensity changes in the substrate resonances over three or more half-lives on the basis of substrate consumption. Data was normalised against the initial substrate concentration $[\text{Substrate}]_{t=0}$ so that:

$$Ct = \frac{[Substrate]_{t=0}}{[Substrate]_{t=0} + [Substrate]_t}$$

Reaction rates were derived from the plot of Ct vs time (or Ln(Ct), 1/Ct) by using linear trendlines generated by Microsoft Excel software. To obtain Arrhenius and Eyring plots, kinetic analyses were conducted at 4-5 different temperatures, each separated by approximately 5 K.

# Propionitrile Hydroboration Kinetics

## Determination of Catalyst order

**Figure S1** *Pseudo*-zero order kinetics of propionitrile dihydroboration with varying [**V**]

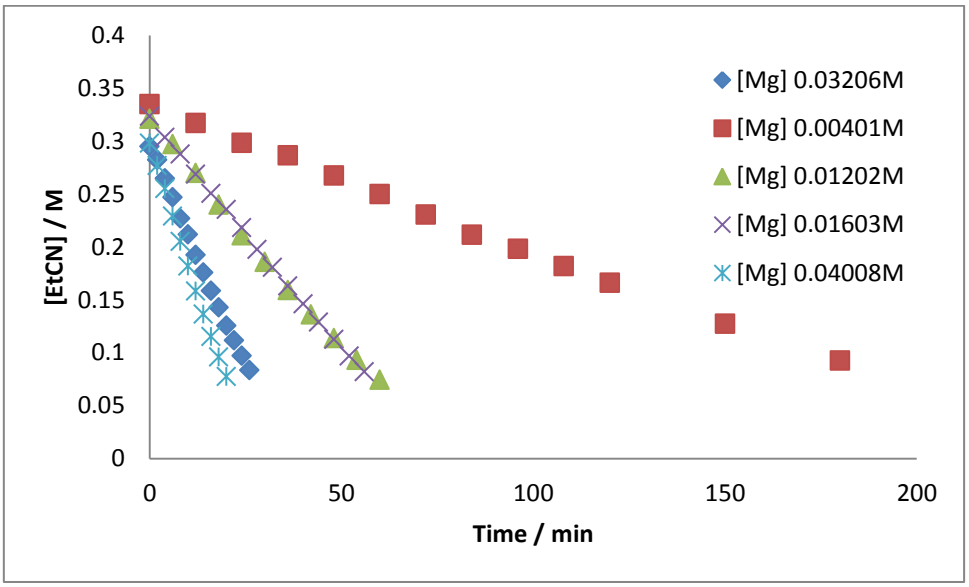


| | [Mg] 0.03206 M | |
|---|---|---|
| | Value | Error |
| $m_1$ | 0.296000 | 0.001437 |
| $m_2$ | -0.008360 | 0.000094 |
| Chisq | 0.00020266 | n/a |
| $R^2$ | 0.99804 | n/a |

| | [Mg] 0.00401 M | |
|---|---|---|
| | Value | Error |
| $m_1$ | 0.331970 | 0.001682 |
| $m_2$ | -0.001370 | 0.000018 |
| Chisq | 0.001751 | n/a |
| $R^2$ | 0.99804 | n/a |

| | [Mg] 0.01202 M | |
|---|---|---|
| | Value | Error |
| $m_1$ | 0.317320 | 0.003780 |
| $m_2$ | -0.004210 | 0.000097 |
| Chisq | 0.001958 | n/a |
| $R^2$ | 0.99601 | n/a |

| | [Mg] 0.01063 M | |
|---|---|---|
| | Value | Error |
| $m_1$ | 0.321200 | 0.001232 |
| $m_2$ | -0.004340 | 0.000035 |
| Chisq | 0.000804 | n/a |
| $R^2$ | 0.99951 | n/a |

| | [Mg] 0.04008 M | |
|---|---|---|
| | Value | Error |
| $m_1$ | 0.297150 | 0.001701 |
| $m_2$ | -0.011260 | 0.000144 |
| Chisq | 0.000197 | n/a |
| $R^2$ | 0.99854 | n/a |

**Figure S2.** ln([EtCN]$_0$/[EtCN]$_t$) vs time; non-linear kinetics

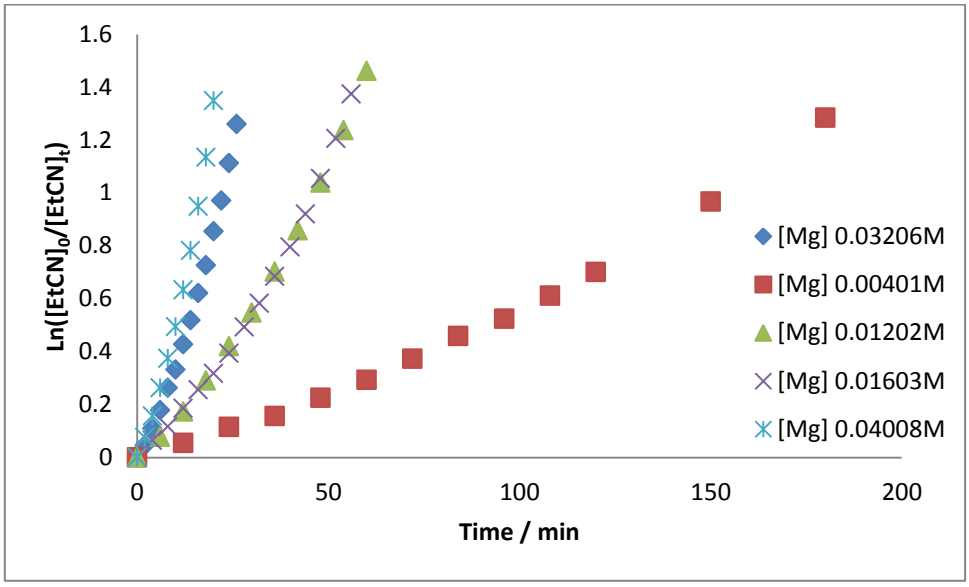


**Figure S3.** 1/[EtCN] vs time; non-linear kinetics

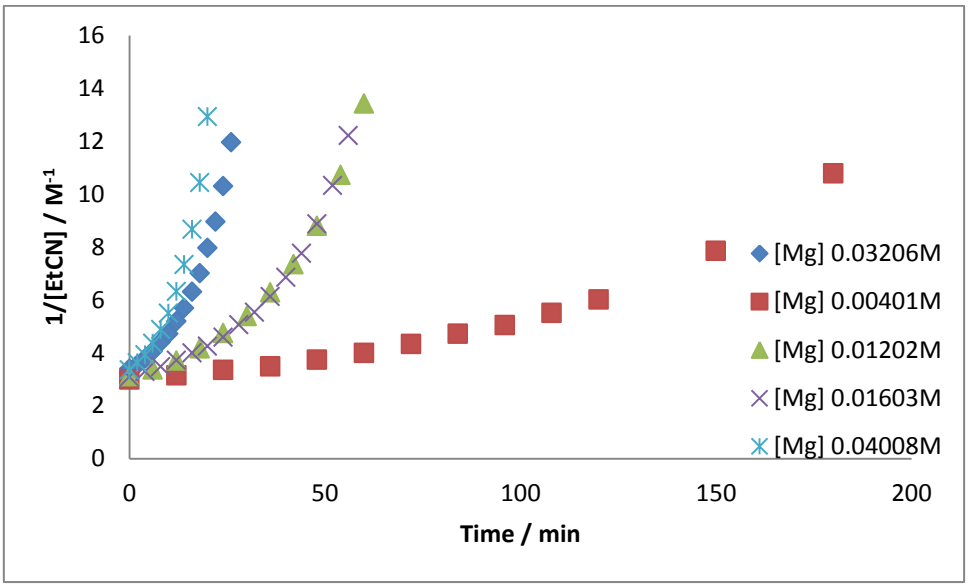

**Figure S4.** [Mg] vs $k_{obs}$ (from Fig. S1); shows first order dependence

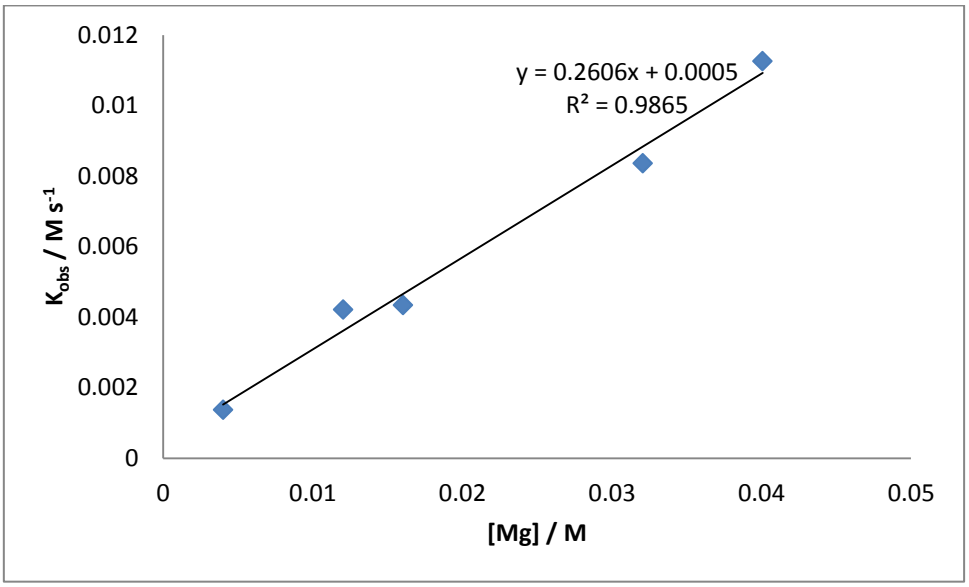


| | Value | Error |
|---|---|---|
| $m_1$ | 0.000477 | 0.000435 |
| $m_2$ | 0.260600 | 0.017616 |
| Chisq | 0.018455 | n/a |
| $R^2$ | 0.9865 | n/a |

## Determination of reaction order with respect to [HBpin]

Varying concentrations of starting reagent HBpin whilst keeping constant [Mg] = 0.04 M and pseudo first order conditions in EtCN (8.0 M).

**Figure S5.** [$EtCH_2N(Bpin)_2$] vs time for varying [HBpin]

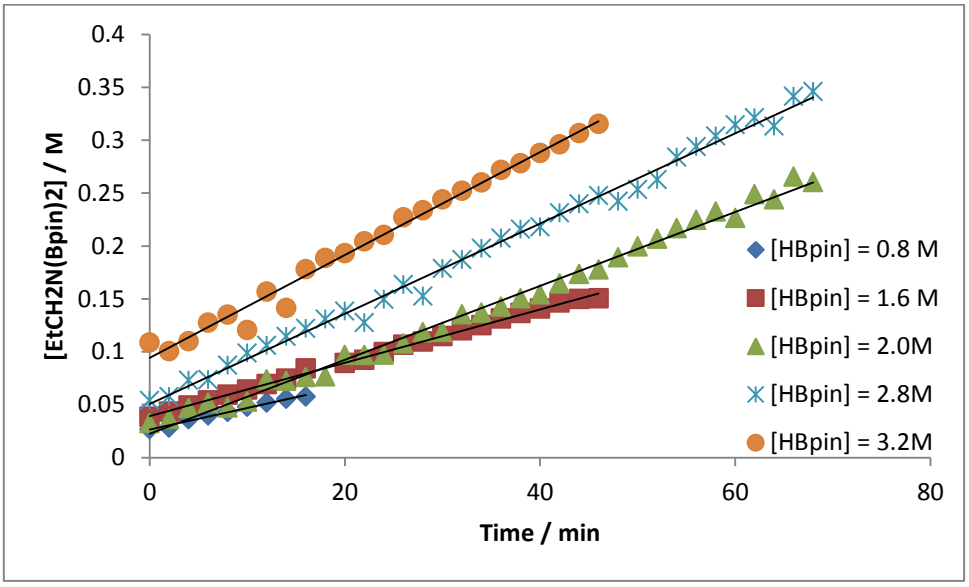

| | [HBpin] = 0.8M | |
|---|---|---|
| | Value | Error |
| $m_1$ | 0.027214 | 0.001114 |
| $m_2$ | 0.001908 | 0.000104 |
| Chisq | 0.00267759 | n/a |
| $R^2$ | 0.976633 | n/a |

| | [HBpin] = 1.6M | |
|---|---|---|
| | Value | Error |
| $m_1$ | 0.038840 | 0.000530 |
| $m_2$ | 0.002547 | 0.000020 |
| Chisq | 8.696E-05 | n/a |
| $R^2$ | 0.998720 | n/a |

| | [HBpin] = 2.0M | |
|---|---|---|
| | Value | Error |
| $m_1$ | 0.022683 | 0.002139 |
| $m_2$ | 0.003491 | 0.000054 |
| Chisq | 0.0192224 | n/a |
| $R^2$ | 0.992143 | n/a |

| | [HBpin] = 2.8M | |
|---|---|---|
| | Value | Error |
| $m_1$ | 0.050577 | 0.002271 |
| $m_2$ | 0.004265 | 0.000057 |
| Chisq | 0.0013212 | n/a |
| $R^2$ | 0.994052 | n/a |

| | [HBpin] = 3.2M | |
|---|---|---|
| | Value | Error |
| $m_1$ | 0.094123 | 0.003163 |
| $m_2$ | 0.004866 | 0.000118 |
| Chisq | 0.044993949 | n/a |
| $R^2$ | 0.987265 | n/a |

**Figure S6.** $\ln([EtCH_2N(Bpin)_2]_0/[EtCH_2N(Bpin)_2]_t)$ vs time; non-linear kinetics

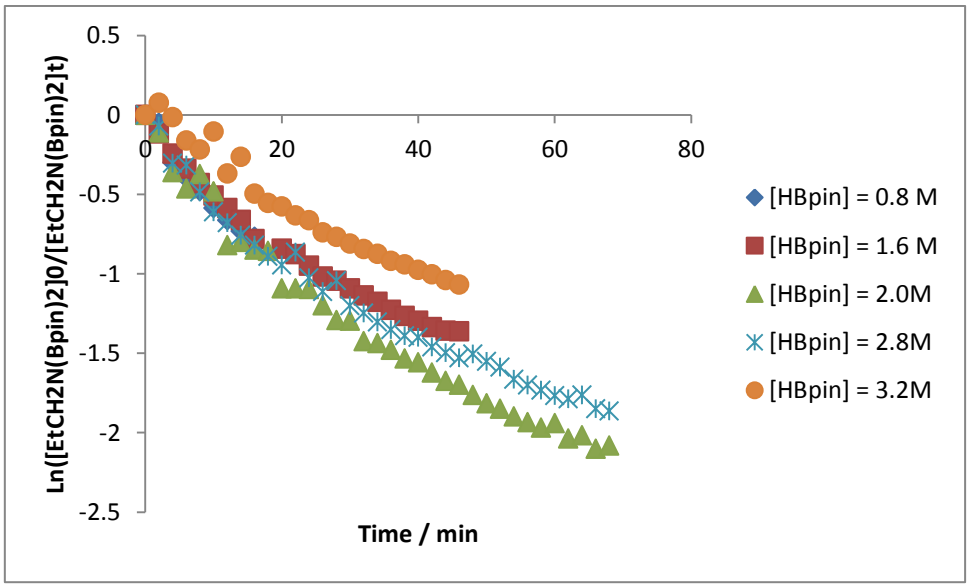

**Figure S7.** 1/[$EtCH_2N(Bpin)_2$] vs time; non-linear kinetics

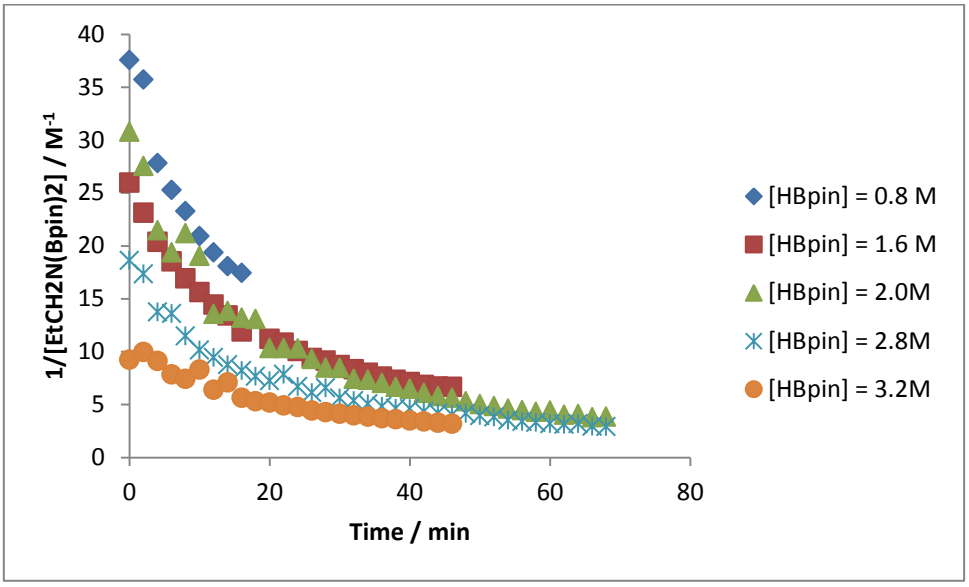


**Figure S8.** [HBpin] vs $k_{obs}$; linear fit indicates 1st order dependence on [HBpin]

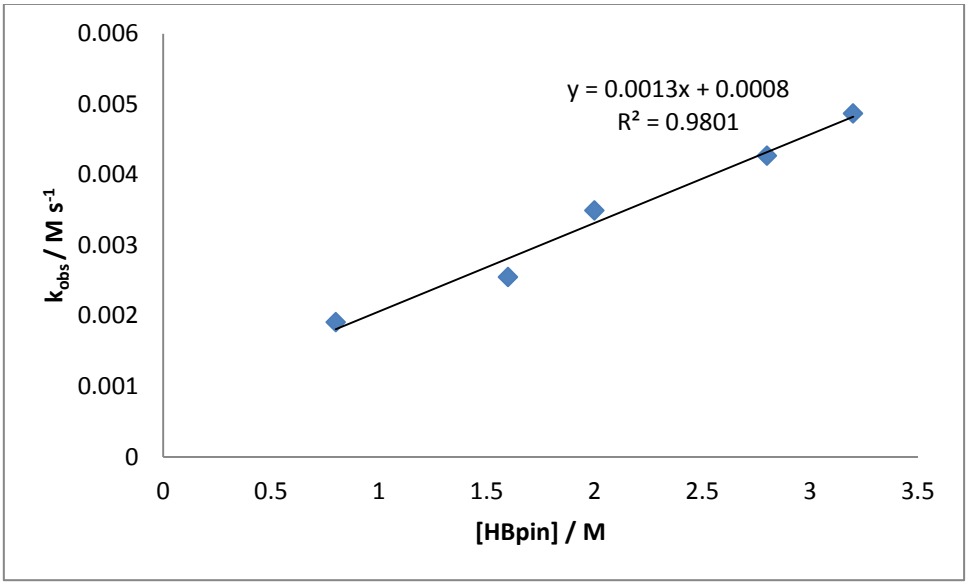


| | Value | Error |
|---|---|---|
| $m_1$ | 0.000806 | 0.000232 |
| $m_2$ | 0.001255 | 0.000103 |
| Chisq | 0.008197128 | n/a |
| $R^2$ | 0.980118 | n/a |

## Determination of reaction order with respect to [EtCN]

Varying concentrations of starting reagent EtCN whilst keeping constant [Mg] = 0.04M and pseudo first order conditions of HBpin (8.0M).

**Figure S9.** [$EtCH_2N(Bpin)_2$] vs time; variable [EtCN]

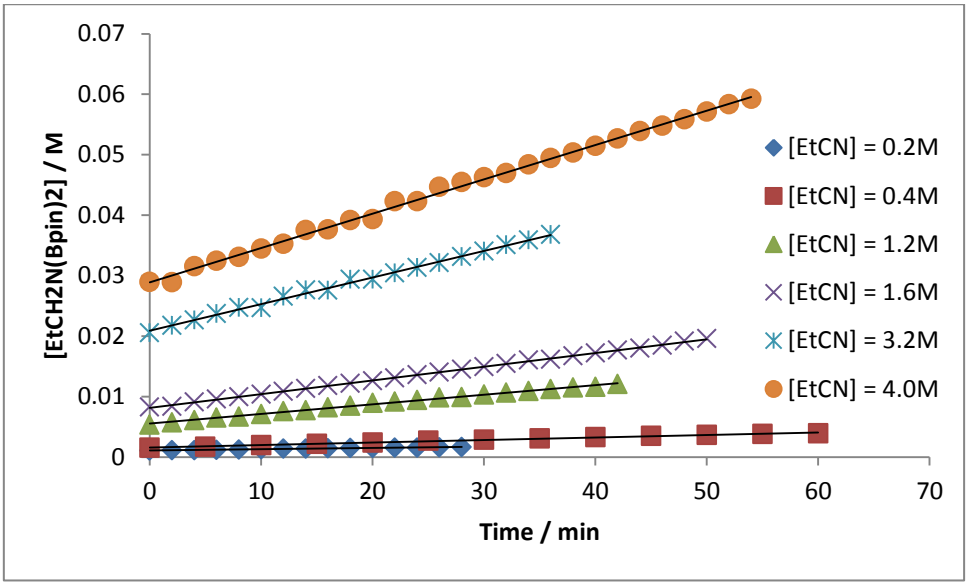


| | [EtCN] = 0.2M | |
|---|---|---|
| | Value | Error |
| $m_1$ | 0.001066 | 0.000012 |
| $m_2$ | 0.000021 | 0.000001 |
| Chisq | 0.009468 | n/a |
| $R^2$ | 0.984067 | n/a |

| | [EtCN] = 0.4M | |
|---|---|---|
| | Value | Error |
| $m_1$ | 0.001572 | 0.000035 |
| $m_2$ | 0.000041 | 0.000001 |
| Chisq | 0.005337 | n/a |
| $R^2$ | 0.993577 | n/a |

| | [EtCN] = 1.2M | |
|---|---|---|
| | Value | Error |
| $m_1$ | 0.005545 | 0.000057 |
| $m_2$ | 0.000158 | 0.000002 |
| Chisq | 0.009731 | n/a |
| $R^2$ | 0.995669 | n/a |

| | [EtCN] = 1.6M | |
|---|---|---|
| | Value | Error |
| $m_1$ | 0.008134 | 0.000038 |
| $m_2$ | 0.000227 | 0.000001 |
| Chisq | 0.000912 | n/a |
| $R^2$ | 0.999219 | n/a |

| | [EtCN] = 3.2M | |
|---|---|---|
| | Value | Error |
| $m_1$ | 0.020904 | 0.000144 |
| $m_2$ | 0.000440 | 0.000007 |
| Chisq | 0.00585 | n/a |
| $R^2$ | 0.995901 | n/a |

| | [EtCN] = 4.0M | |
|---|---|---|
| | Value | Error |
| $m_1$ | 0.028883 | 0.000179 |
| $m_2$ | 0.000568 | 0.000006 |
| Chisq | 7.38E-05 | n/a |
| $R^2$ | 0.997399 | n/a |

**Figure S10**. ln([$EtCH_2N(Bpin)_2$]$_0$/[$EtCH_2N(Bpin)_2$]$_t$) vs time; non-linear kinetics

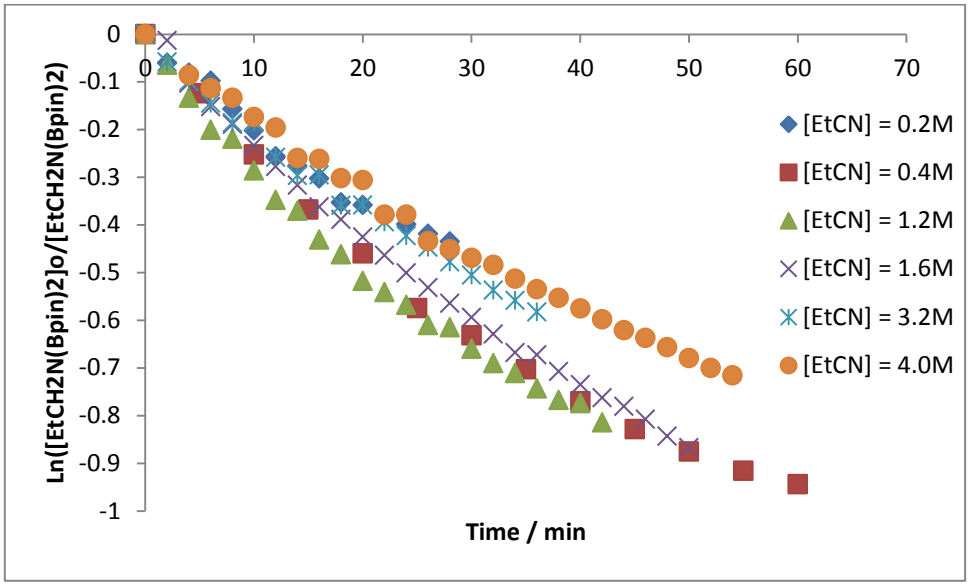


**Figure S11.** 1/[$EtCH_2N(Bpin)_2$] vs time; non-linear kinetics

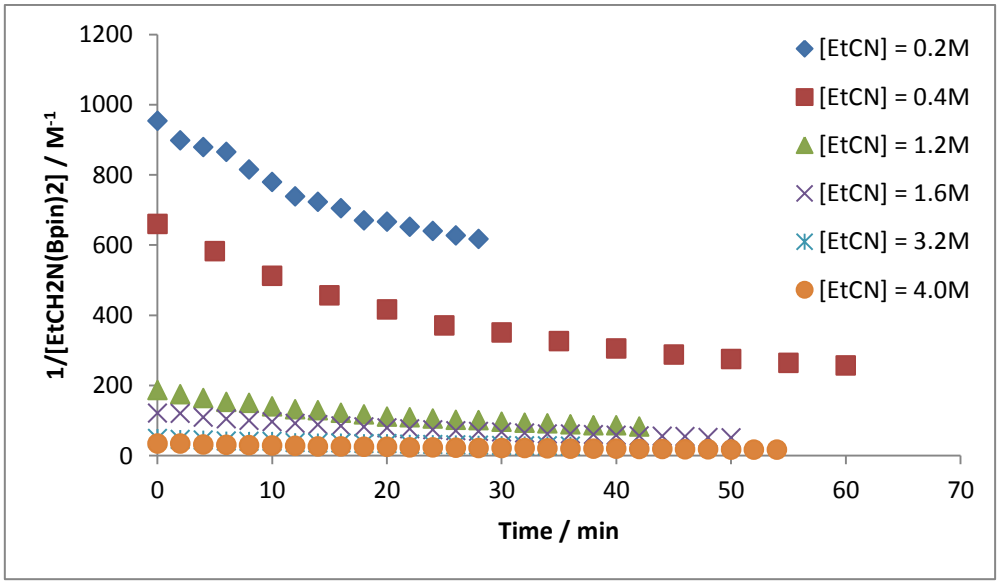

**Figure S12.** [EtCN] vs $k_{obs}$; indicates a first order dependence on [EtCN] under *pseudo*-first order conditions in HBpin

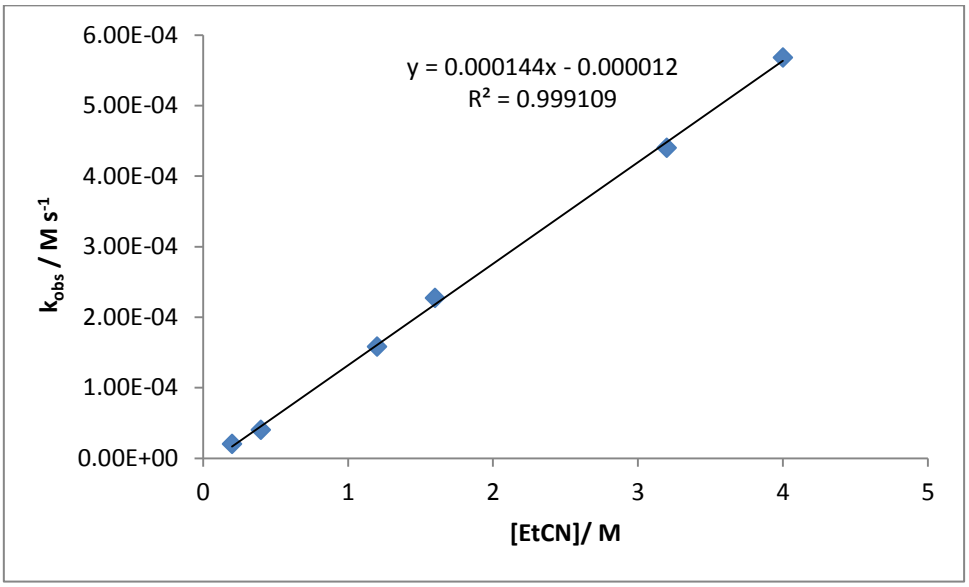


| | Value | Error |
|---|---|---|
| $m_1$ | -0.000012 | 0.000005 |
| $m_2$ | 0.000144 | 0.000002 |
| Chisq | 0.000253 | n/a |
| $R^2$ | 0.999109 | n/a |

## Variable [Mg] under *pseudo*-first order in [HBpin]

**Figure S13.** [$EtCH_2N(Bpin)_2$] vs time; variation in [Mg] whilst under *pseudo*-first order conditions in [HBpin] = 8.0M and keeping [EtCN] = 0.4M constant

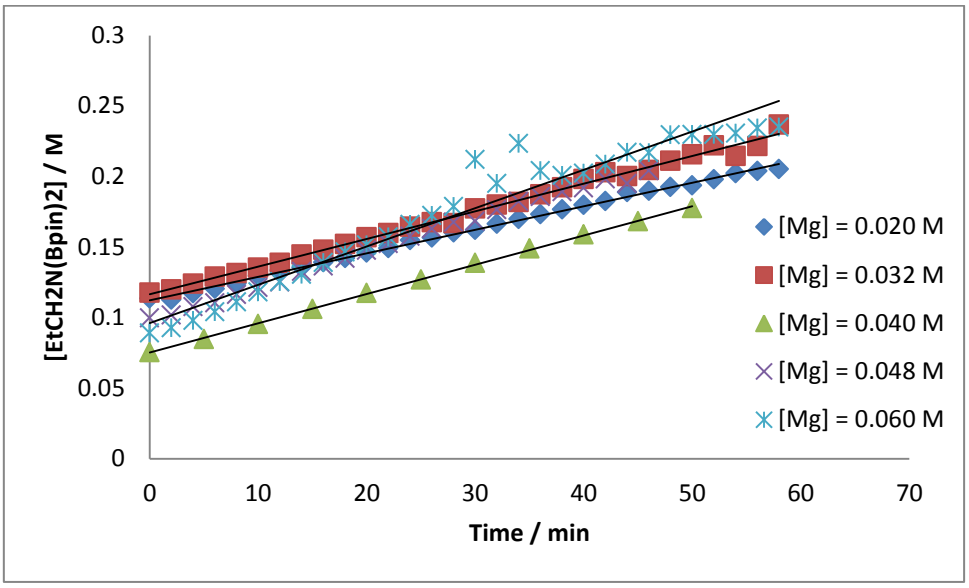


| | [Mg] = 0.020 M | |
|---|---|---|
| | Value | Error |
| $m_1$ | 0.112321 | 0.000556 |
| $m_2$ | 0.001664 | 0.000016 |
| Chisq | 0.001359 | n/a |
| $R^2$ | 0.997272 | n/a |

| | [Mg] = 0.032 M | |
|---|---|---|
| | Value | Error |
| $m_1$ | 0.108293 | 0.001005 |
| $m_2$ | 0.001914 | 0.000030 |
| Chisq | 0.001194 | n/a |
| $R^2$ | 0.993732 | n/a |

| | [Mg] = 0.040 M | |
|---|---|---|
| | Value | Error |
| $m_1$ | 0.075126 | 0.000482 |
| $m_2$ | 0.002078 | 0.000016 |
| Chisq | 1.94E-05 | n/a |
| $R^2$ | 0.999448 | n/a |

| | [Mg] = 0.048 M | |
|---|---|---|
| | Value | Error |
| $m_1$ | 0.098833 | 0.000985 |
| $m_2$ | 0.002352 | 0.000037 |
| Chisq | 0.000583 | n/a |
| $R^2$ | 0.994673 | n/a |

| | [Mg] = 0.060 M | |
|---|---|---|
| | Value | Error |
| $m_1$ | 0.090021 | 0.001977 |
| $m_2$ | 0.002954 | 0.000075 |
| Chisq | 0.000654 | n/a |
| $R^2$ | 0.943791 | n/a |

**Figure S14**. ln([$EtCH_2N(Bpin)_2$]$_0$/[$EtCH_2N(Bpin)_2$]$_t$) vs time; non-linear kinetics

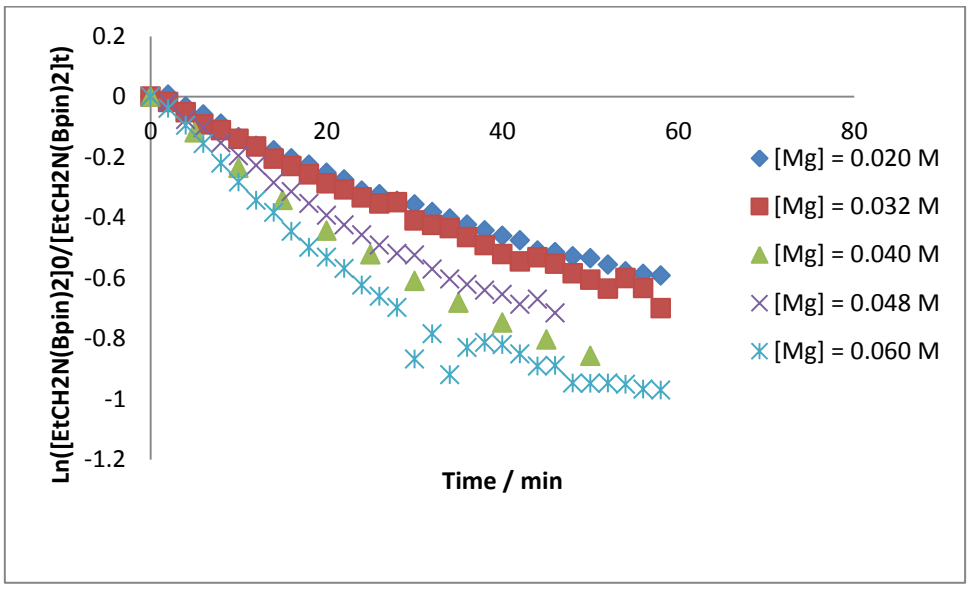


**Figure S15**. 1/[$EtCH_2N(Bpin)_2$] vs time; non-linear kinetics

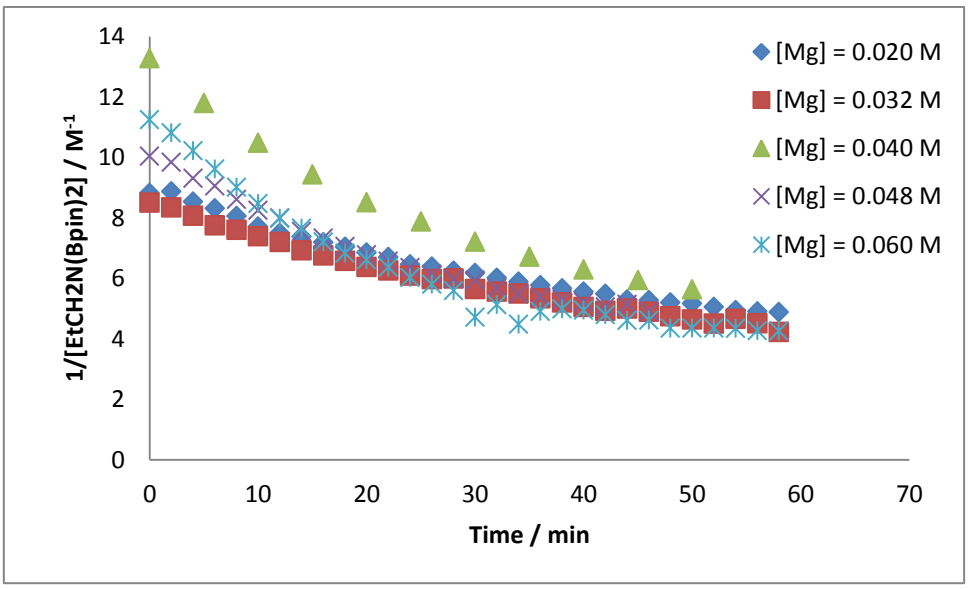

**Figure S16.** [Mg] vs $k_{obs}$; non-linear

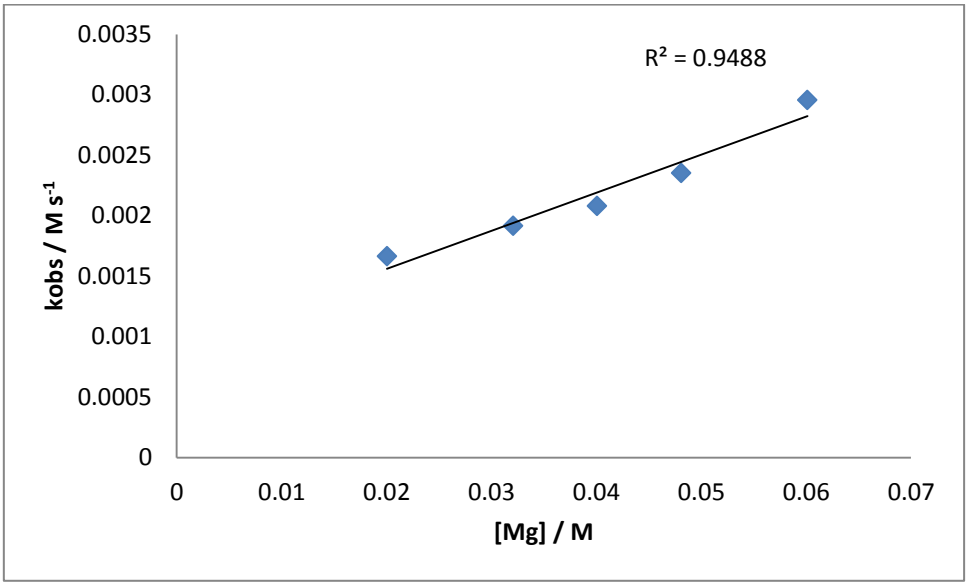


**Figure S17.** $[Mg]^2$ vs $k_{obs}$

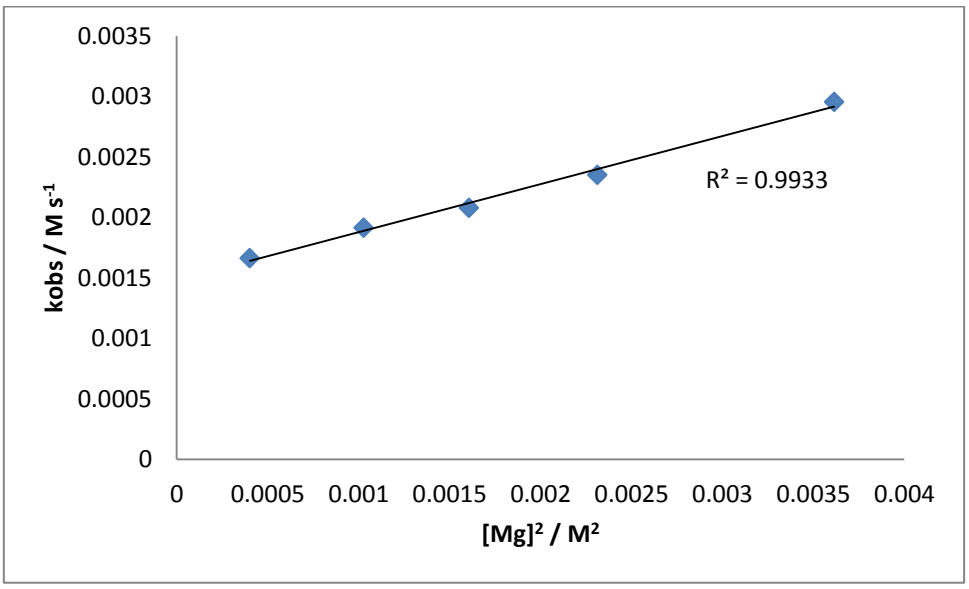


| | Value | Error |
|---|---|---|
| $m_1$ | 0.001481 | 0.000040 |
| $m_2$ | 0.397084 | 0.018813 |
| Chisq | 0.002838 | n/a |
| $R^2$ | 0.993311 | n/a |

**Figure S18.** $[Mg]^3$ vs $k_{obs}$

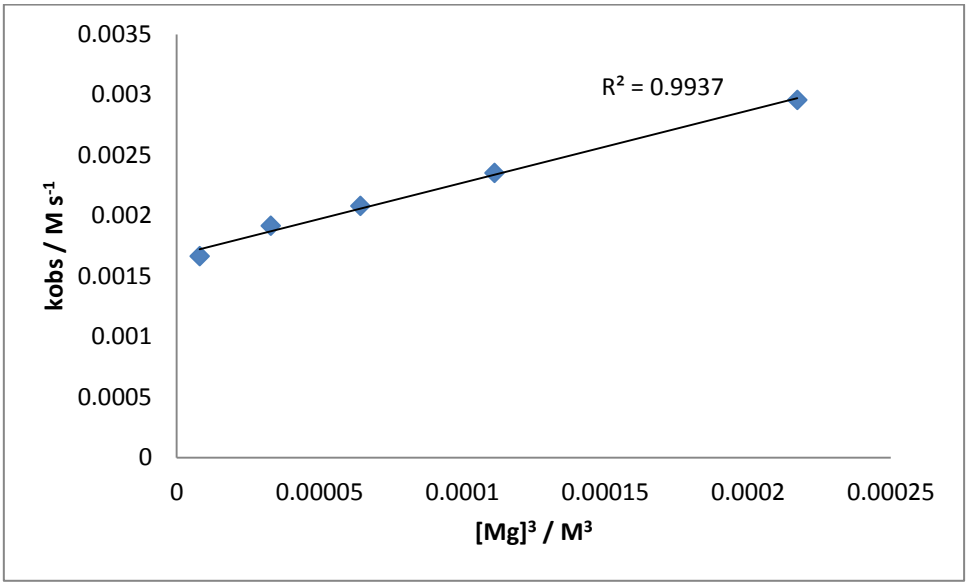


| | Value | Error |
|---|---|---|
| $m_1$ | 0.001675 | 0.000031 |
| $m_2$ | 5.965861 | 0.273449 |
| Chisq | 0.017854 | n/a |
| $R^2$ | 0.993737 | n/a |

## Variable [Mg] under *pseudo*-first order in [EtCN]

**Figure S19.** $[EtCH_2N(Bpin)_2]$ vs time; variable [Mg] under *pseudo*-first order in [EtCN] (4.0M) whilst keeping [HBpin] (0.8 M) invariant

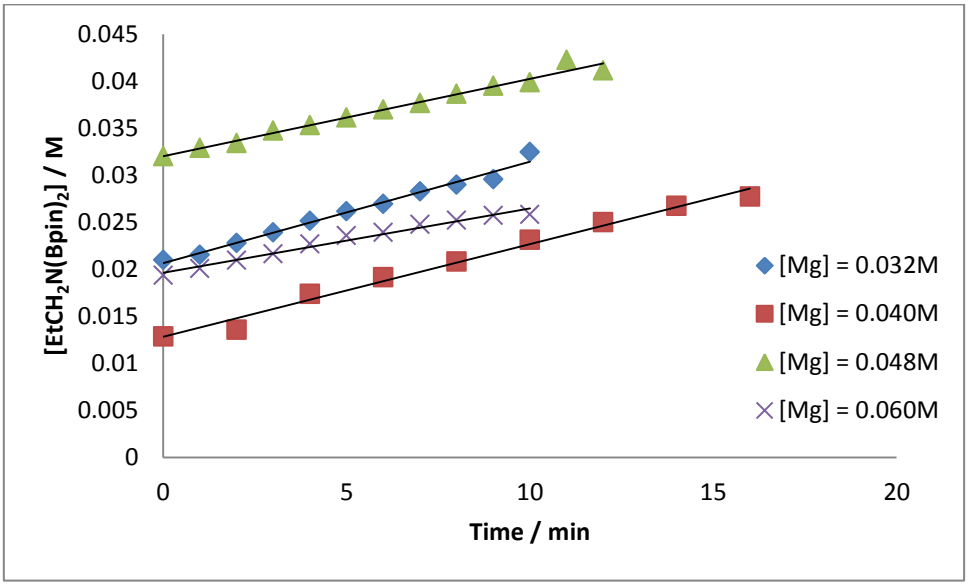

| | [Mg] = 0.032M | |
|---|---|---|
| | Value | Error |
| $m_1$ | 0.020662 | 0.000261 |
| $m_2$ | 0.001077 | 0.000044 |
| Chisq | 0.007186 | n/a |
| $R^2$ | 0.985102 | n/a |

| | [Mg] = 0.040M | |
|---|---|---|
| | Value | Error |
| $m_1$ | 0.012806 | 0.000411 |
| $m_2$ | 0.000985 | 0.000043 |
| Chisq | 3.5E-05 | n/a |
| $R^2$ | 0.986742 | n/a |

| | [Mg] = 0.048M | |
|---|---|---|
| | Value | Error |
| $m_1$ | 0.032003 | 0.000238 |
| $m_2$ | 0.000825 | 0.000034 |
| Chisq | 3.97E-05 | n/a |
| $R^2$ | 0.981993 | n/a |

| | [Mg] = 0.060M | |
|---|---|---|
| | Value | Error |
| $m_1$ | 0.019622 | 0.000198 |
| $m_2$ | 0.000684 | 0.000034 |
| Chisq | 0.019062 | n/a |
| $R^2$ | 0.978871 | n/a |

**Figure S20.** $\ln([EtCH_2N(Bpin)_2]_0/[EtCH_2N(Bpin)_2]_t)$ vs time; non-linear kinetics

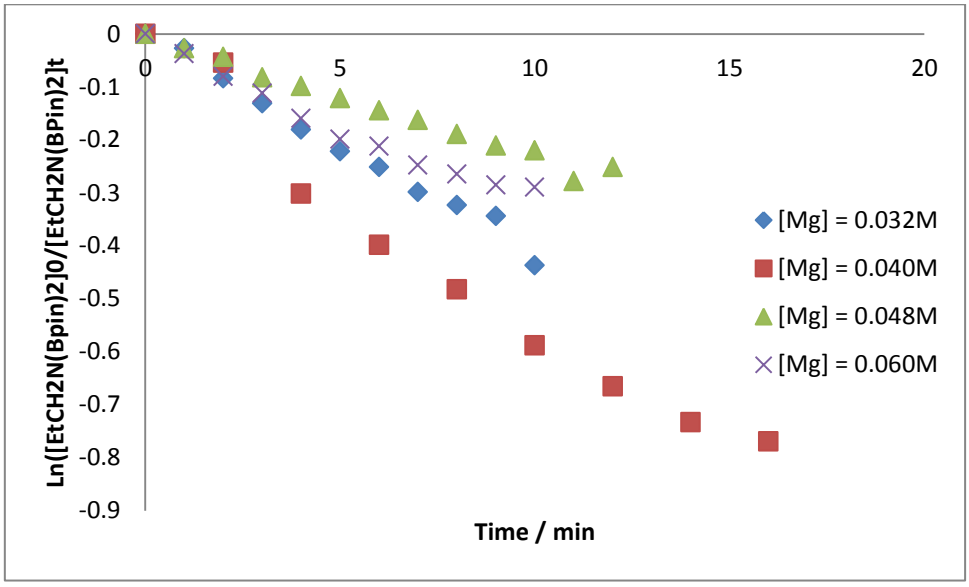


**Figure S21.** $1/[EtCH_2N(Bpin)_2]$ vs time; non-linear kinetics

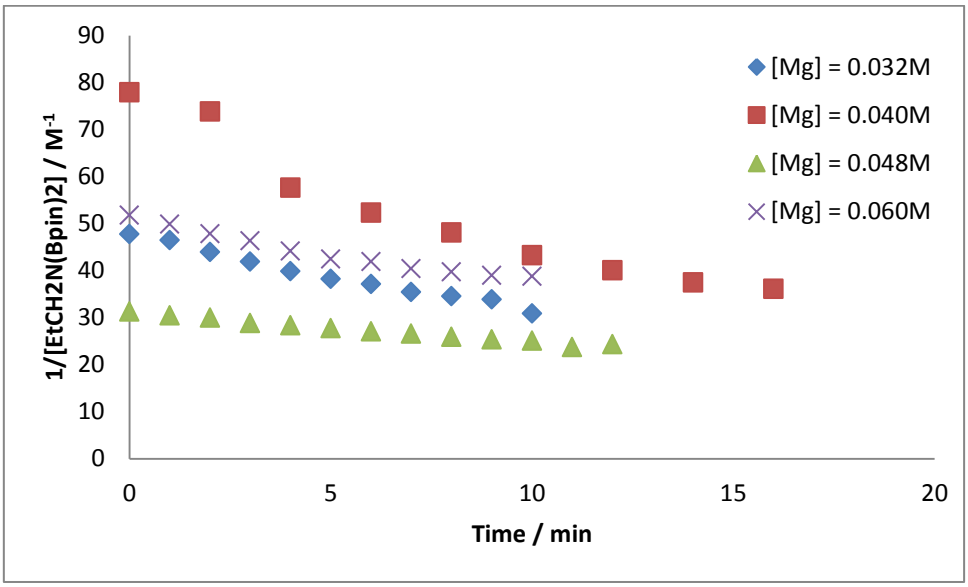

**Figure S22.** [Mg] vs $k_{obs}$ ; indicates 1st order dependence on [Mg]

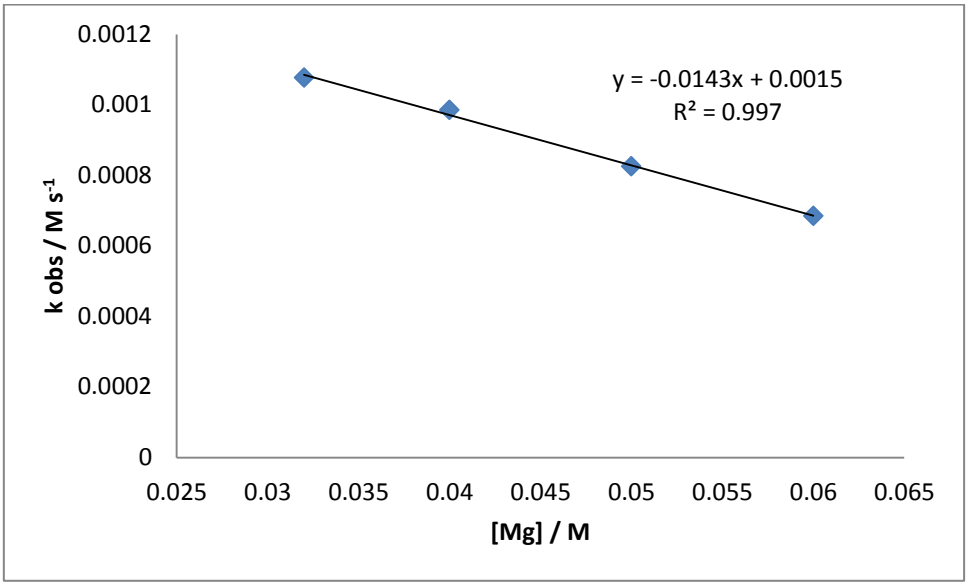


| | Value | Error |
|---|---|---|
| $m_1$ | 0.001543 | 0.000026 |
| $m_2$ | -0.014281 | 0.000558 |
| Chisq | 0.003582 | n/a |
| $R^2$ | 0.996957 | n/a |

## Variable [EtCN] approaching 2:1 reaction stoichiometry

**Figure S23.** [$EtCH_2N(Bpin)_2$] vs time; variable [EtCN] whilst keeping [Mg] = 0.04M and [HBpin] = 0.84M

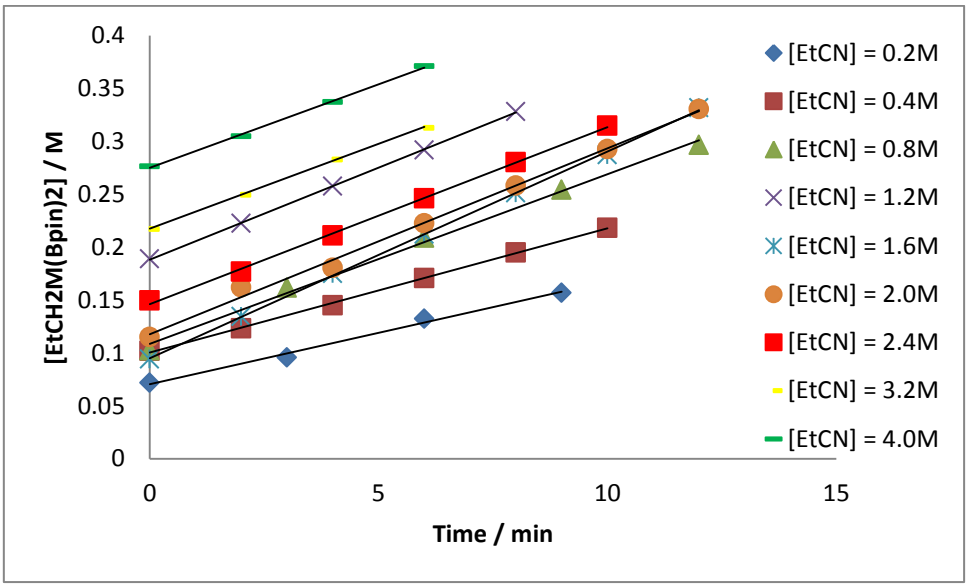

| | [EtCN] = 0.2M | |
|---|---|---|
| | Value | Error |
| $m_1$ | 0.070346 | 0.003208 |
| $m_2$ | 0.009723 | 0.000572 |
| Chisq | 0.00172655 | n/a |
| $R^2$ | 0.993134 | n/a |

| | [EtCN] = 0.4M | |
|---|---|---|
| | Value | Error |
| $m_1$ | 0.101748 | 0.001263 |
| $m_2$ | 0.011449 | 0.000118 |
| Chisq | 2.398E-06 | n/a |
| $R^2$ | 0.999147 | n/a |

| | [EtCN] = 0.8M | |
|---|---|---|
| | Value | Error |
| $m_1$ | 0.108361 | 0.010890 |
| $m_2$ | 0.016036 | 0.000680 |
| Chisq | 0.0031748 | n/a |
| $R^2$ | 0.995617 | n/a |

| | [EtCN] = 1.2M | |
|---|---|---|
| | Value | Error |
| $m_1$ | 0.188108 | 0.000651 |
| $m_2$ | 0.017388 | 0.000133 |
| Chisq | 0.00023175 | n/a |
| $R^2$ | 0.999825 | n/a |

| | [EtCN] = 1.6M | |
|---|---|---|
| | Value | Error |
| $m_1$ | 0.094968 | 0.001308 |
| $m_2$ | 0.019539 | 0.000181 |
| Chisq | 9.846E-05 | n/a |
| $R^2$ | 0.999569 | n/a |

| | [EtCN] = 2.0M | |
|---|---|---|
| | Value | Error |
| $m_1$ | 0.117474 | 0.003765 |
| $m_2$ | 0.017587 | 0.000522 |
| Chisq | 0.0012035 | n/a |
| $R^2$ | 0.995613 | n/a |

| | [EtCN] = 2.4M | |
|---|---|---|
| | Value | Error |
| $m_1$ | 0.146617 | 0.001870 |
| $m_2$ | 0.016518 | 0.000309 |
| Chisq | 0.00276225 | n/a |
| $R^2$ | 0.997931 | n/a |

| | [EtCN] = 3.2M | |
|---|---|---|
| | Value | Error |
| $m_1$ | 0.217298 | 0.000913 |
| $m_2$ | 0.016029 | 0.000244 |
| Chisq | 7.272E-05 | n/a |
| $R^2$ | 0.999536 | n/a |

| | [EtCN] = 4.0M | |
|---|---|---|
| | Value | Error |
| $m_1$ | 0.274767 | 0.001674 |
| $m_2$ | 0.015817 | 0.000448 |
| Chisq | 0.0018655 | n/a |
| $R^2$ | 0.998402 | n/a |

**Figure S24.** $\ln([EtCH_2N(Bpin)_2]_0/[EtCH_2N(Bpin)_2]_t)$ vs time; non-linear kinetics

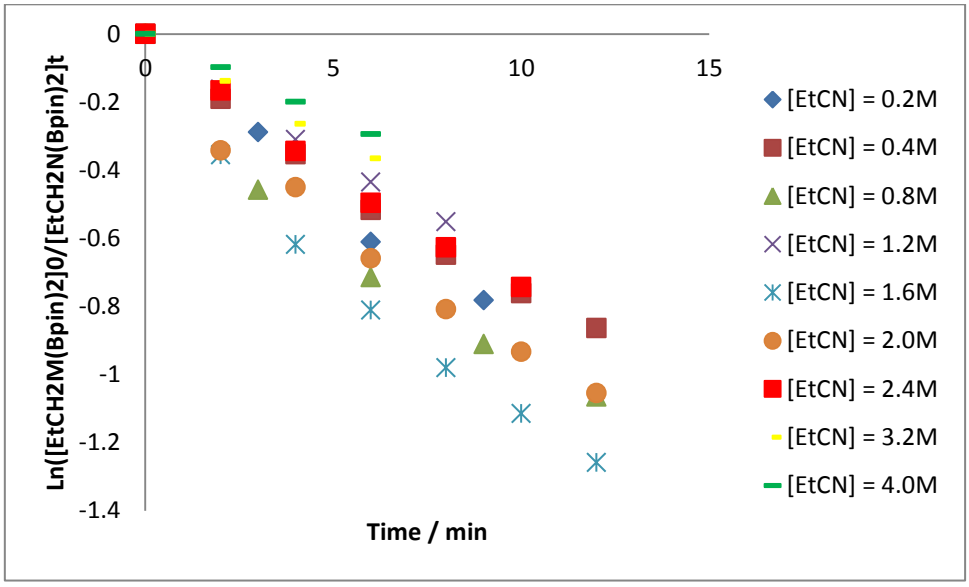

**Figure S25.** 1/[$EtCH_2N(Bpin)_2$] vs time; non-linear kinetics

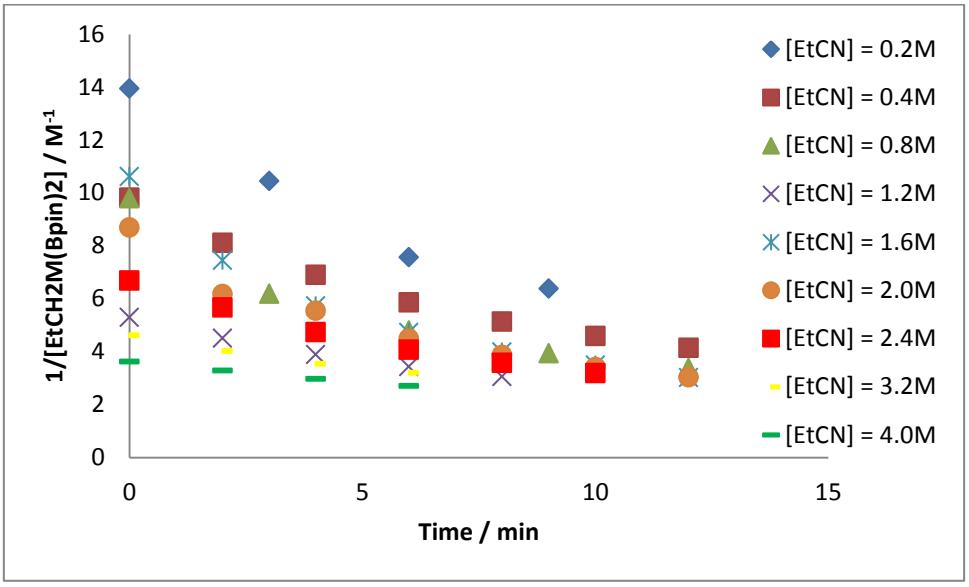


**Figure S26.** [EtCN] vs $k_{obs}$; indicating variable dependence on [EtCN] upon rate of reaction

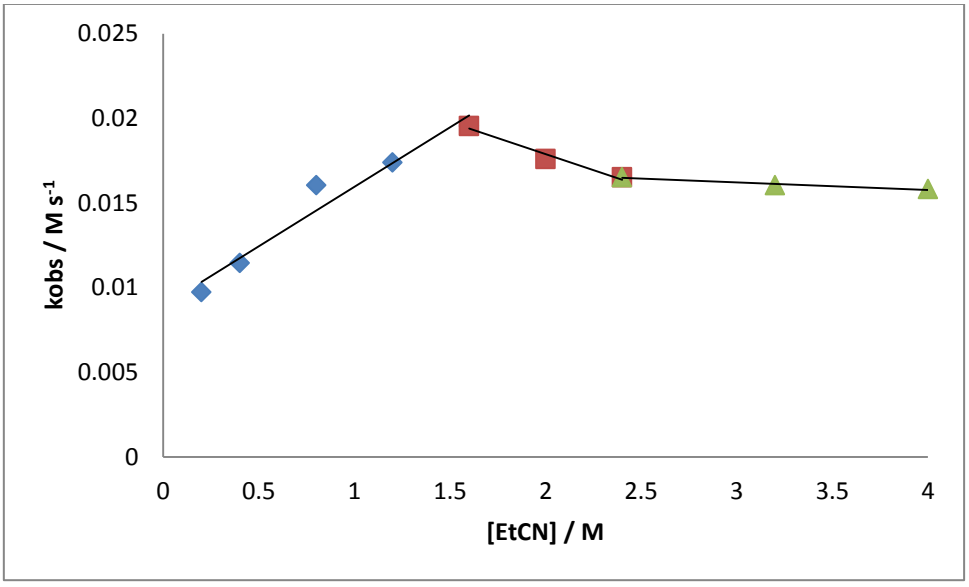


| | [EtCN] = 0.2 – 1.6M | |
|---|---|---|
| | Value | Error |
| $m_1$ | 0.008930 | 0.000868 |
| $m_2$ | 0.007020 | 0.000883 |
| Chisq | 0.02757781 | n/a |
| $R^2$ | 0.95470 | n/a |

| | [EtCN] = 1.6 – 2.4M | |
|---|---|---|
| | Value | Error |
| $m_1$ | 0.025434 | 0.001291 |
| $m_2$ | -0.003776 | 0.000637 |
| Chisq | 0.0137380 | n/a |
| $R^2$ | 0.9592 | n/a |

| | [EtCN] = 2.4 – 4.0M | |
|---|---|---|
| | Value | Error |
| $m_1$ | 0.017523 | 0.000326 |
| $m_2$ | -0.000438 | 0.000100 |
| Chisq | 0.0247721 | n/a |
| $R^2$ | 0.9262 | n/a |

## Variable [HBpin] approaching 2:1 reaction stoichiometry

**Figure S27.** [$EtCH_2N(Bpin)_2$] vs time for variable [HBpin] whilst keeping [Mg] = 0.04M and [EtCN] = 0.4M

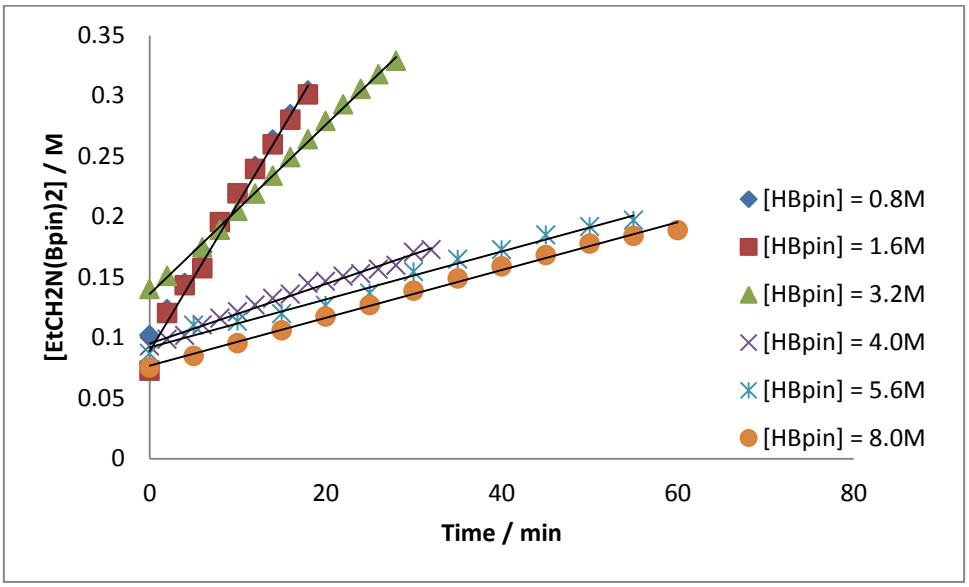


| | [HBpin] = 0.8M | |
|---|---|---|
| | Value | Error |
| $m_1$ | 0.101748 | 0.001263 |
| $m_2$ | 0.011449 | 0.000118 |
| Chisq | 2.3979E-06 | n/a |
| $R^2$ | 0.999147 | n/a |

| | [HBpin] = 1.6M | |
|---|---|---|
| | Value | Error |
| $m_1$ | 0.090523 | 0.004952 |
| $m_2$ | 0.011946 | 0.000419 |
| Chisq | 0.0561306 | n/a |
| $R^2$ | 0.989071 | n/a |

| | [HBpin] = 3.2M | |
|---|---|---|
| | Value | Error |
| $m_1$ | 0.136191 | 0.001343 |
| $m_2$ | 0.007001 | 0.000079 |
| Chisq | 0.0039901 | n/a |
| $R^2$ | 0.998473 | n/a |

| | [HBpin] = 4.0M | |
|---|---|---|
| | Value | Error |
| $m_1$ | 0.095307 | 0.098612 |
| $m_2$ | 0.002462 | 0.000767 |
| Chisq | 7.5365E-06 | n/a |
| $R^2$ | 0.989688 | n/a |

| | [HBpin] = 5.6M | |
|---|---|---|
| | Value | Error |
| $m_1$ | 0.091912 | 0.002417 |
| $m_2$ | 0.001987 | 0.000074 |
| Chisq | 0.0205431 | n/a |
| $R^2$ | 0.986156 | n/a |

| | [HBpin] = 8.0M | |
|---|---|---|
| | Value | Error |
| $m_1$ | 0.076936 | 0.001491 |
| $m_2$ | 0.001976 | 0.000042 |
| Chisq | 0.0020196 | n/a |
| $R^2$ | 0.995011 | n/a |

**Figure S28**. ln([$EtCH_2N(Bpin)_2$]$_0$/[$EtCH_2N(Bpin)_2$]$_t$) vs time; non-linear kinetics

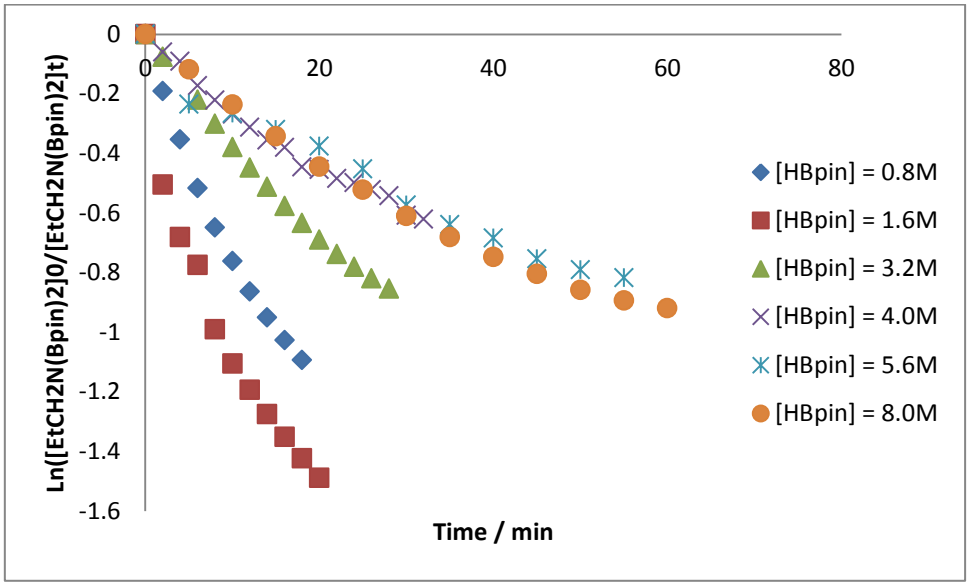


**Figure S29**. 1/[$EtCH_2N(Bpin)_2$] vs time; non-linear kinetics

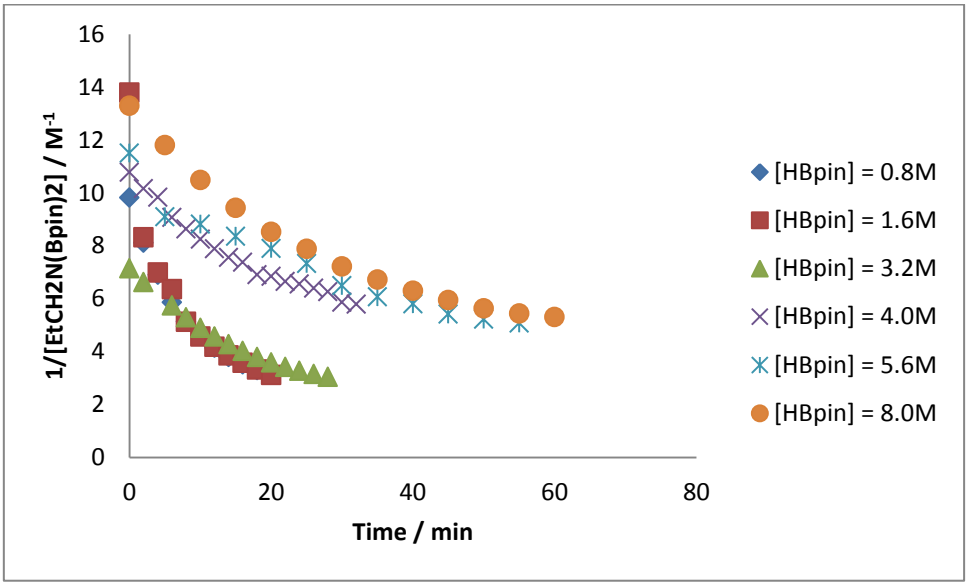

**Figure S30.** [HBpin] vs $k_{obs}$; indicates a variable dependence upon rate of reaction with changing [HBpin]

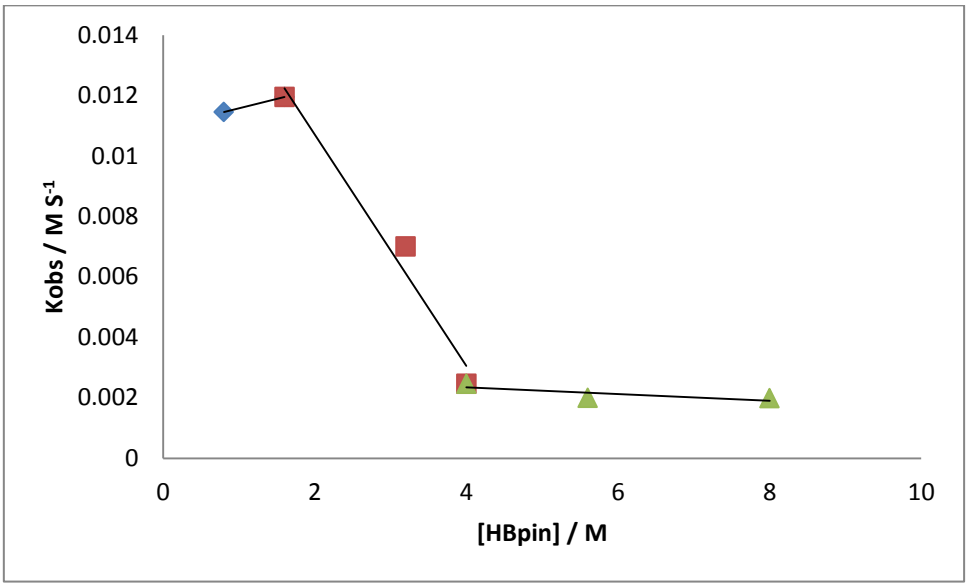


| | [HBpin] = 1.6 – 4.0M | |
|---|---|---|
| | Value | Error |
| $m_1$ | 0.018367 | 0.001980 |
| $m_2$ | -0.003829 | 0.000639 |
| Chisq | 0.0057859 | n/a |
| $R^2$ | 0.972887 | n/a |

| | [HBpin] = 4.0-8.0M | |
|---|---|---|
| | Value | Error |
| $m_1$ | 0.002800 | 0.000487 |
| $m_2$ | -0.000112 | 0.000080 |
| Chisq | 0.2357439 | n/a |
| $R^2$ | 0.99847 | n/a |

## Variable Temperature Studies

**Figure S31.** [EtCN] vs time; variable temperature

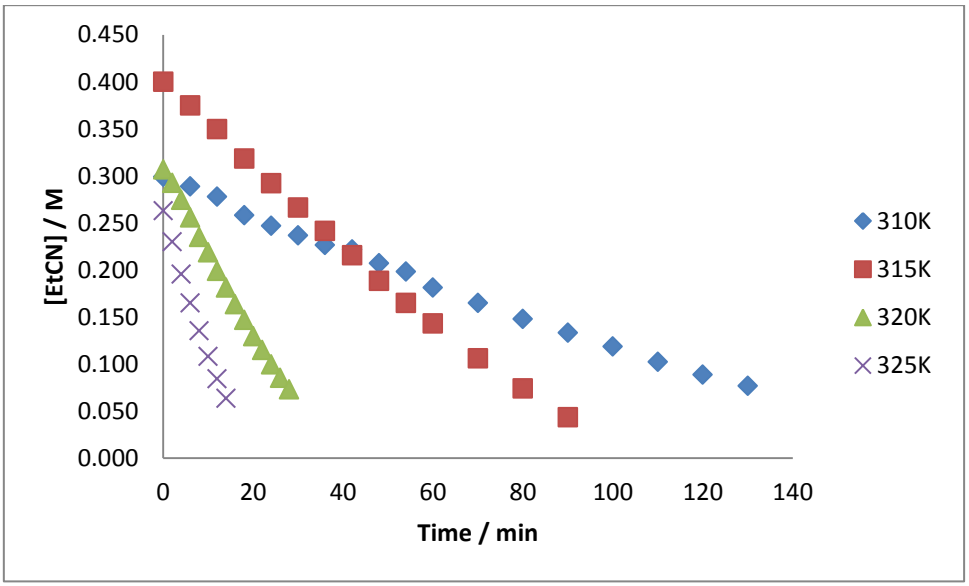

| | T = 310 K | |
|---|---|---|
| | Value | Error |
| $m_1$ | 0.293231 | 0.006892 |
| $m_2$ | -0.001765 | 0.000097 |
| Chisq | 0.007775 | n/a |
| $R^2$ | 0.995548 | n/a |

| | T = 315 K | |
|---|---|---|
| | Value | Error |
| $m_1$ | 0.391690 | 0.003811 |
| $m_2$ | -0.004048 | 0.000078 |
| Chisq | 0.005843 | n/a |
| $R^2$ | 0.995542 | n/a |

| | T = 320 K | |
|---|---|---|
| | Value | Error |
| $m_1$ | 0.305263 | 0.001915 |
| $m_2$ | -0.008599 | 0.000116 |
| Chisq | 0.000411 | n/a |
| $R^2$ | 0.997624 | n/a |

| | T = 325 k | |
|---|---|---|
| | Value | Error |
| $m_1$ | 0.256095 | 0.003864 |
| $m_2$ | -0.014385 | 0.000462 |
| Chisq | 0.010242 | n/a |
| $R^2$ | 0.993854 | n/a |

**Figure S32.** $\ln([EtCN]_0/[EtCN]_t)$ vs time; non-linear kinetics

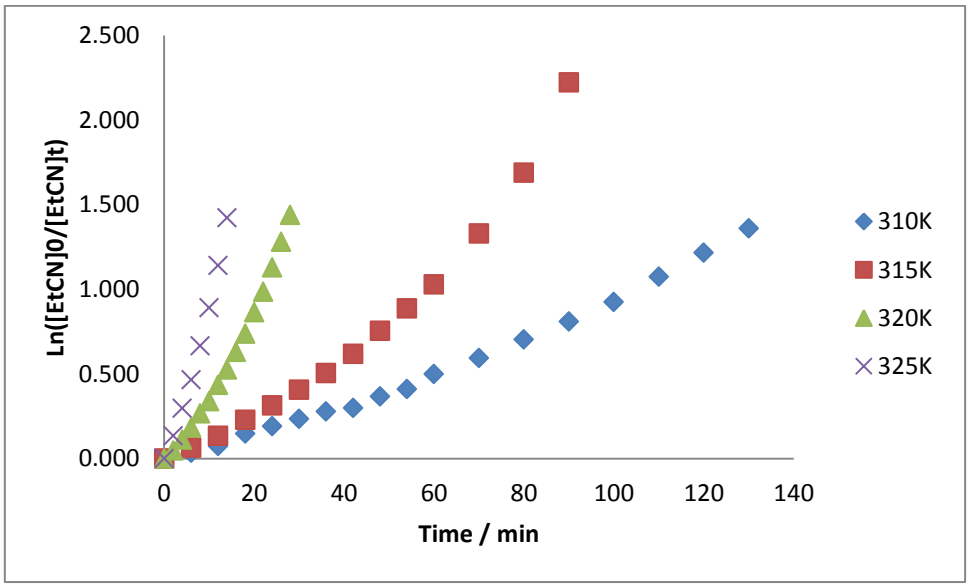


**Figure S33.** 1/[EtCN] vs time; non-linear kinetics

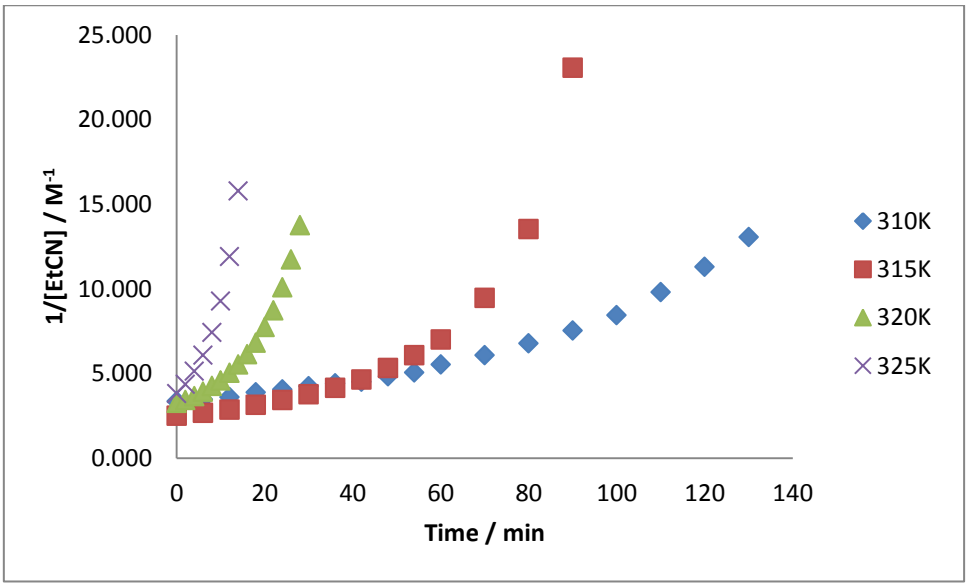

**Figure S34.** Eyring Plot – Ln(k/T) vs 1/T

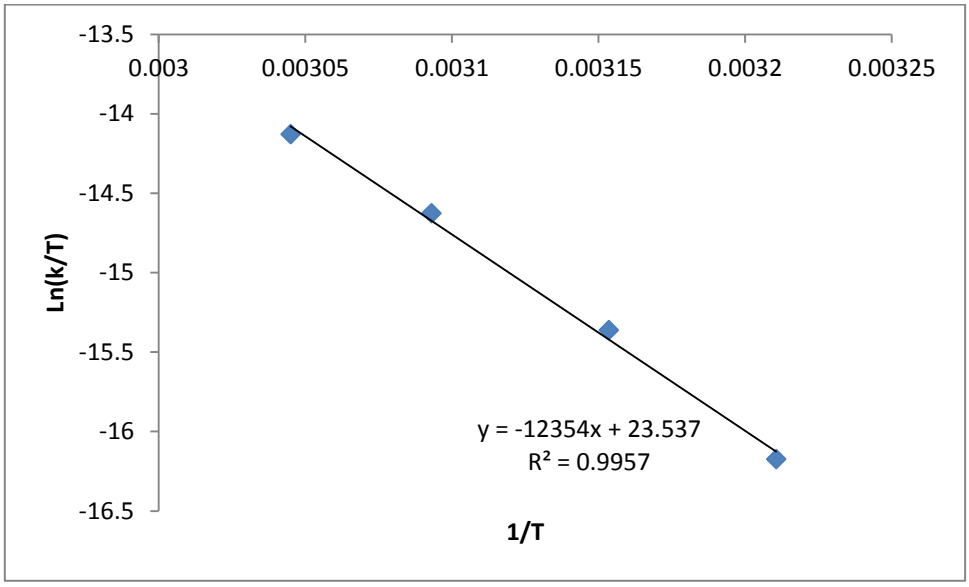


| | Value | Error |
|---|---|---|
| $m_1$ | 23.537 | 1.790 |
| $m_2$ | -12354 | 572.60 |
| Chisq | 0.00398094 | n/a |
| $R^2$ | 0.9957 | n/a |

This graph was used to calculate the following Activation Energy Parameters, least square error analysis was also carried to provide accurate error information.

| | Value | Error |
|---|---|---|
| ΔH | 102.71 kJ $mol^{-1}$ | ± 4.76 |
| ΔS | -1.85 J $k^{-1}$ $mol^{-1}$ | ± 14.88 |

**Figure S35**. Arrhenius Plot - Ln(k) vs 1/T

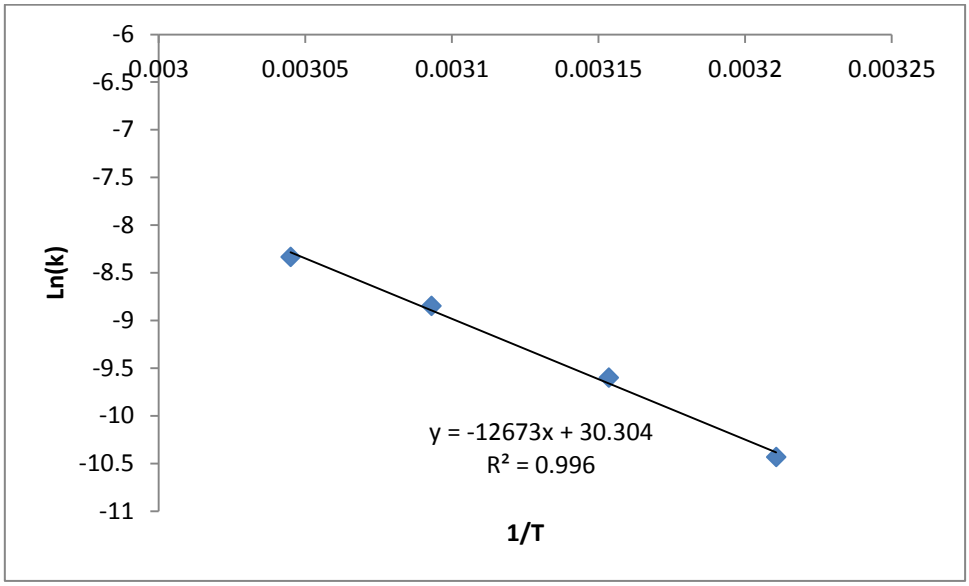

| | Value | Error |
|---|---|---|
| $m_1$ | 30.304 | 1.785 |
| $m_2$ | -12673 | 570.876 |
| Chisq | 0.004023456 | n/a |
| $R^2$ | 0.9960 | n/a |

This graph was used to calculate the following Activation Energy Parameter; least square error analysis was also carried to provide accurate error information.

| | Value | Error |
|---|---|---|
| Ea | 105.36 kJ $mol^{-1}$ | ± 4.75 |

# Aryl Nitrile Kinetics

## Hammett plot

Standard reaction used of 10 mg (0.02 mmol, ie. 10 mol%) of LMgBu was dissolved in 0.5 ml of $C_6D_6$, 60.9 µL (0.42 mmol) of pinacolborane was then added followed by 0.2 mmol of Nitrile. $^1H$ NMR spectra were collected at consistent intervals until reaction reached the desired 3 half-lives (80 % product conversion). Reaction was carried out with 8 different aryl substituted nitriles: 4-methoxybenzonitrile, para-tolunitrile, meta-tolunitrile, 3-methoxybenzonitrile, 3-Fluorobenzonitrile, 4-Chlorobenzonitrile, 4-(trifluoromethyl)benzonitrile, and benzonitrile. All reactions were carried out at 323 K.

**Figure S36.** [ArCN] vs time; non-linear kinetics

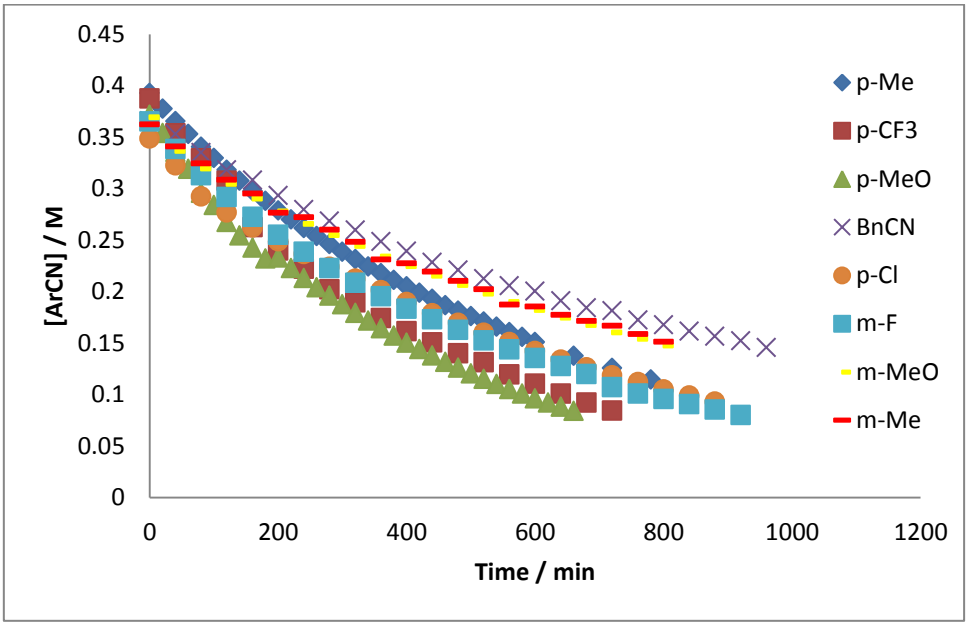

**Figure S37.** ln([ArCN]$_0$/[ArCN]$_t$) vs time for a series of different aryl nitriles

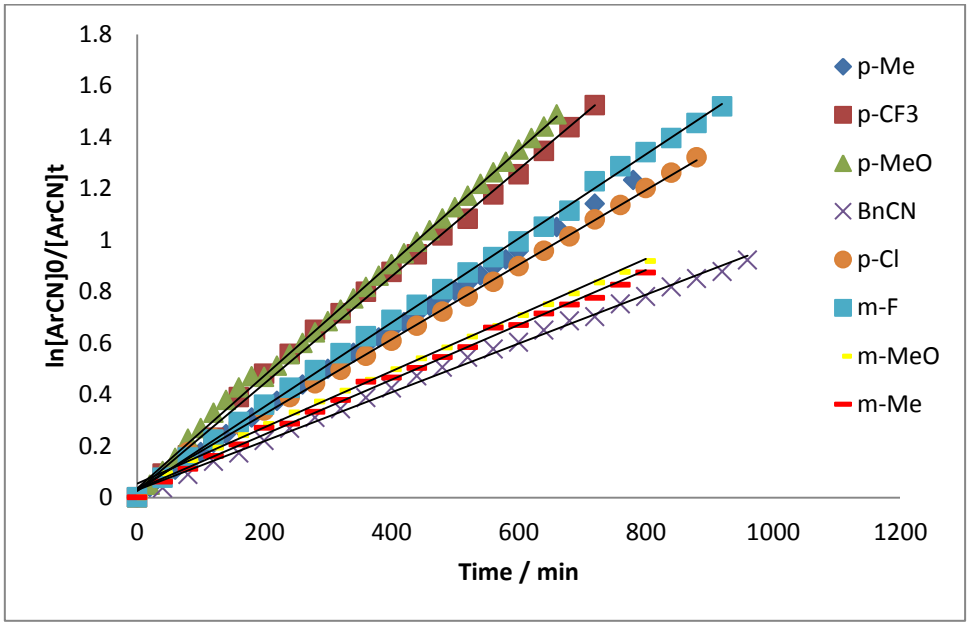


| | p-Me | |
|---|---|---|
| | Value | Error |
| $m_1$ | 0.021810 | 0.002473 |
| $m_2$ | 0.001560 | 0.000006 |
| Chisq | 0.004459 | n/a |
| $R^2$ | 0.99949 | n/a |

| | p-CF$_3$ | |
|---|---|---|
| | Value | Error |
| $m_1$ | 0.027300 | 0.011683 |
| $m_2$ | 0.002080 | 0.000028 |
| Chisq | 0.003583 | n/a |
| $R^2$ | 0.99699 | n/a |

| | p-MeO | |
|---|---|---|
| | Value | Error |
| $m_1$ | 0.035330 | 0.005828 |
| $m_2$ | 0.002190 | 0.000015 |
| Chisq | 0.006753 | n/a |
| $R^2$ | 0.99846 | n/a |

| | BnCN | |
|---|---|---|
| | Value | Error |
| $m_1$ | 0.029425 | 0.006618 |
| $m_2$ | 0.000949 | 0.000012 |
| Chisq | 0.011518 | n/a |
| $R^2$ | 0.996445 | n/a |

| | m-F | |
|---|---|---|
| | Value | Error |
| $m_1$ | 0.019040 | 0.002459 |
| $m_2$ | 0.001360 | 0.000005 |
| Chisq | 0.002541 | n/a |
| $R^2$ | 0.99975 | n/a |

| | p-Cl | |
|---|---|---|
| | Value | Error |
| $m_1$ | -0.097600 | 0.005398 |
| $m_2$ | 0.048200 | 0.000011 |
| Chisq | 0.064175 | n/a |
| $R^2$ | 0.99890 | n/a |

| | m-MeO | |
|---|---|---|
| | Value | Error |
| $m_1$ | 0.054630 | 0.006236 |
| $m_2$ | 0.001090 | 0.000013 |
| Chisq | 0.042573 | n/a |
| $R^2$ | 0.99717 | n/a |

| | m-Me | |
|---|---|---|
| | Value | Error |
| $m_1$ | 0.032360 | 0.006857 |
| $m_2$ | 0.001060 | 0.000015 |
| Chisq | 0.015722 | n/a |
| $R^2$ | 0.99640 | n/a |

**Figure S38.** 1/[ArCN] vs time; non-linear kinetics

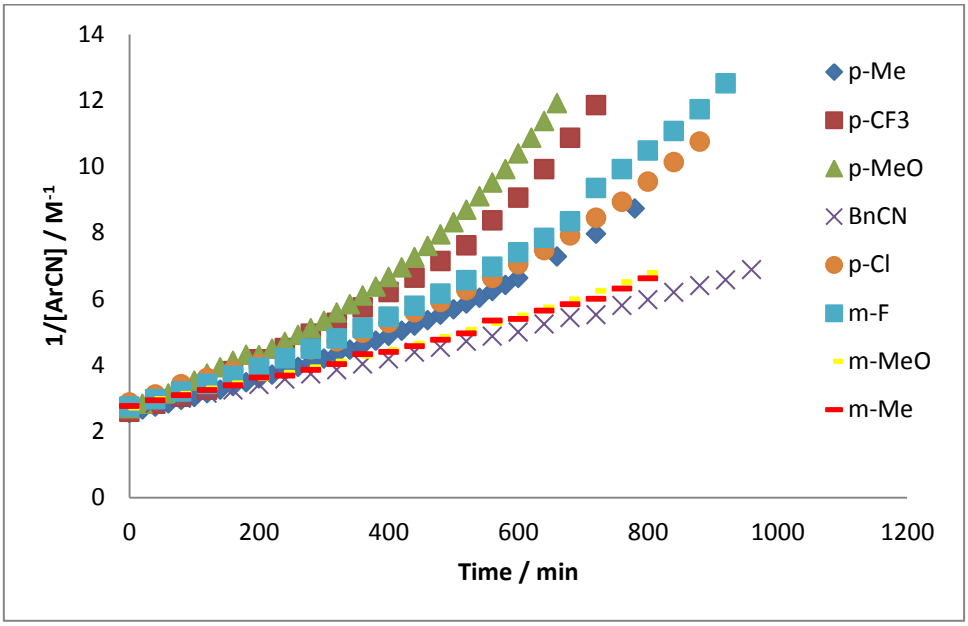


**Figure S39.** Hammett Plot; $k_{obs}$ taken from 1st order plots

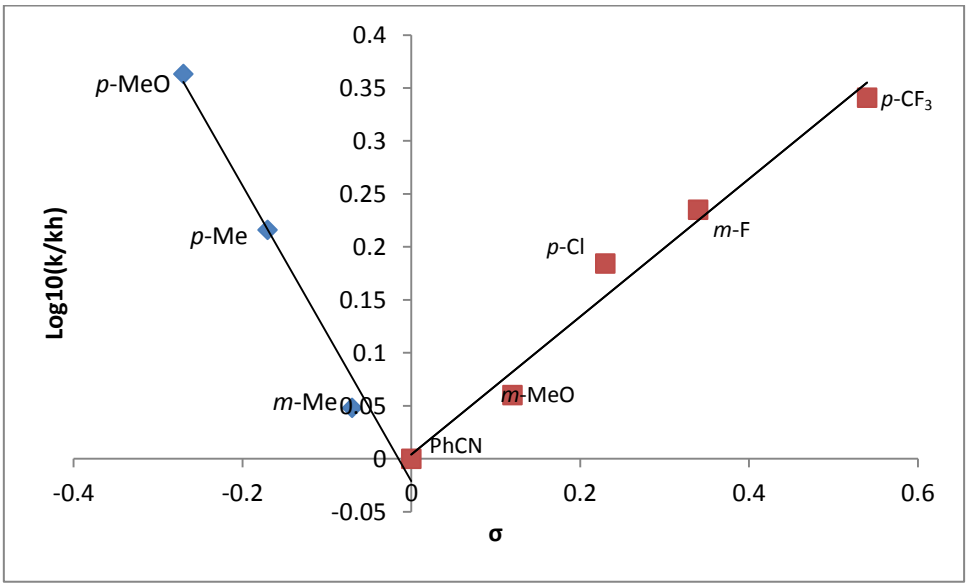


| | Electron Donating Groups (EDG) | |
|---|---|---|
| | Value | Error |
| $m_1$ | -0.021180 | 0.020524 |
| $m_2$ | -1.395670 | 0.125666 |
| Chisq | 0.021751 | n/a |
| $R^2$ | 0.98404 | n/a |

| | Electron Withdrawing Groups (EWG) | |
|---|---|---|
| | Value | Error |
| $m_1$ | 0.004090 | 0.017839 |
| $m_2$ | 0.650020 | 0.057909 |
| Chisq | 0.001125 | n/a |
| $R^2$ | 0.97674 | n/a |

| | **ρ value** |
|---|---|
| **Electron donating group (EDG)** | -1.40 |
| **Electron withdrawing group (EWG)** | +0.65 |

## Electron Donating Aryl nitrile (*p*-$MeOC_6H_4CN$)

### Determination of Catalyst order

**Figure S40.** [*p*-$MeOC_6H_4CN$] vs time; non-linear kinetics for 1:2 *p*-$MeOC_6H_4CN$:HBpin

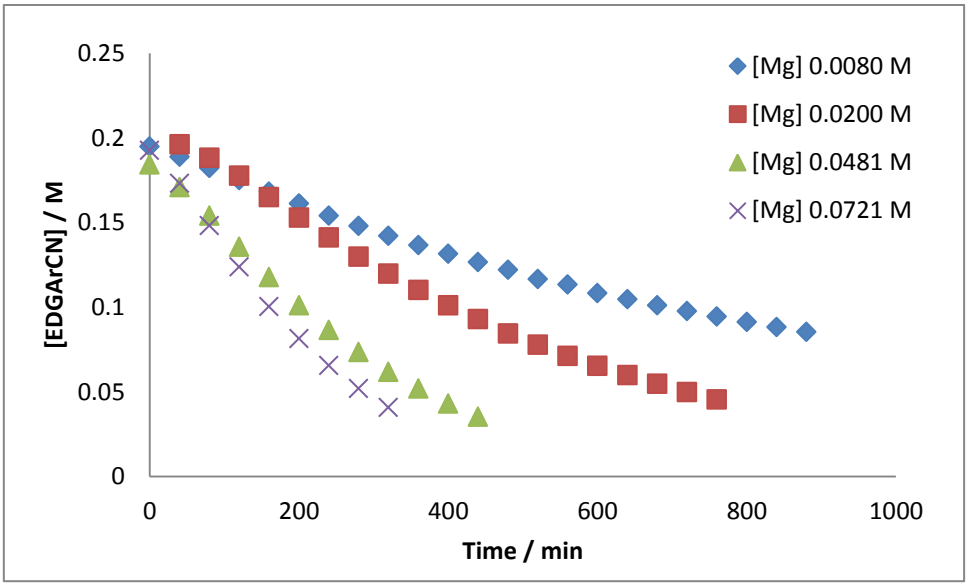


**Figure S41.** ln([*p*-$MeOC_6H_4CN$]$_0$/[p-$MeOC_6H_4CN$]$_t$) vs time for 1:2 *p*-$MeOC_6H_4CN$:HBpin

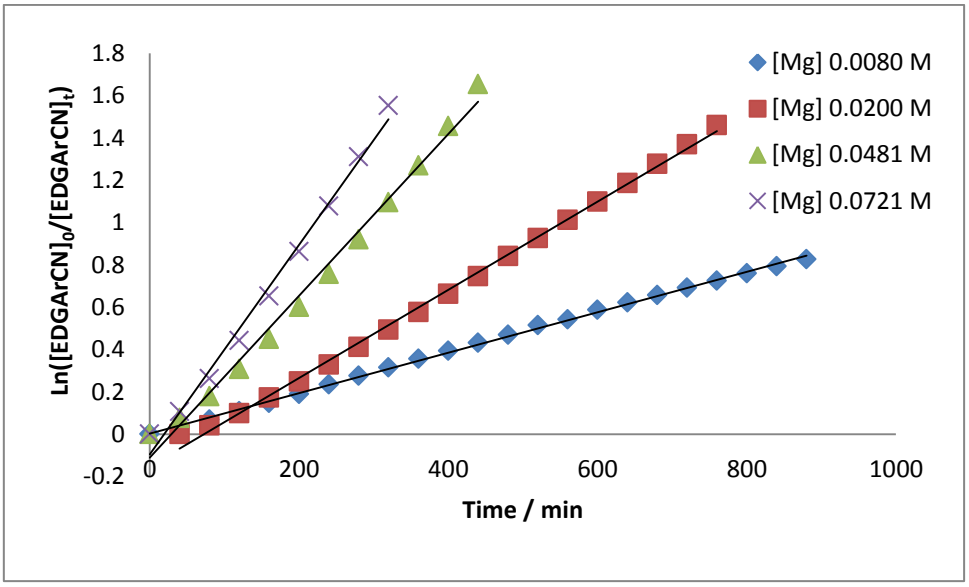


| | [Mg] 0.00802 M | |
|---|---|---|
| | Value | Error |
| $m_1$ | 0.002229 | 0.003687 |
| $m_2$ | 0.000957 | 0.000007 |
| Chisq | 7.7E-05 | n/a |
| $R^2$ | 0.998821 | n/a |

| | [Mg] 0.02004 M | |
|---|---|---|
| | Value | Error |
| $m_1$ | -0.071470 | 0.010574 |
| $m_2$ | 0.002100 | 0.000024 |
| Chisq | 0.021781 | n/a |
| $R^2$ | 0.99769 | n/a |

| | [Mg] 0.0481 M | |
|---|---|---|
| | Value | Error |
| $m_1$ | -0.110970 | 0.031377 |
| $m_2$ | 0.003820 | 0.000121 |
| Chisq | 0.043733 | n/a |
| $R^2$ | 0.99012 | n/a |

| | [Mg] 0.0721 M | |
|---|---|---|
| | Value | Error |
| $m_1$ | -0.095350 | 0.034113 |
| $m_2$ | 0.004950 | 0.000179 |
| Chisq | 0.034514 | n/a |
| $R^2$ | 0.99090 | n/a |

**Figure S42.** 1/[*p*-$MeOC_6H_4CN$] vs time; non-linear kinetics for 1:2 *p*-$MeOC_6H_4CN$:HBpin

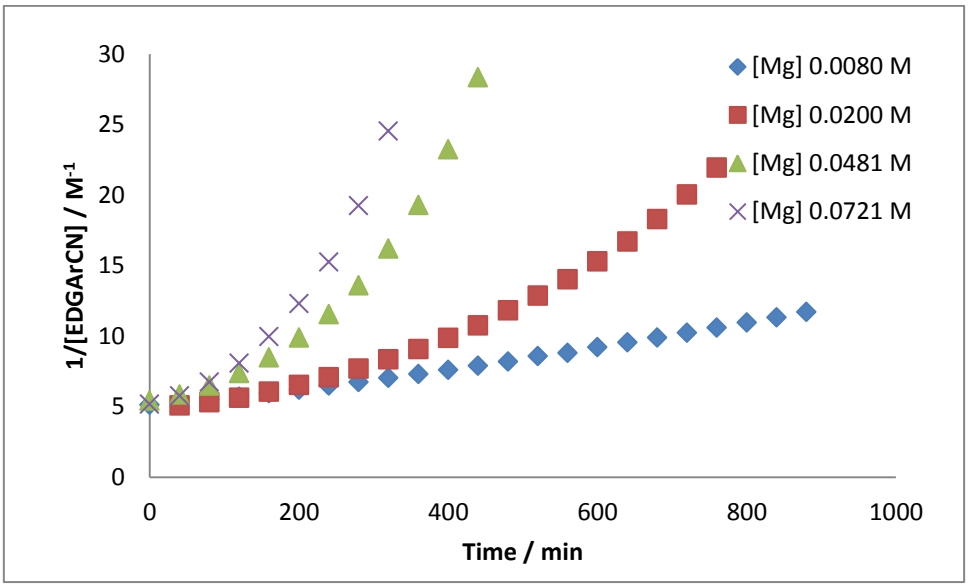


**Figure S43.** [Mg] vs $k_{obs}$; indicating a first order dependence on [Mg]

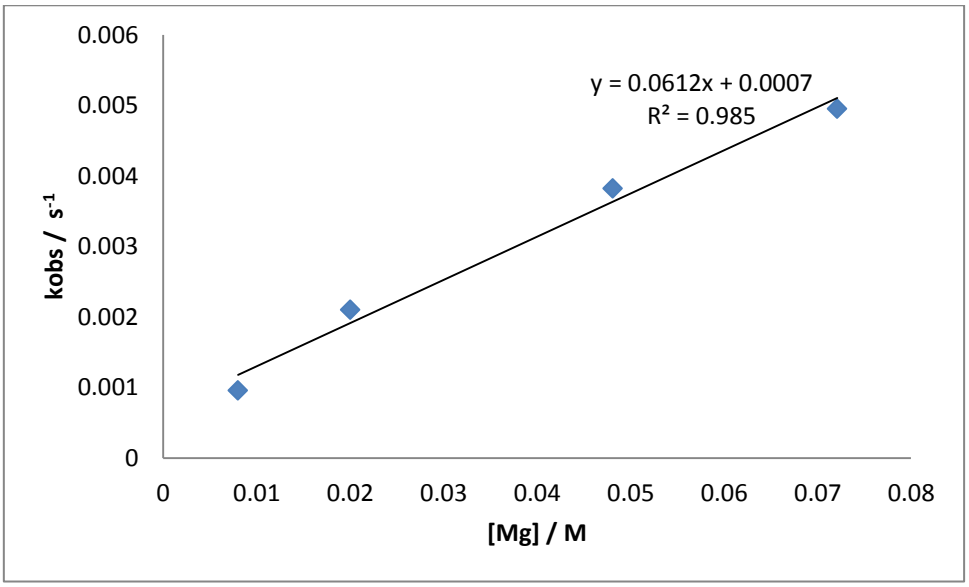


| | Value | Error |
|---|---|---|
| $m_1$ | 0.000688 | 0.000239 |
| $m_2$ | 0.061193 | 0.005354 |
| Chisq | 0.020769 | n/a |
| $R^2$ | 0.984918 | n/a |

## Determination of order in [*p*-MeOC$_6$H$_4$CN]

**Figure S44.** [*p*-MeOC$_6$H$_4$CH$_2$N(Bpin)$_2$] vs time; non-linear kinetics

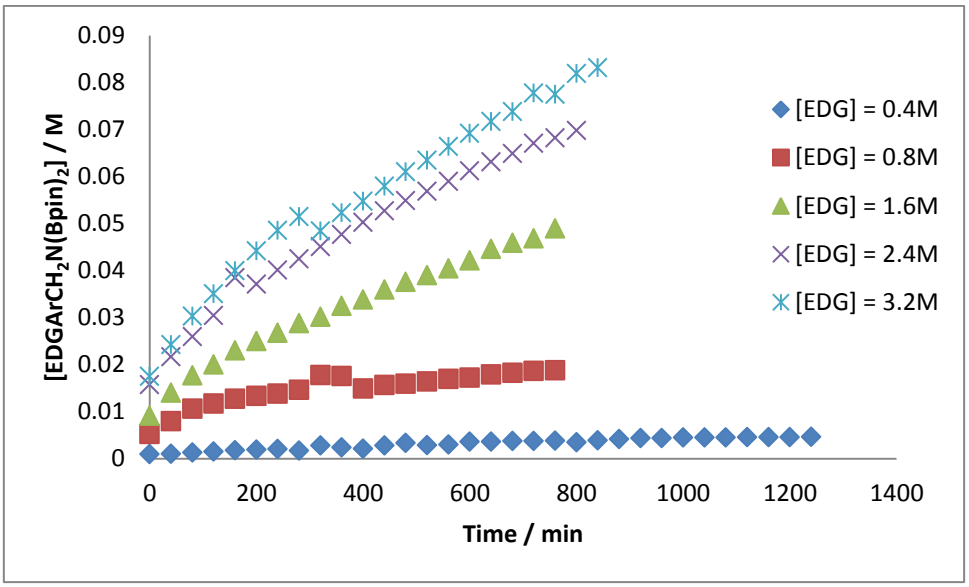


**Figure S45.** ln([*p*-MeOC$_6$H$_4$CH$_2$N(Bpin)$_2$]$_0$/[ *p*-MeOC$_6$H$_4$CH$_2$N(Bpin)$_2$]$_t$) vs time; non-linear kinetics

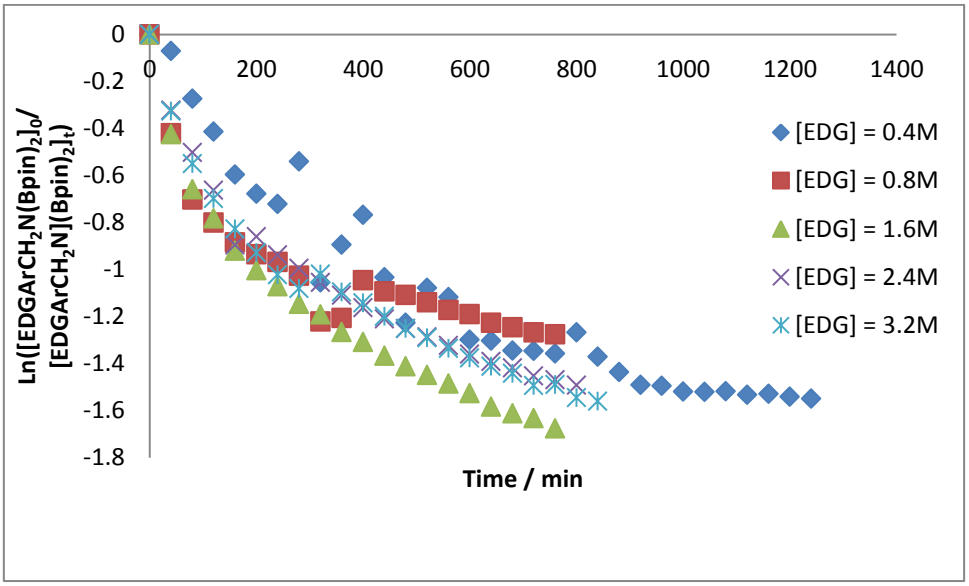

**Figure S46**. 1/[ *p*-MeOC$_6$H$_4$CH$_2$N(Bpin)$_2$] vs time; non-linear kinetics

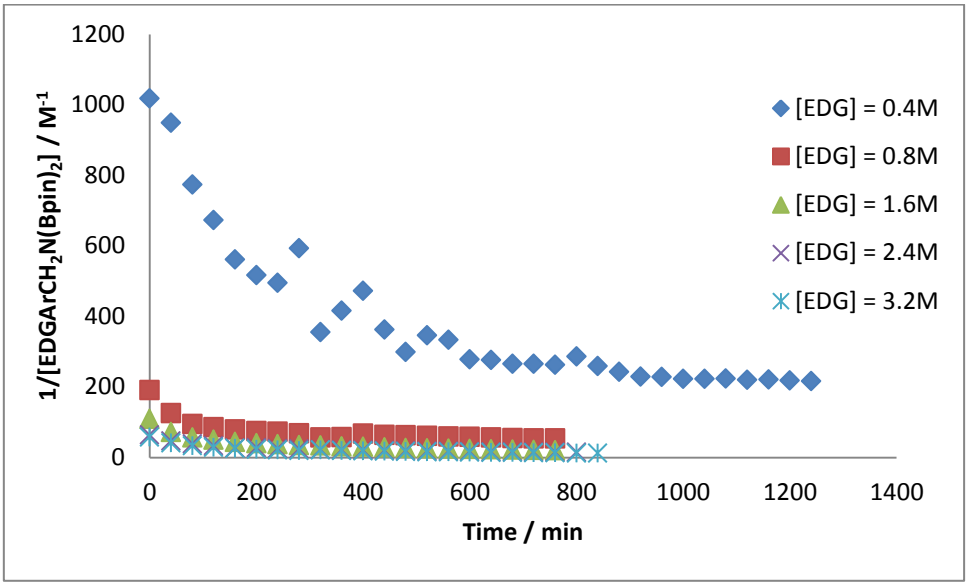


**Figure S47.** [*p*-MeOC$_6$H$_4$CH$_2$N(Bpin)$_2$]$^2$ vs time

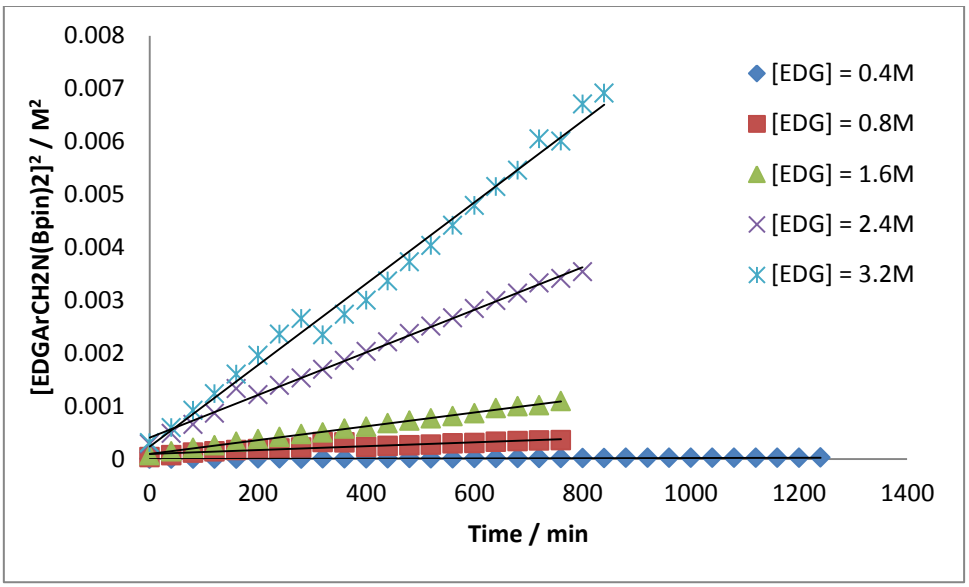


| | [EDG] = 0.4M | |
|---|---|---|
| | Value | Error |
| $m_1$ | 8.0000E-08 | 4.89E-07 |
| $m_2$ | 2.0000E-08 | 6.78E-10 |
| Chisq | 0.01609483 | n/a |
| $R^2$ | 0.961347 | n/a |

| | [EDG] = 0.8M | |
|---|---|---|
| | Value | Error |
| $m_1$ | 0.000102 | 3.018E-05 |
| $m_2$ | 0.000000 | 6.790E-08 |
| Chisq | 0.746088 | n/a |
| $R^2$ | 0.985122 | n/a |

| | [EDG] = 1.6M | |
|---|---|---|
| | Value | Error |
| $m_1$ | 0.000094 | 6.287E-06 |
| $m_2$ | 0.000001 | 1.414E-08 |
| Chisq | 0.007088 | n/a |
| $R^2$ | 0.997887 | n/a |

| | [EDG] = 2.4M | |
|---|---|---|
| | Value | Error |
| $m_1$ | 0.000401 | 3.360E-05 |
| $m_2$ | 0.000004 | 7.185E-08 |
| Chisq | 0.01585 | n/a |
| $R^2$ | 0.993990 | n/a |

| | [EDG] = 3.2M | |
|---|---|---|
| | Value | Error |
| $m_1$ | 0.000235 | 8.774E-05 |
| $m_2$ | 0.000008 | 1.788E-07 |
| Chisq | 0.001265 | n/a |
| $R^2$ | 0.98930136 | n/a |

**Figure S48**. [*p*-MeOC$_6$H$_4$CN] vs $k_{obs}$; non-linear fit

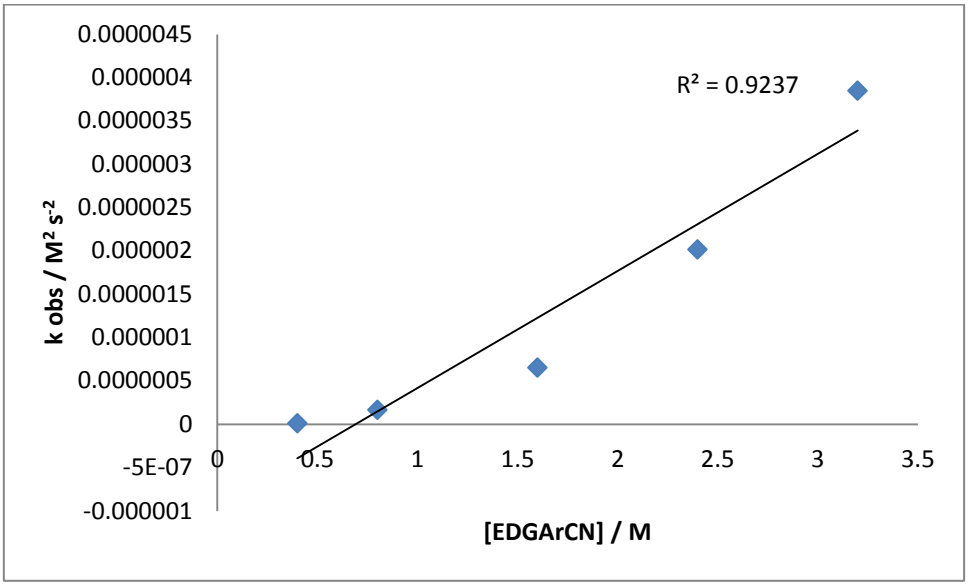


**Figure S49.** [*p*-MeOC$_6$H$_4$CN]$^{-1}$ vs $k_{obs}$; non-linear fit

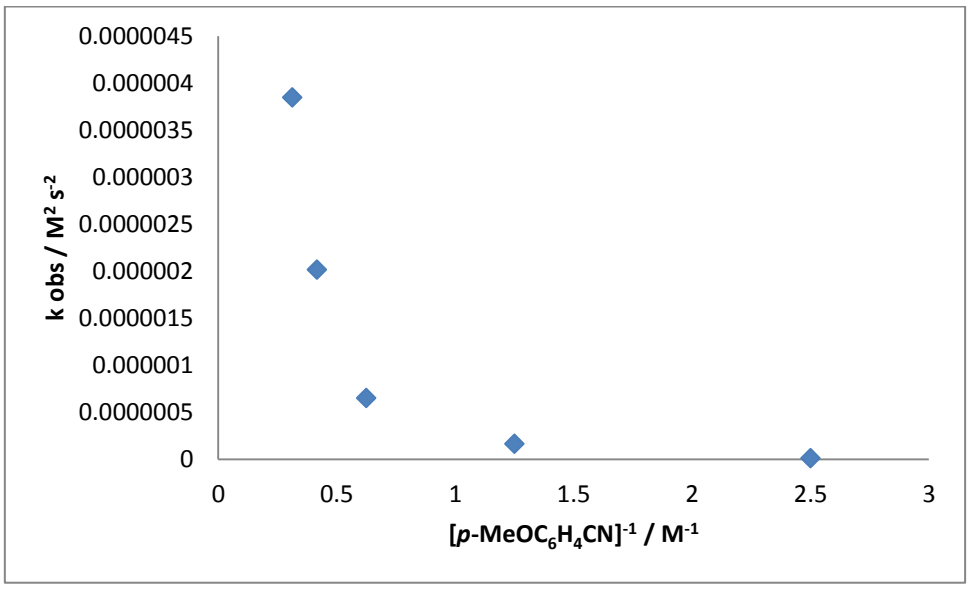

**Figure S50.** [*p*-MeOC$_6$H$_4$CN]$^{-1}$ vs $k_{obs}$

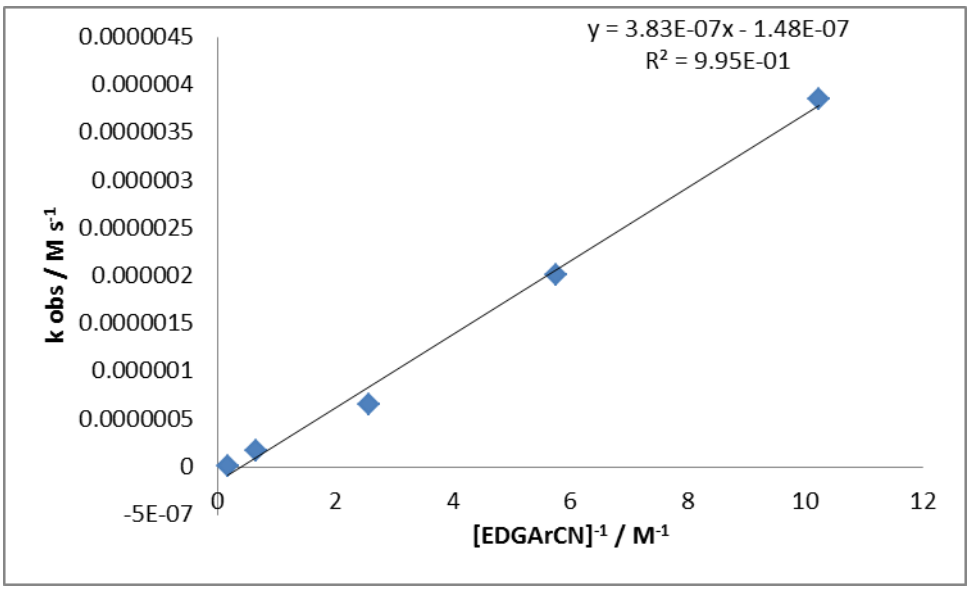


| | Value | Error |
|---|---|---|
| $m_1$ | -1.4800E-07 | 8.6431E-08 |
| $m_2$ | 3.8300E-07 | 1.6048E-08 |
| Chisq | 0.00451649 | n/a |
| $R^2$ | 0.994773 | n/a |

## Determination of order in [HBpin]

**Figure S51.** [*p*-MeOC$_6$H$_4$CH$_2$N(Bpin)$_2$] vs time; non-linear kinetics

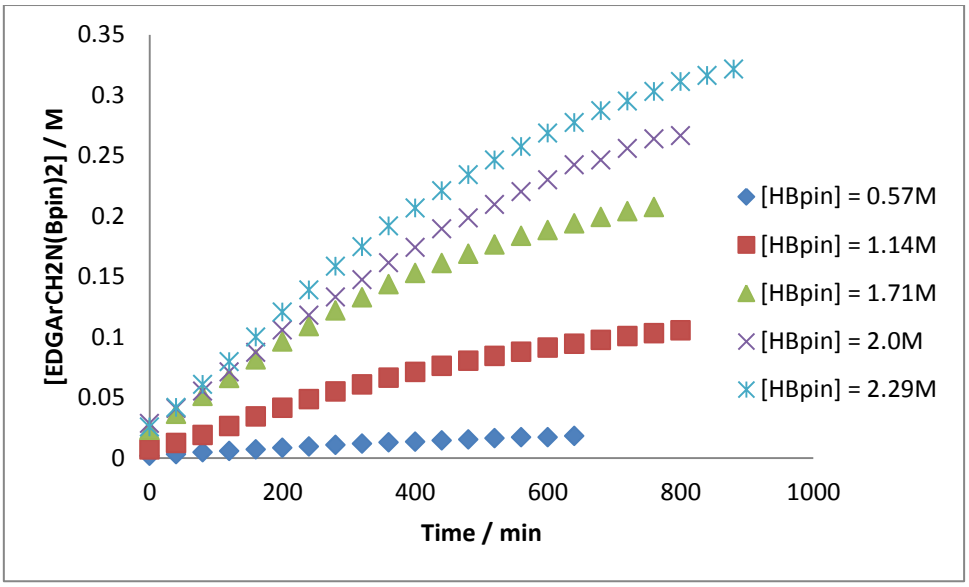

**Figure S52**. ln([*p*-MeOC$_6$H$_4$CH$_2$N(Bpin)$_2$]$_0$/[ *p*-MeOC$_6$H$_4$CH$_2$N(Bpin)$_2$]$_t$) vs time; non-linear kinetics

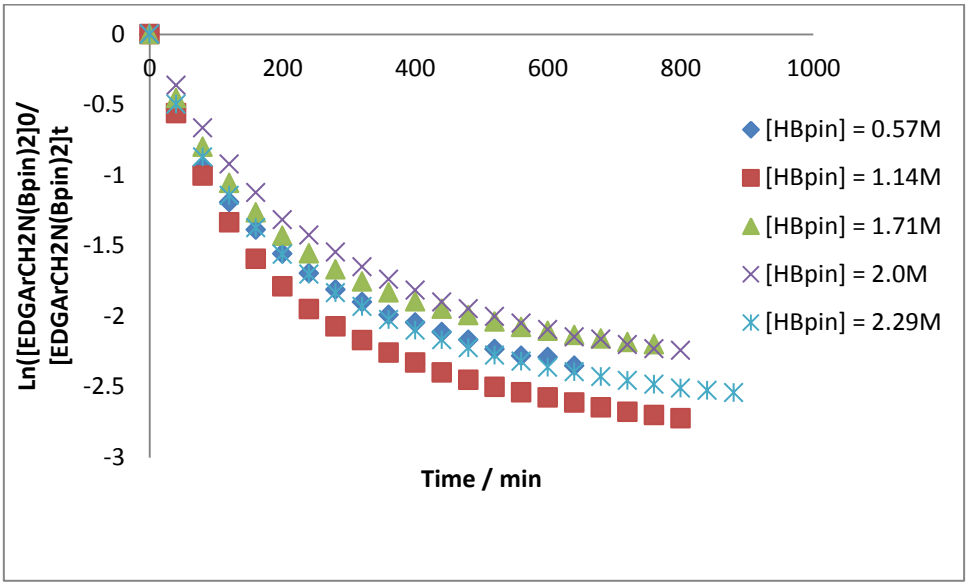


**Figure S53.** 1/[ *p*-MeOC$_6$H$_4$CH$_2$N(Bpin)$_2$] vs time; non-linear kinetics

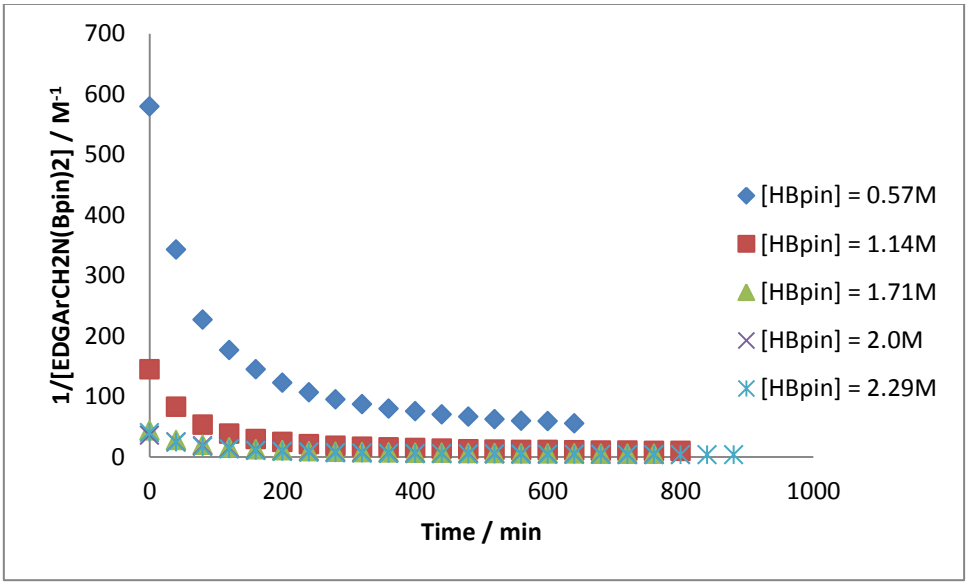

**Figure S54.** [*p*-MeOC$_6$H$_4$CH$_2$N(Bpin)$_2$]$^2$ vs time; induction period of 120 mins observed

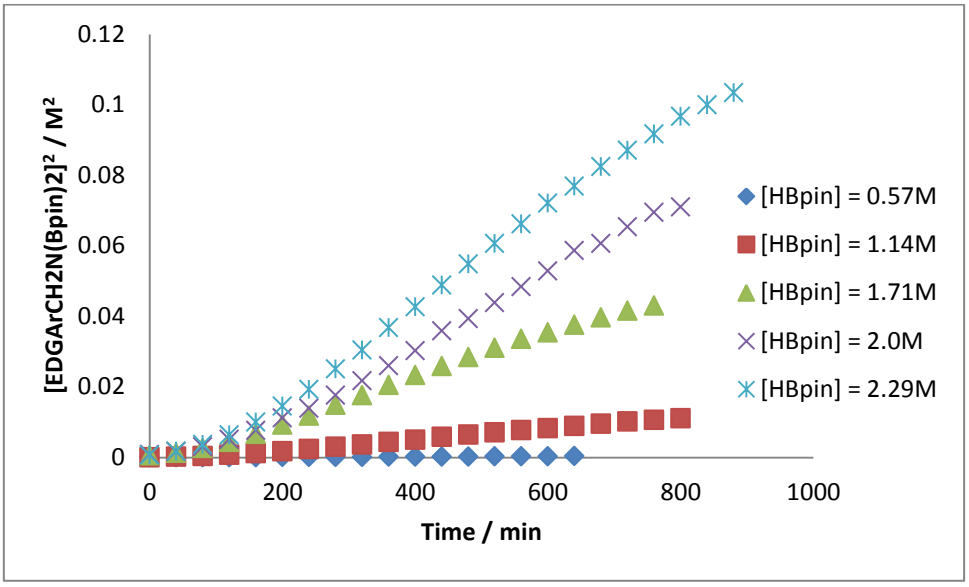


**Figure S55.** [*p*-MeOC$_6$H$_4$CH$_2$N(Bpin)$_2$]$^2$ vs time; induction period of 120 minutes removed

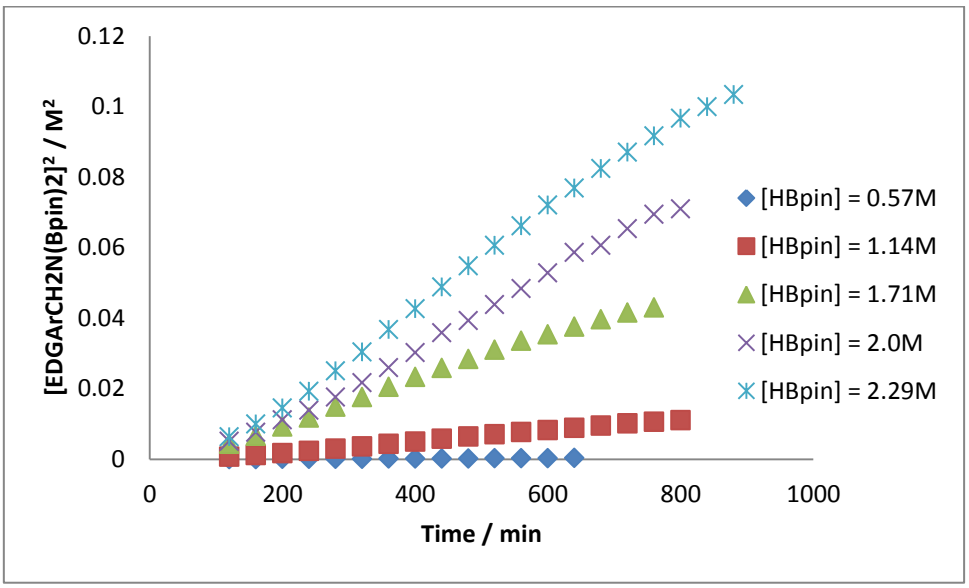


| | [HBpin] = 0.57M | |
|---|---|---|
| | Value | Error |
| $m_1$ | -0.000048 | 0.000004 |
| $m_2$ | 0.000001 | 0.000000 |
| Chisq | 0.011388 | n/a |
| $R^2$ | 0.9967516 | n/a |

| | [HBpin] = 1.14M | |
|---|---|---|
| | Value | Error |
| $m_1$ | -0.001327 | 0.000074 |
| $m_2$ | 0.000016 | 0.000000 |
| Chisq | 0.001187 | n/a |
| $R^2$ | 0.998651 | n/a |

| | [HBpin] = 1.71M | |
|---|---|---|
| | Value | Error |
| $m_1$ | -0.002571 | 0.000544 |
| $m_2$ | 0.000063 | 0.000001 |
| Chisq | 0.002314 | n/a |
| $R^2$ | 0.995136 | n/a |

| | [HBpin] = 2.0M | |
|---|---|---|
| | Value | Error |
| $m_1$ | -0.009919 | 0.000752 |
| $m_2$ | 0.000104 | 0.000001 |
| Chisq | 0.014046 | n/a |
| $R^2$ | 0.996698 | n/a |

| | [HBpin] = 2.29M | |
|---|---|---|
| | Value | Error |
| $m_1$ | -0.011227 | 0.000939 |
| $m_2$ | 0.000135 | 0.000002 |
| Chisq | 0.001852 | n/a |
| $R^2$ | 0.997134 | n/a |

**Figure S56.** [HBpin] vs $k_{oba}$; non-linear fit

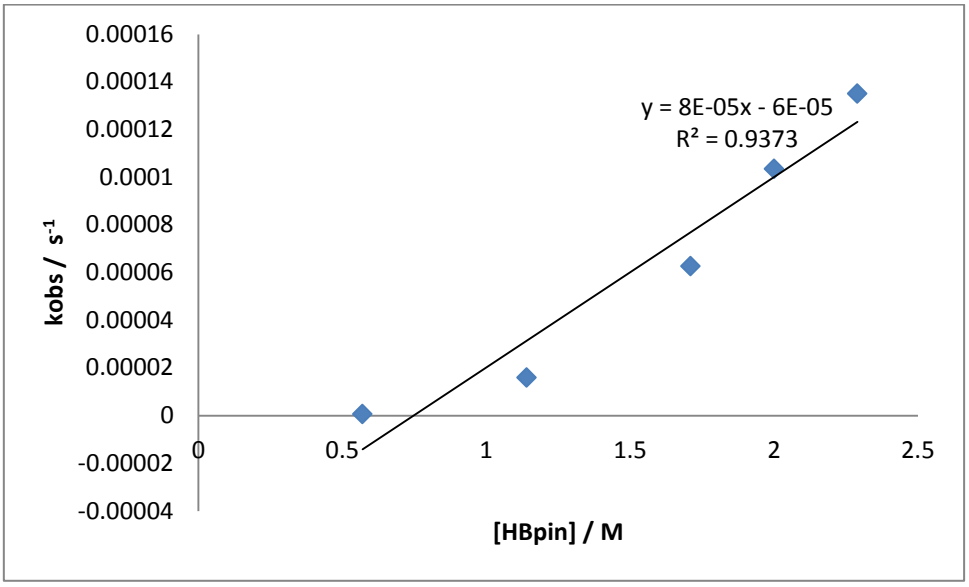


**Figure S57.** $[HBpin]^2$ vs $k_{obs}$; linear fit indicates a second order dependence on [HBpin]

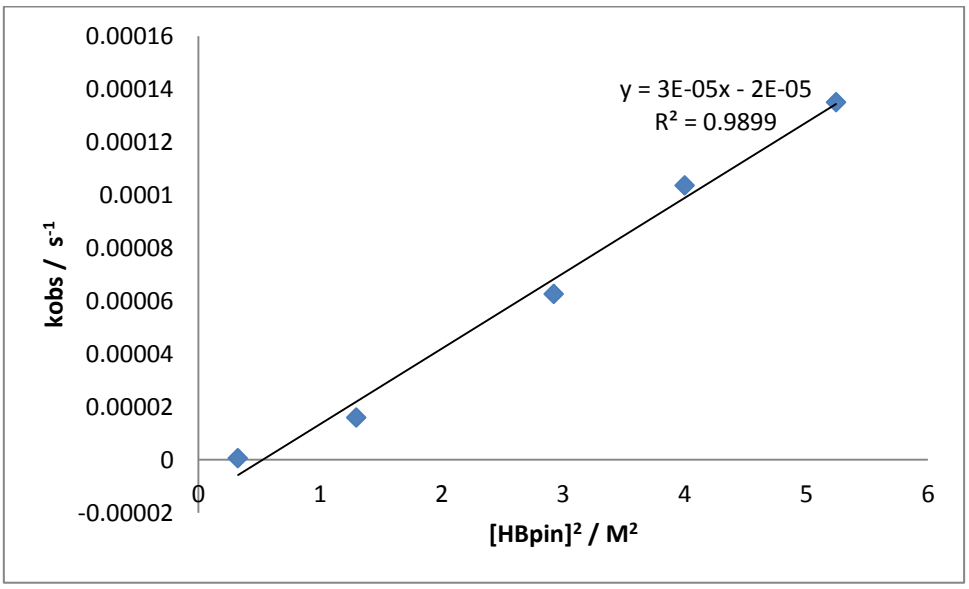


| | Value | Error |
|---|---|---|
| $m_1$ | -0.000015 | 0.000005 |
| $m_2$ | 0.000028 | 0.000002 |
| Chisq | 0.015630413 | n/a |
| $R^2$ | 0.98985985 | n/a |

**Figure S58.** $[HBpin]^3$ vs $k_{obs}$

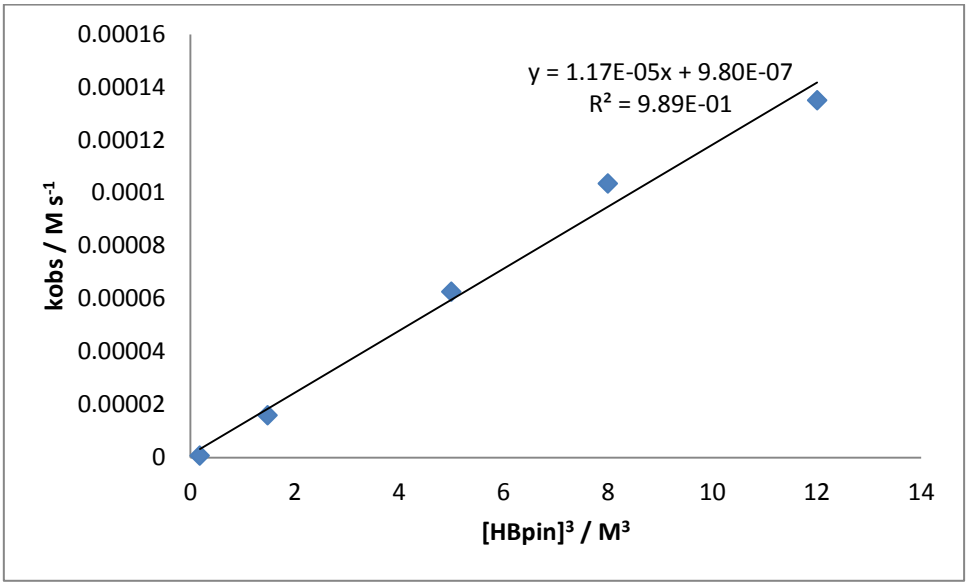


| | Value | Error |
|---|---|---|
| $m_1$ | 9.80E-07 | 4.93E-06 |
| $m_2$ | 1.17E-05 | 7.19E-07 |
| Chisq | 0.002553085 | n/a |
| $R^2$ | 0.98884400 | n/a |

## Variable [Mg] under *pseudo*-first order conditions in [HBpin]

**Figure S59.** [*p*-$MeOC_6H_4CN$] vs time; non-linear kinetics

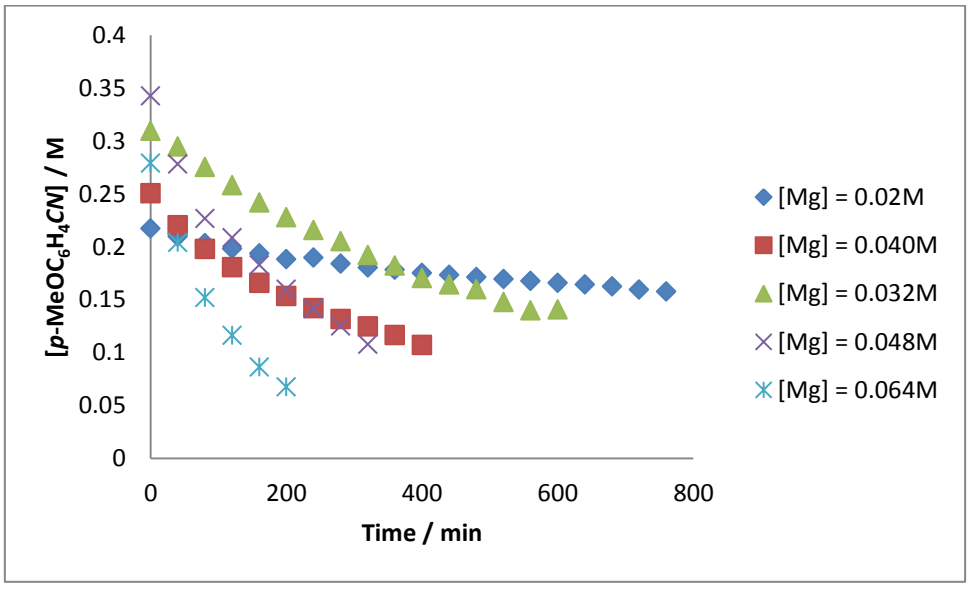

**Figure S60.** ln([*p*-MeOC$_6$H$_4$CN]$_0$/[ *p*-MeOC$_6$H$_4$CN]$_t$) vs time; variable [Mg] under *pseudo*-first order conditions in [HBpin] (8.0 M) whilst keeping [*p*-MeOC$_6$H$_4$CN] (0.4 M) invariant

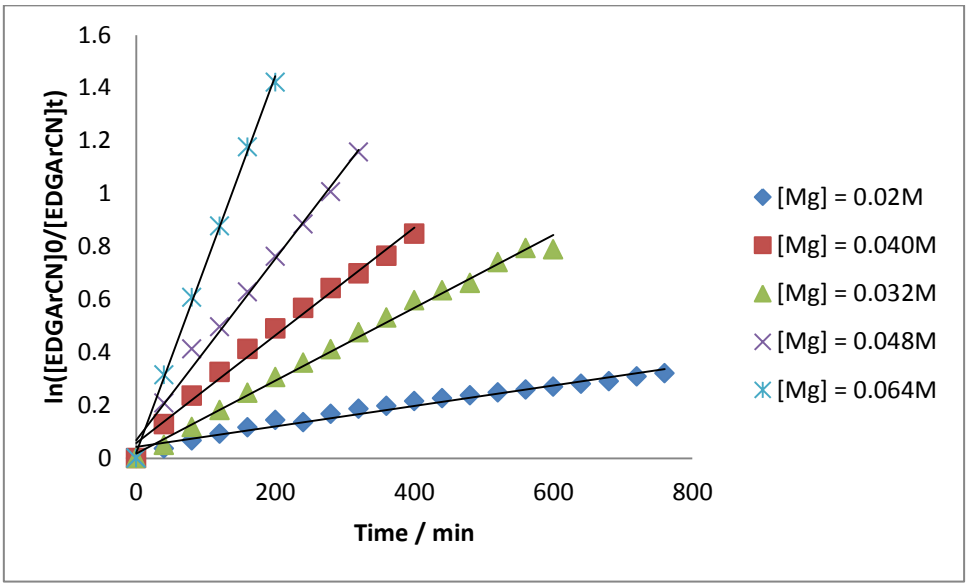


| | [Mg] = 0.020M | |
|---|---|---|
| | Value | Error |
| $m_1$ | 0.043055 | 0.007416 |
| $m_2$ | 0.000386 | 0.000017 |
| Chisq | 0.225892 | n/a |
| $R^2$ | 0.967518 | n/a |

| | [Mg] = 0.040M | |
|---|---|---|
| | Value | Error |
| $m_1$ | 0.057696 | 0.016640 |
| $m_2$ | 0.002037 | 0.000070 |
| Chisq | 0.049623 | n/a |
| $R^2$ | 0.989386 | n/a |

| | [Mg] = 0.032M | |
|---|---|---|
| | Value | Error |
| $m_1$ | 0.018183 | 0.016640 |
| $m_2$ | 0.001376 | 0.000070 |
| Chisq | 0.004929 | n/a |
| $R^2$ | 0.993879 | n/a |

| | [Mg] = 0.048M | |
|---|---|---|
| | Value | Error |
| $m_1$ | 0.068100 | 0.023870 |
| $m_2$ | 0.003433 | 0.000125 |
| Chisq | 0.036552 | n/a |
| $R^2$ | 0.990754 | n/a |

| | [Mg] = 0.064M | |
|---|---|---|
| | Value | Error |
| $m_1$ | 0.021445 | 0.014694 |
| $m_2$ | 0.007113 | 0.000121 |
| Chisq | 0.001945 | n/a |
| $R^2$ | 0.998838 | n/a |

**Figure S61.** 1/[ *p*-MeOC$_6$H$_4$CN] vs time; non-linear kinetics

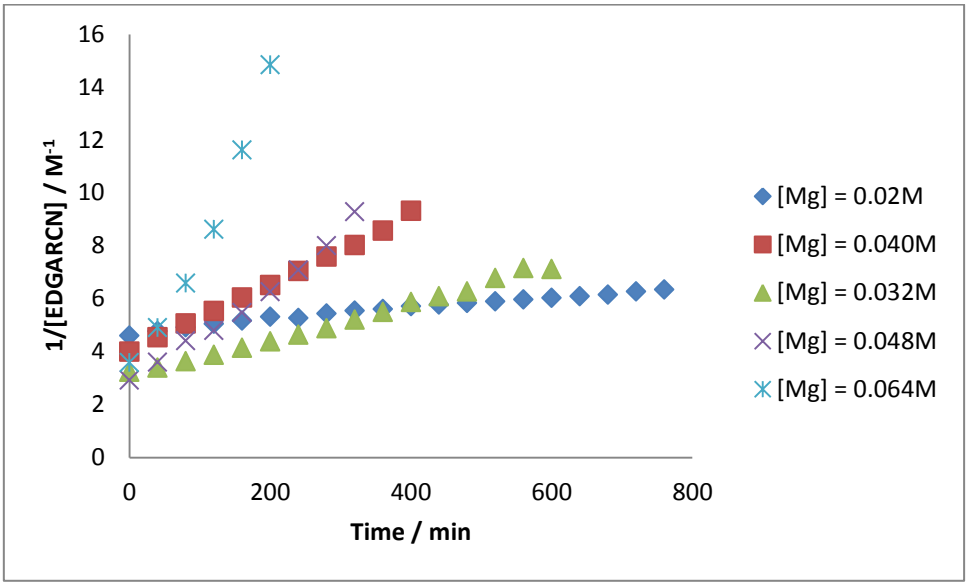


**Figure S62.** [Mg] vs $k_{obs}$; non-linear fit. $k_{obs}$ values taken from 1$^{st}$ order plot

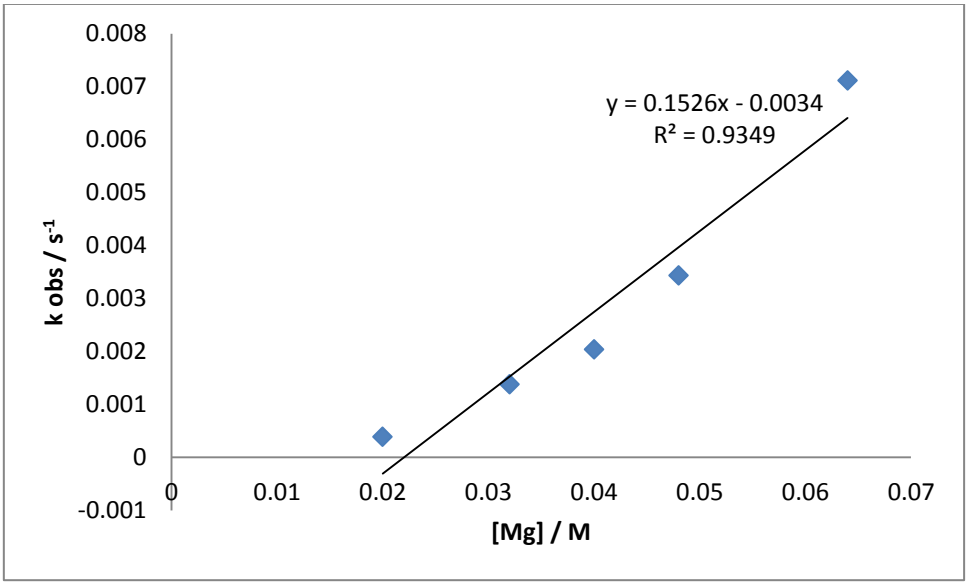

**Figure S63.** $[Mg]^2$ vs $k_{obs}$

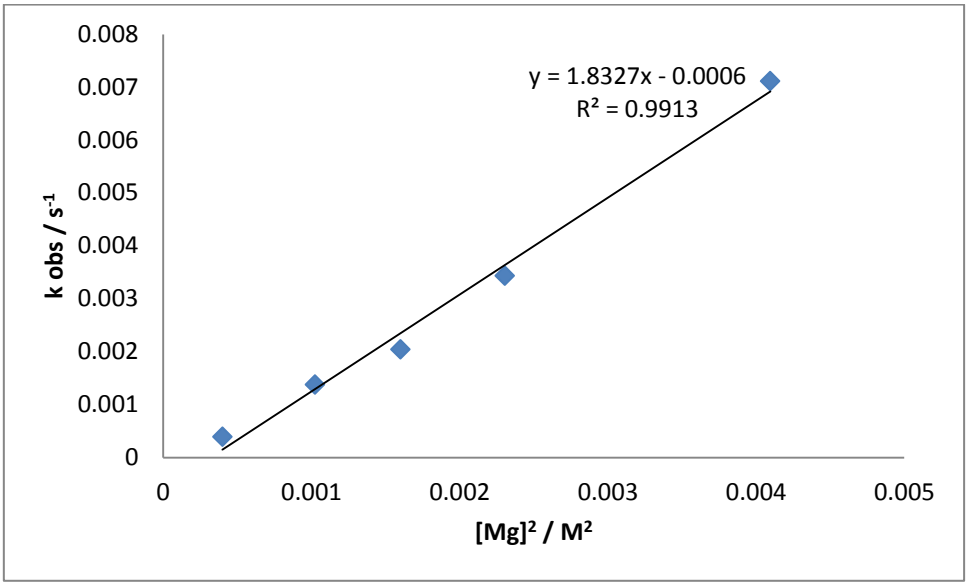


| | Value | Error |
|---|---|---|
| $m_1$ | -0.000585 | 0.000225 |
| $m_2$ | 1.832664 | 0.099105 |
| Chisq | 0.010325 | n/a |
| $R^2$ | 0.991303 | n/a |

**Figure S64.** $[Mg]^3$ vs $k_{obs}$

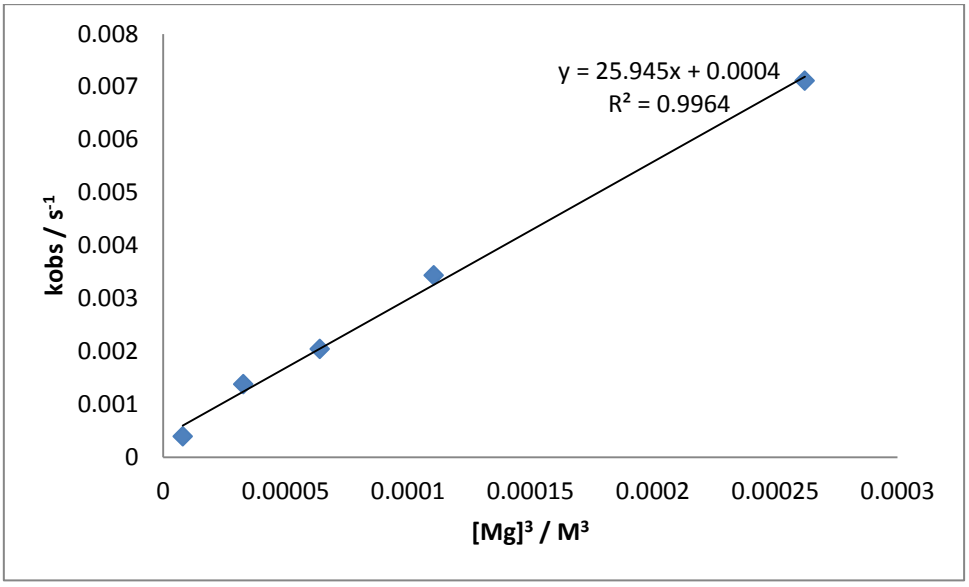


| | Value | Error |
|---|---|---|
| $m_1$ | 0.000391 | 0.000119 |
| $m_2$ | 25.944599 | 0.904880 |
| Chisq | 0.008239727 | n/a |
| $R^2$ | 0.996364 | n/a |

## Variable [HBpin] under near stoichiometric reaction conditions

**Figure S65**. [*p*-MeOC$_6$H$_4$CN] vs time; non-linear kinetics

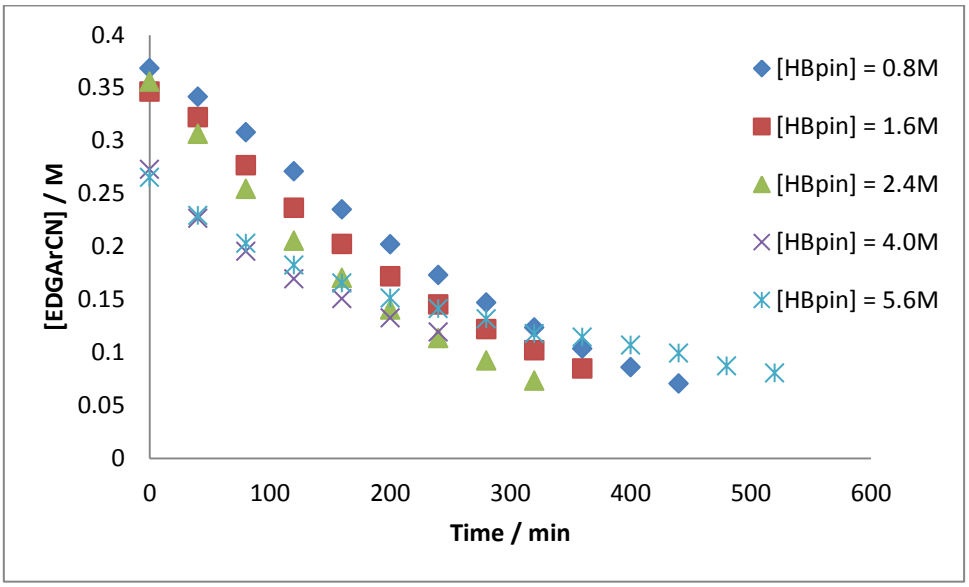


**Figure S66**. ln([*p*-MeOC$_6$H$_4$CN]$_0$/[ *p*-MeOC$_6$H$_4$CN]$_t$) vs time

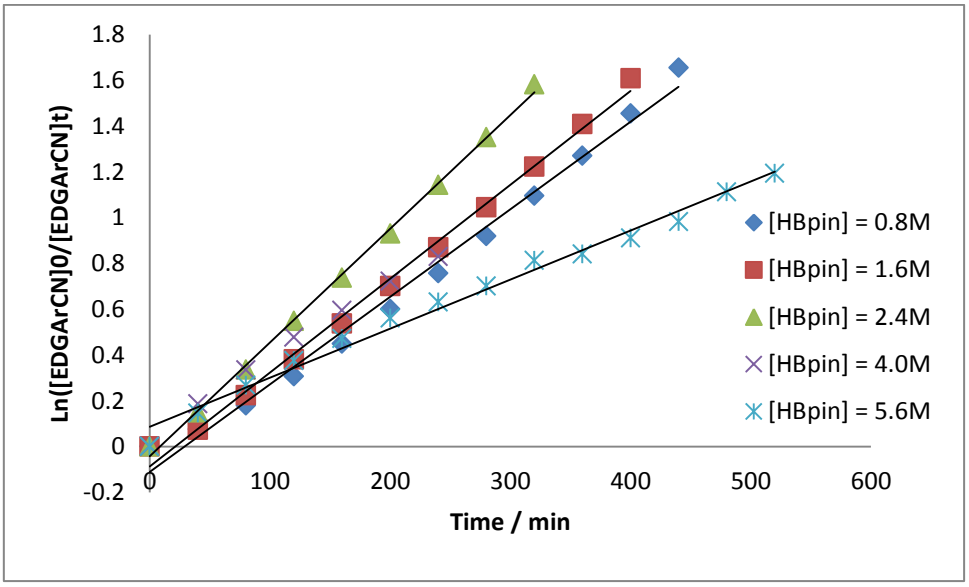


| | [HBpin] = 0.8M | |
|---|---|---|
| | Value | Error |
| $m_1$ | -0.095968 | 0.028964 |
| $m_2$ | 0.003711 | 0.000122 |
| Chisq | 0.041384 | n/a |
| $R^2$ | 0.990307 | n/a |

| | [HBpin] = 1.6M | |
|---|---|---|
| | Value | Error |
| $m_1$ | -0.075344 | 0.021288 |
| $m_2$ | 0.004009 | 0.000100 |
| Chisq | 0.026625 | n/a |
| $R^2$ | 0.995078 | n/a |

| | [HBpin] = 2.4M | |
|---|---|---|
| | Value | Error |
| $m_1$ | -0.042223 | 0.015034 |
| $m_2$ | 0.004969 | 0.000079 |
| Chisq | 0.006756 | n/a |
| $R^2$ | 0.998236 | n/a |

| | [HBpin] = 4.0M | |
|---|---|---|
| | Value | Error |
| $m_1$ | 0.039869 | 0.019001 |
| $m_2$ | 0.003409 | 0.000132 |
| Chisq | 0.021209 | n/a |
| $R^2$ | 0.992589 | n/a |

| | [HBpin] = 5.6M | |
|---|---|---|
| | Value | Error |
| $m_1$ | 0.086297 | 0.020508 |
| $m_2$ | 0.002142 | 0.000067 |
| Chisq | 0.061684 | n/a |
| $R^2$ | 0.988388 | n/a |

**Figure S67**. 1/[ *p*-MeOC$_6$H$_4$CN] vs time; non-linear kinetics

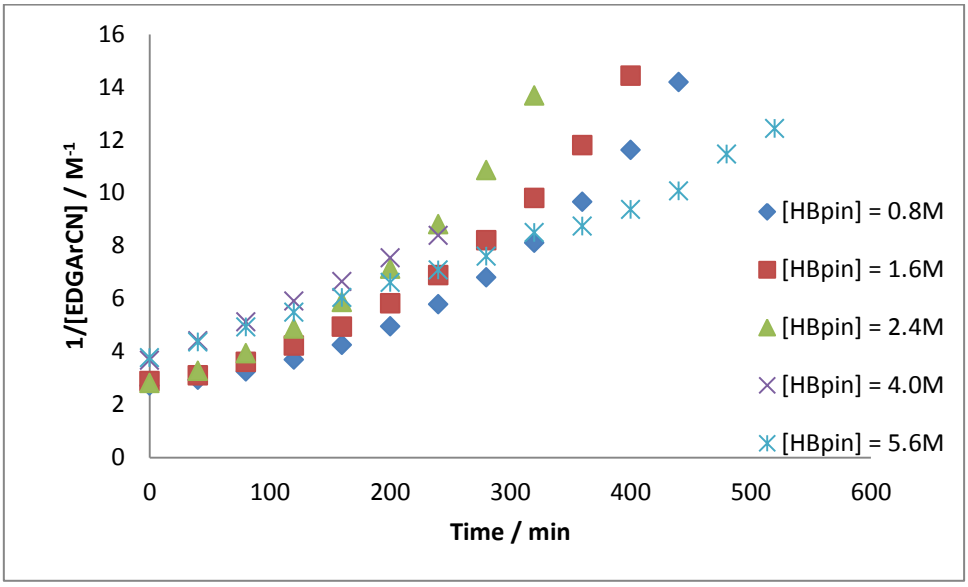


**Figure S68.** [HBpin] vs $k_{obs}$; indicates a variable dependence upon [HBpin] with respect to rate of reaction

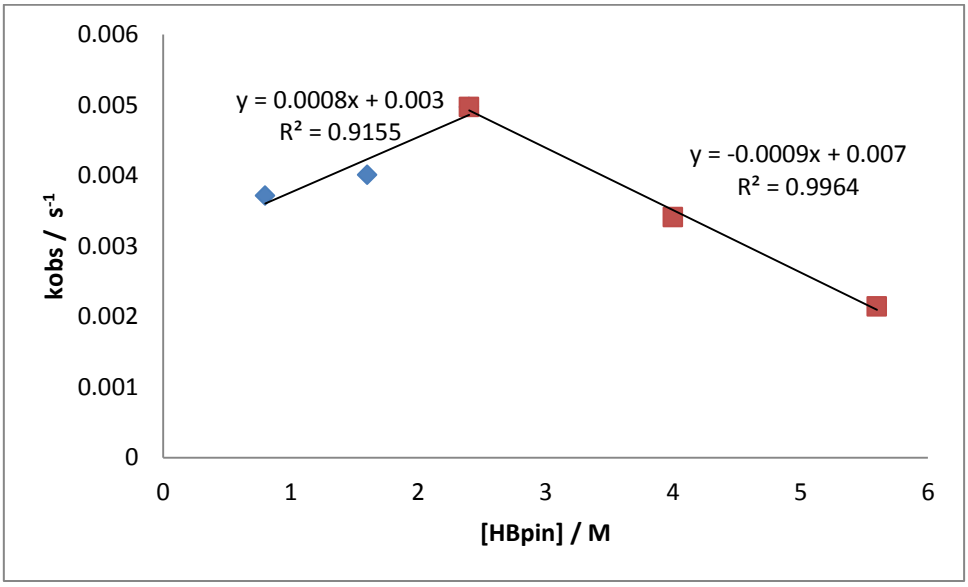


| | [HBpin] 0.8 – 2.4M | |
|---|---|---|
| | Value | Error |
| $m_1$ | 0.002957 | 0.000413 |
| $m_2$ | 0.000794 | 0.000239 |
| Chisq | 0.048987 | n/a |
| $R^2$ | 0.919695 | n/a |

| | [HBpin] = 2.4 – 5.6M | |
|---|---|---|
| | Value | Error |
| $m_1$ | 0.007081 | 0.000222 |
| $m_2$ | -0.000897 | 0.000053 |
| Chisq | 0.001245 | n/a |
| $R^2$ | 0.997477 | n/a |

**Figure S69.** $[HBpin]^2$ vs $k_{obs}$; increased linearity for 0.8-2.4M

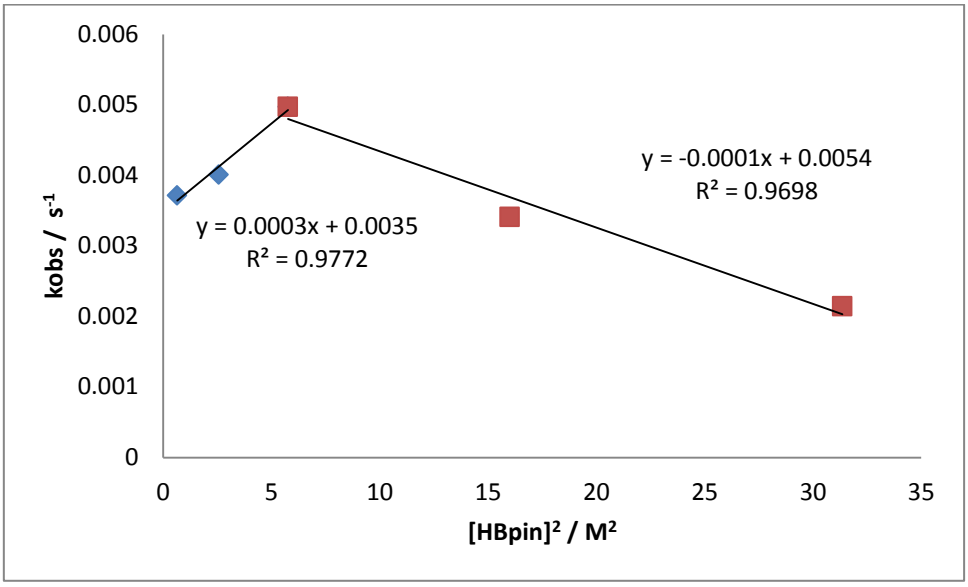


| | [HBpin] 0.8 – 2.4M | |
|---|---|---|
| | Value | Error |
| $m_1$ | 0.003479 | 0.000140 |
| $m_2$ | 0.000251 | 0.000038 |
| Chisq | 0.017675 | n/a |
| $R^2$ | 0.977190 | n/a |

| | [HBpin] = 2.4 – 5.6M | |
|---|---|---|
| | Value | Error |
| $m_1$ | 0.005423 | 0.000393 |
| $m_2$ | -0.000108 | 0.000019 |
| Chisq | 0.021134 | n/a |
| $R^2$ | 0.969779 | n/a |

**Figure S70.** $[HBpin]^3$ vs $k_{obs}$; increased linearity for 0.8 - 2.4M

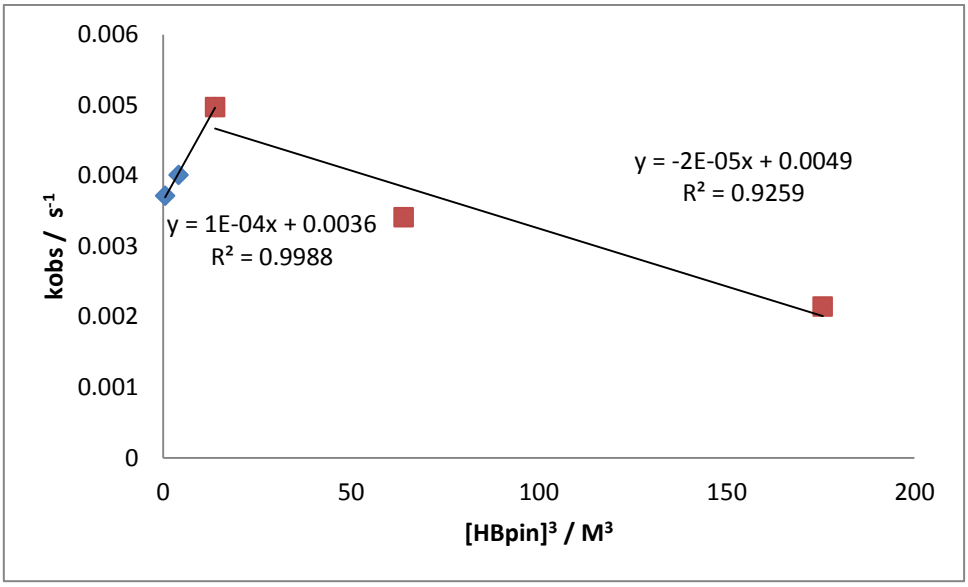


| | [HBpin] 0.8 – 2.4M | |
|---|---|---|
| | Value | Error |
| $m_1$ | 0.003644 | 0.000027 |
| $m_2$ | 0.000095 | 0.000003 |
| Chisq | 0.00117 | n/a |
| $R^2$ | 0.998807 | n/a |

| | [HBpin] = 2.4 – 5.6M | |
|---|---|---|
| | Value | Error |
| $m_1$ | 0.004897 | 0.000503 |
| $m_2$ | -0.000016 | 0.000005 |
| Chisq | 0.064303 | n/a |
| $R^2$ | 0.925949 | n/a |

## Variable Temperature Studies

**Figure S71.** [*p*-$MeOC_6H_4CN$] vs time; non-linear kinetics

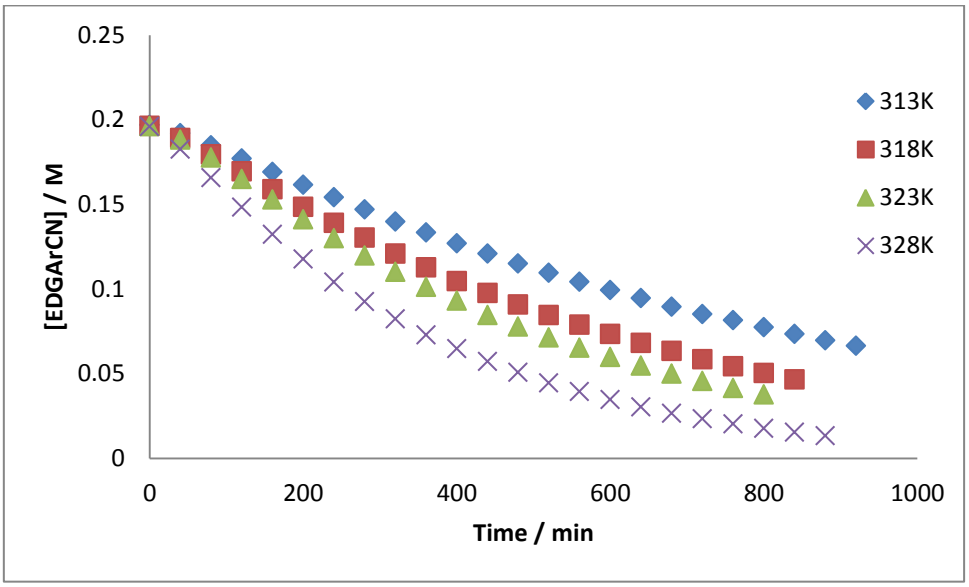


**Figure S72.** ln([*p*-$MeOC_6H_4CN$]$_0$/[ *p*-$MeOC_6H_4CN$]$_t$) vs time

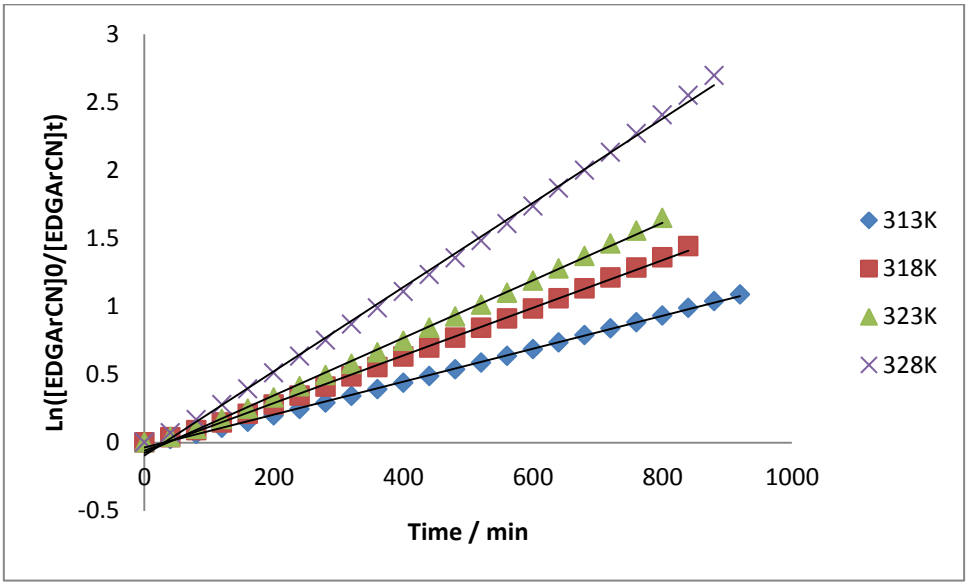


| | 313 K | |
|---|---|---|
| | Value | Error |
| $m_1$ | -0.036570 | 0.004240 |
| $m_2$ | 0.001210 | 0.000008 |
| Chisq | 0.011917 | n/a |
| $R^2$ | 0.99906 | n/a |

| | 318 K | |
|---|---|---|
| | Value | Error |
| $m_1$ | -0.058620 | 0.008199 |
| $m_2$ | 0.001750 | 0.000017 |
| Chisq | 0.017399 | n/a |
| $R^2$ | 0.99818 | n/a |

| | 323 K | |
|---|---|---|
| | Value | Error |
| $m_1$ | -0.074960 | 0.010727 |
| $m_2$ | 0.002110 | 0.000023 |
| Chisq | 0.021446 | n/a |
| $R^2$ | 0.99776 | n/a |

| | 328 K | |
|---|---|---|
| | Value | Error |
| $m_1$ | -0.056910 | 0.010357 |
| $m_2$ | 0.002930 | 0.000031 |
| Chisq | 0.012625 | n/a |
| $R^2$ | 0.99850 | n/a |

**Figure S73.** 1/[ *p*-MeOC$_6$H$_4$CN] vs time; non-linear kinetics

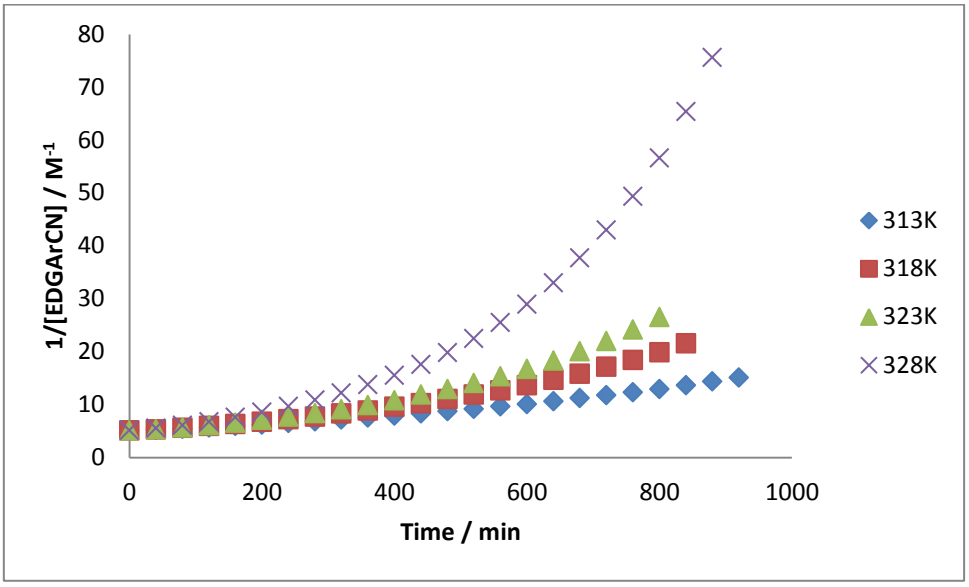


**Figure S74.** Eyring Plot; 1/T vs Ln(k/T)

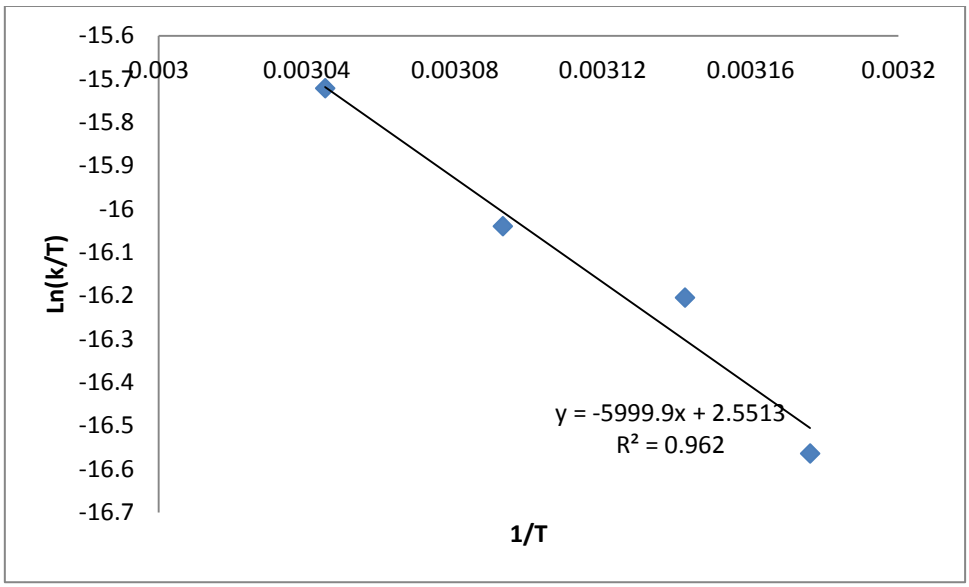


| | Value | Error |
|---|---|---|
| $m_1$ | 2.551282 | 2.627555 |
| $m_2$ | -5999.875772 | 843.654844 |
| Chisq | 0.038217588 | n/a |
| $R^2$ | 0.961961 | n/a |

The graph shown as Fig. S74 was used to calculate the following Activation Energy Parameters, least square error analysis was also carried to provide accurate error information.

| | Value | Error |
|---|---|---|
| ΔH | 49.88 kJ mol$^{-1}$ | ± 7.01 |
| ΔS | -176.33 J k$^{-1}$ mol$^{-1}$ | ± 21.85 |

**Figure S75.** Arrhenius Plot; 1/T vs Ln(k)

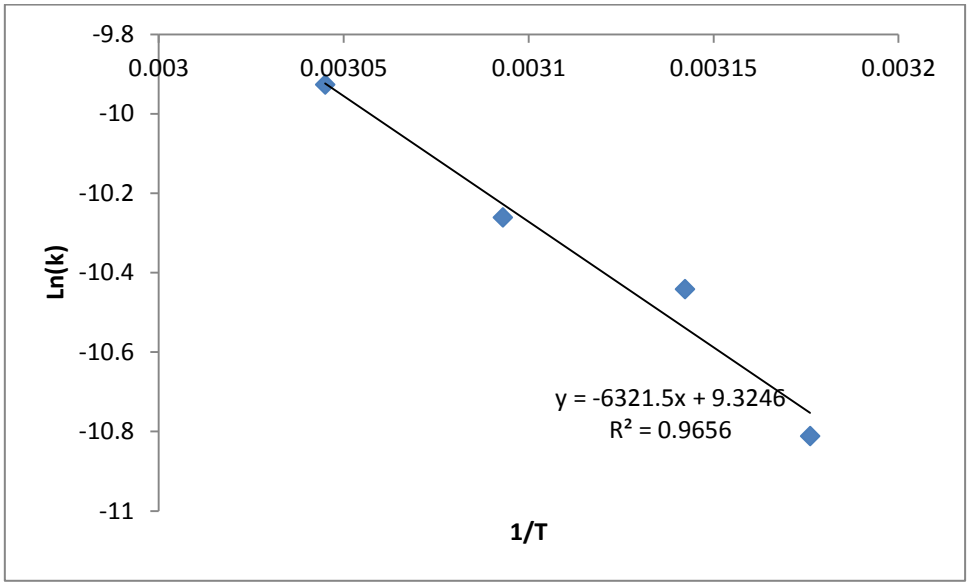


| | Value | Error |
|---|---|---|
| $m_1$ | 9.324641 | 2.625809 |
| $m_2$ | -6321.450699 | 843.094344 |
| Chisq | 0.034447917 | n/a |
| $R^2$ | 0.965647 | n/a |

This graph was used to calculate the following Activation Energy Parameter; least square error analysis was also carried to provide accurate error information.

| | Value | Error |
|---|---|---|
| Ea | 52.56 kJ $mol^{-1}$ | ± 7.01 |

## Electron Withdrawing aryl nitrile – *m*-$MeOC_6H_4CN$

### Determination of order in [Mg]

**Figure S76.** [*m*-$MeOC_6H_4CN$] vs time; non-linear kinetics

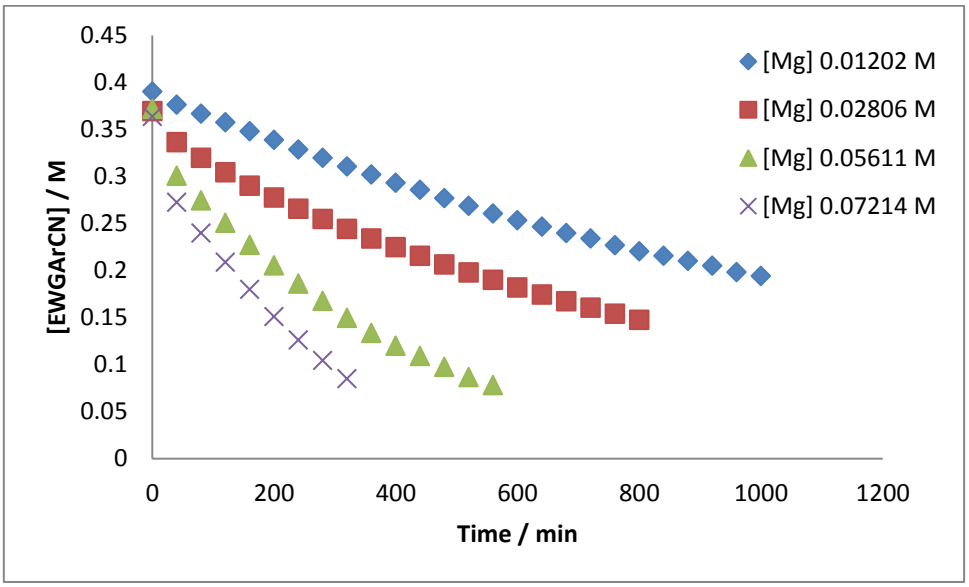


**Figure S77.** ln([*m*-$MeOC_6H_4CN$]$_0$/[ *m*-$MeOC_6H_4CN$]$_t$) vs time

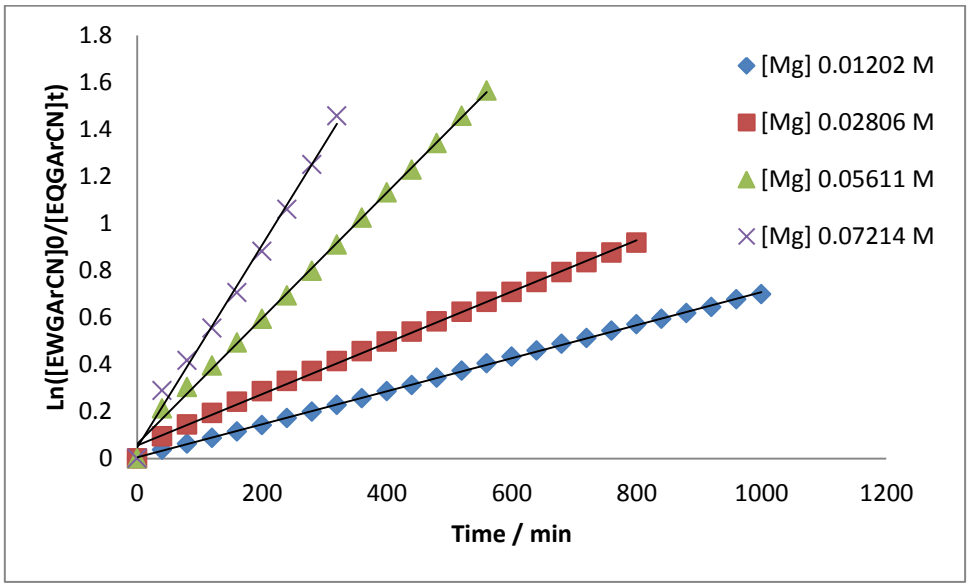

| | [Mg] 0.01202 M | |
|---|---|---|
| | Value | Error |
| $m_1$ | 0.004713 | 0.001563 |
| $m_2$ | 0.000702 | 0.000003 |
| Chisq | 0.0005 | n/a |
| $R^2$ | 0.999650 | n/a |

| | [Mg] 0.02806 M | |
|---|---|---|
| | Value | Error |
| $m_1$ | 0.054630 | 0.006236 |
| $m_2$ | 0.001090 | 0.000013 |
| Chisq | 0.042573 | n/a |
| $R^2$ | 0.99717 | n/a |

| | [Mg] 0.05611 M | |
|---|---|---|
| | Value | Error |
| $m_1$ | 0.061530 | 0.011542 |
| $m_2$ | 0.002670 | 0.000035 |
| Chisq | 0.017716 | n/a |
| $R^2$ | 0.99776 | n/a |

| | [Mg] 0.0.07214 M | |
|---|---|---|
| | Value | Error |
| $m_1$ | 0.046350 | 0.024226 |
| $m_2$ | 0.004300 | 0.000127 |
| Chisq | 0.010818 | n/a |
| $R^2$ | 0.99392 | n/a |

**Figure S78.** 1/[ *m*-$MeOC_6H_4CN$] vs time; non-linear kinetics

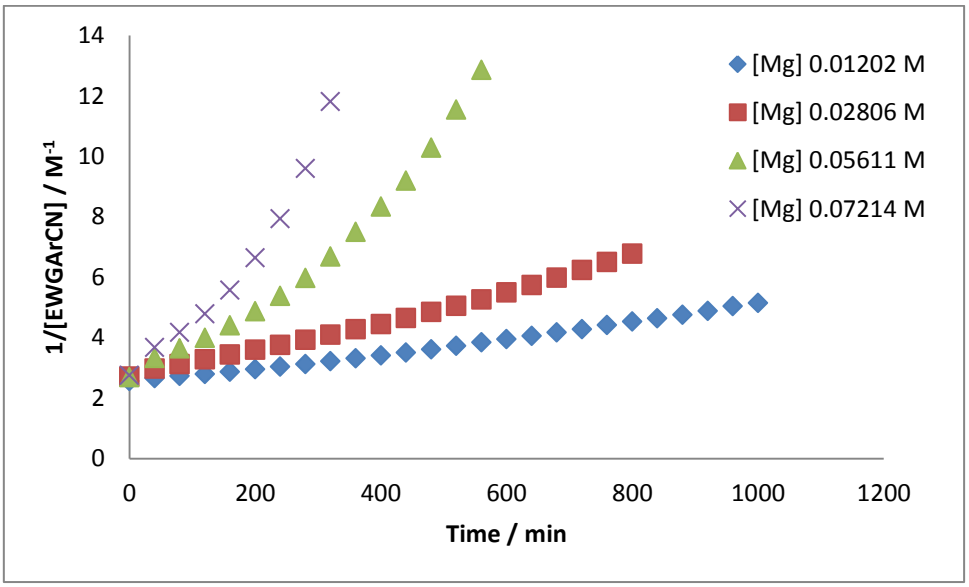

**Figure S79.** [Mg] vs $k_{obs}$; non-linear fit

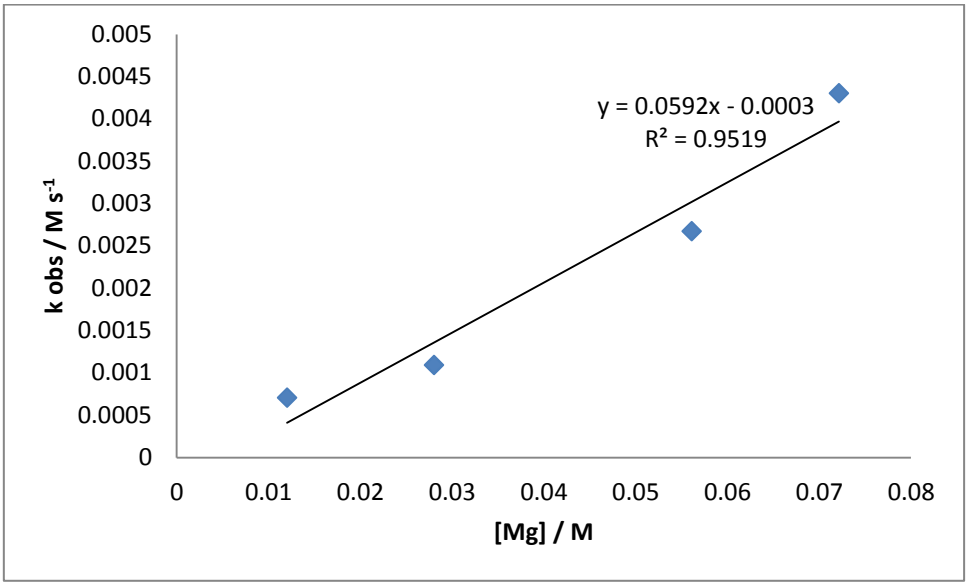


**Figure S80.** $[Mg]^2$ vs $k_{obs}$; indicating a second order dependence upon [Mg]

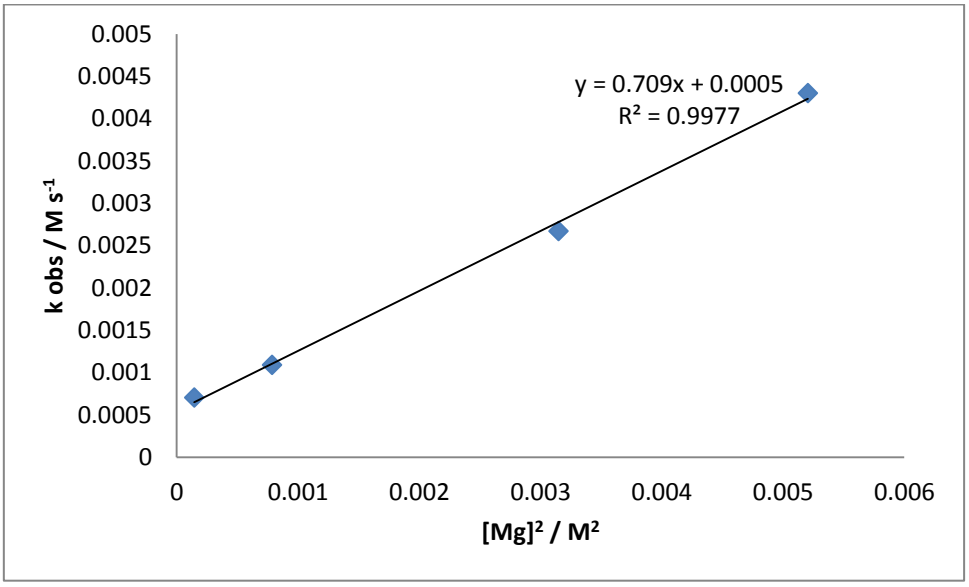


| | Value | Error |
|---|---|---|
| $m_1$ | 0.000545 | 0.000074 |
| $m_2$ | 0.708969 | 0.024210 |
| Chisq | 0.001466 | n/a |
| $R^2$ | 0.997673 | n/a |

**Figure S81.** $[Mg]^{1/2}$ vs $k_{obs}$; non-linear fit

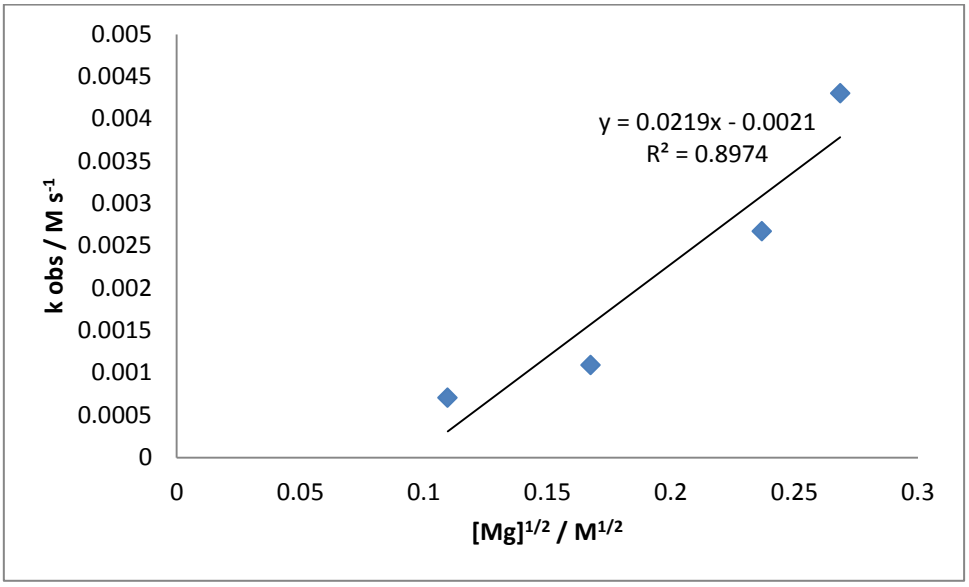


## Determination of order in [Ar(EWG)CN]

**Figure S82.** [*m*-$MeOC_6H_4CN$] vs time; non-linear fit

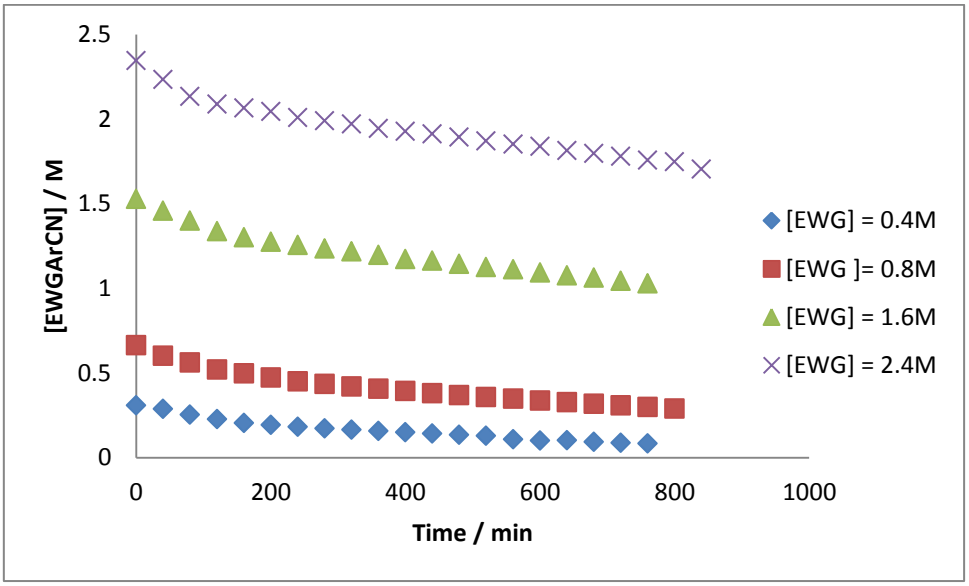

**Figure S83.** ln([*m*-MeOC$_6$H$_4$CN]$_0$/[ *m*-MeOC$_6$H$_4$CN]$_t$) vs time; linear fit with induction period 0-160 min

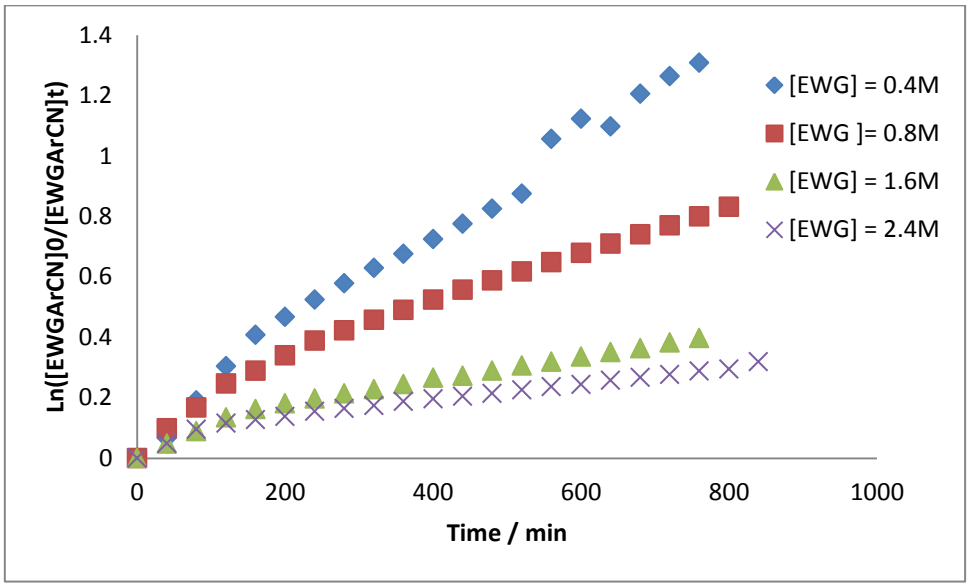


**Figure S84.** ln([*m*-MeOC$_6$H$_4$CN]$_0$/[ *m*-MeOC$_6$H$_4$CN]$_t$) vs time; induction period omitted for $k_{obs}$ values

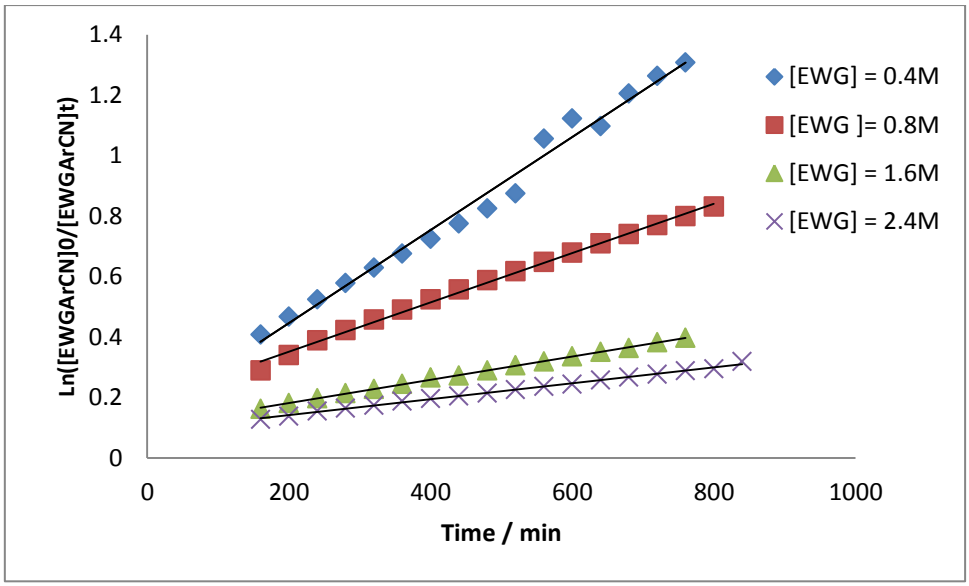


| | [EWG] 0.4M | |
|---|---|---|
| | Value | Error |
| $m_1$ | 0.137358 | 0.024792 |
| $m_2$ | 0.001540 | 0.000050 |
| Chisq | 0.006875 | n/a |
| $R^2$ | 0.985440 | n/a |

| | [EWG] 0.8M | |
|---|---|---|
| | Value | Error |
| $m_1$ | 0.188078 | 0.006876 |
| $m_2$ | 0.000816 | 0.000013 |
| Chisq | 0.03394 | n/a |
| $R^2$ | 0.996050 | n/a |

| | [EWG] 1.6M | |
|---|---|---|
| | Value | Error |
| $m_1$ | 0.104483 | 0.001651 |
| $m_2$ | 0.000385 | 0.000003 |
| Chisq | 0.003903 | n/a |
| $R^2$ | 0.998953 | n/a |

| | [EWG] 2.4M | |
|---|---|---|
| | Value | Error |
| $m_1$ | 0.088384 | 0.002056 |
| $m_2$ | 0.000264 | 0.000004 |
| Chisq | 0.003444 | n/a |
| $R^2$ | 0.996701 | n/a |

**Figure S85.** 1/[ *m*-MeOC$_6$H$_4$CN] vs time; non-linear fit

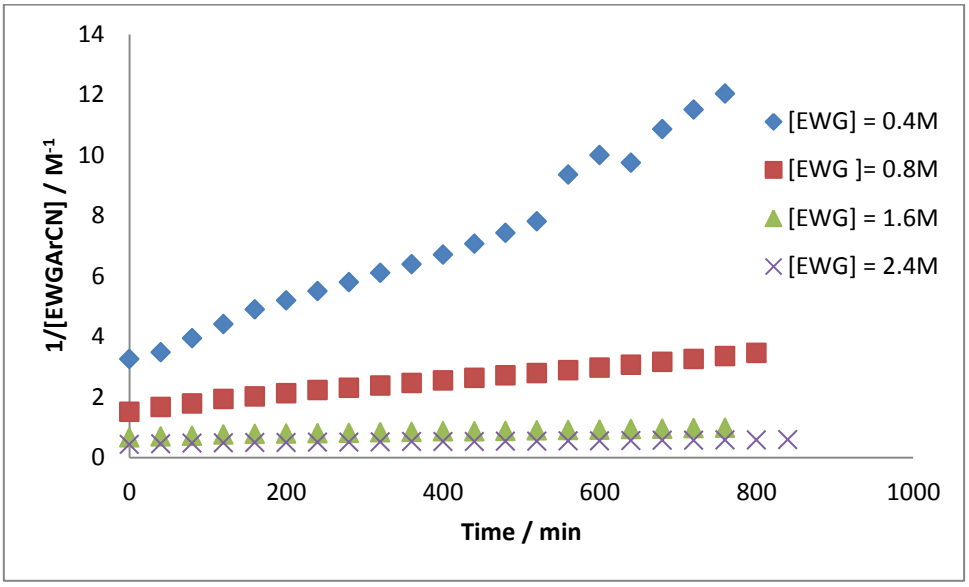


**Figure S86.** [*m*-MeOC$_6$H$_4$CN] vs $k_{obs}$; non-linear kinetics

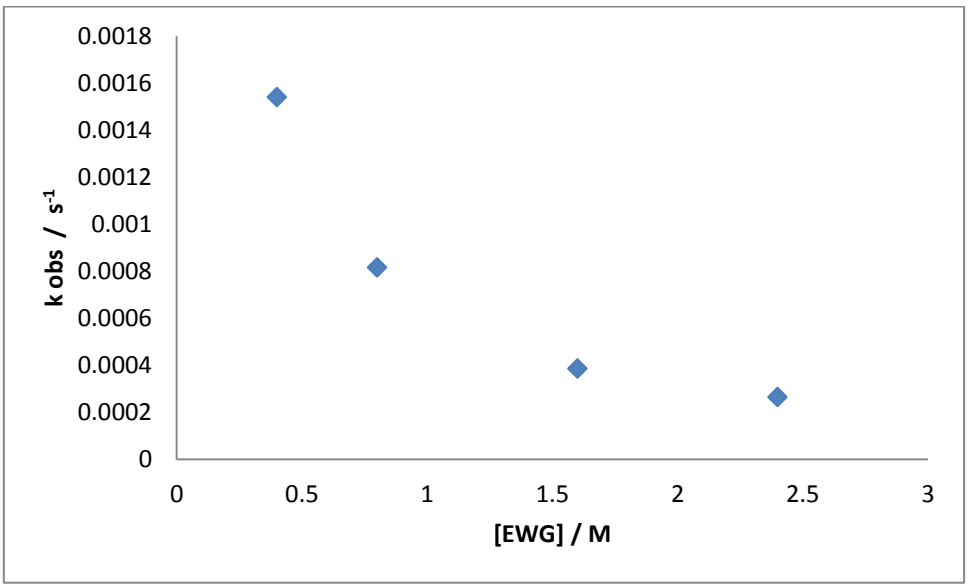

**Figure S87.** [*m*-$MeOC_6H_4CN$]$^{-1}$ vs $k_{obs}$; indicating a -1 order dependence upon [Ar(EWG)CN]

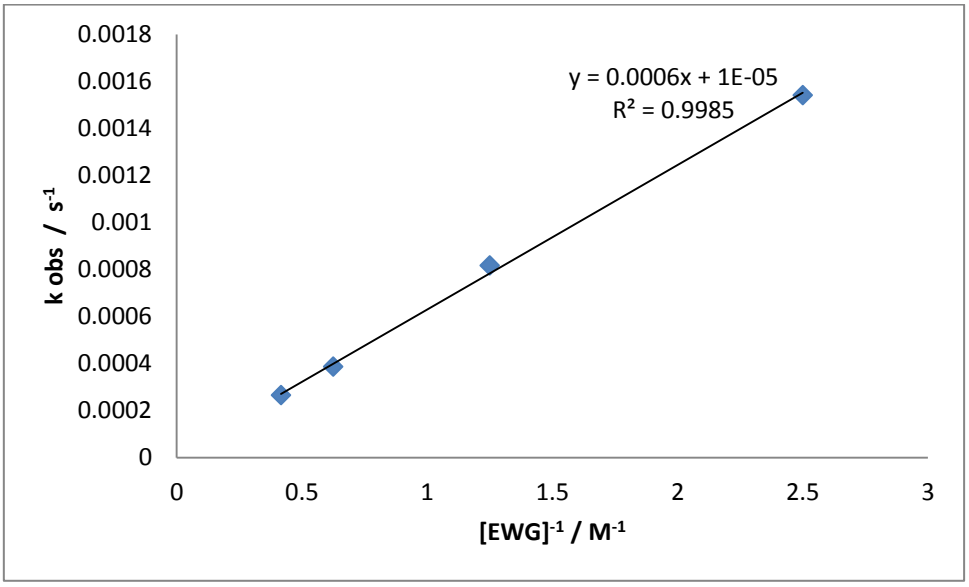


| | Value | Error |
|---|---|---|
| $m_1$ | 0.000015 | 0.000024 |
| $m_2$ | 0.000615 | 0.000017 |
| Chisq | 0.000626 | n/a |
| $R^2$ | 0.998542 | n/a |

## Variable [Mg] under *pseudo*-first order in [HBpin]

**Figure S88.** [*m*-$MeOC_6H_4CN$] vs time; non-linear fit

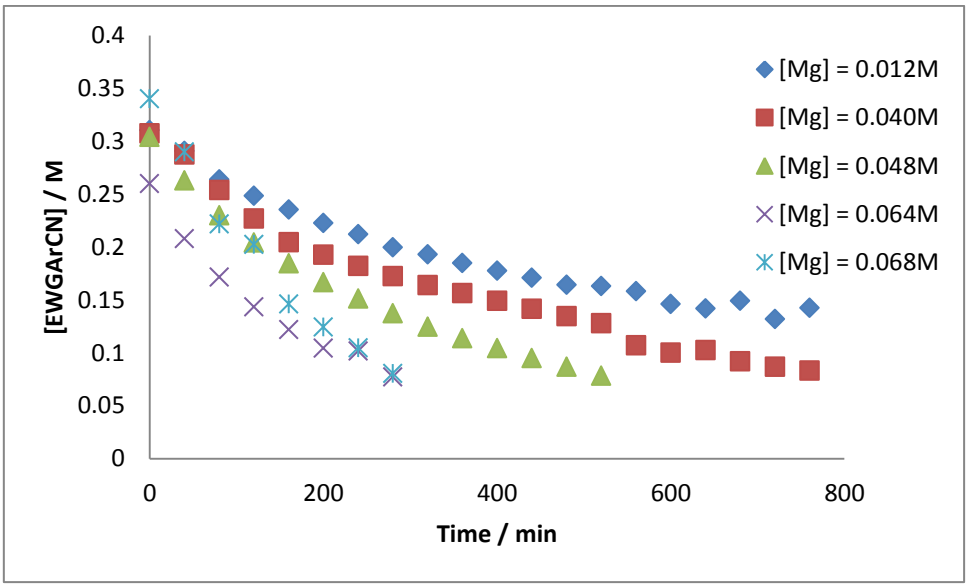


**Figure S891.** ln([*m*-$MeOC_6H_4CN$]$_0$/[ *m*-$MeOC_6H_4CN$]$_t$) vs time; induction period observed at lower [Mg]

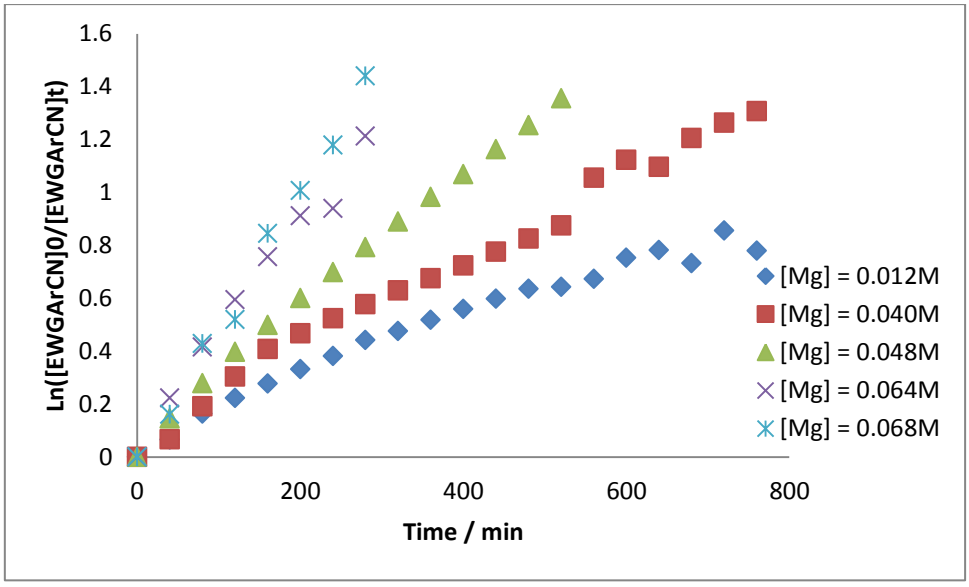

**Figure S90.** ln([*m*-MeOC$_6$H$_4$CN]$_0$/[ *m*-MeOC$_6$H$_4$CN]$_t$) vs time; induction period of 120 min removed for 2 lowest [Mg]

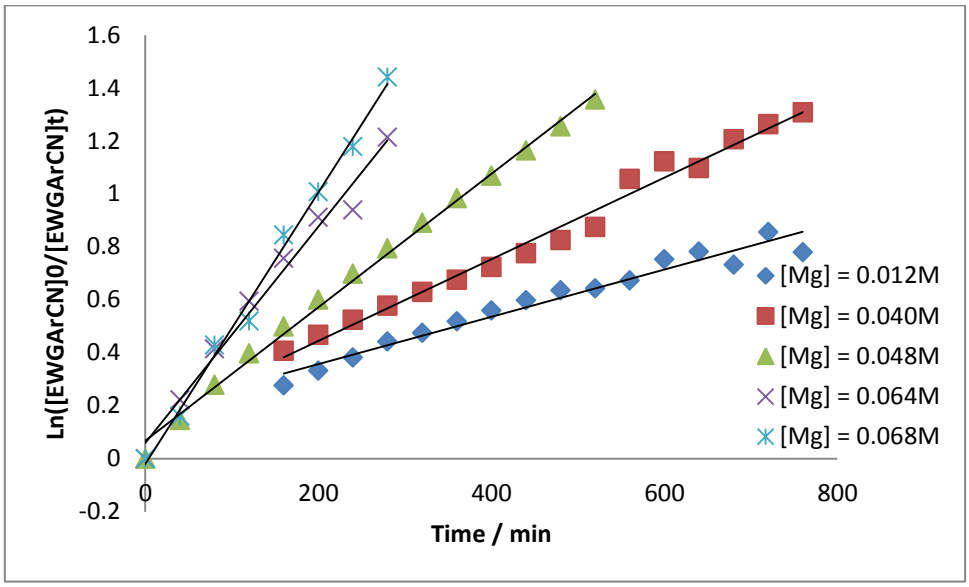


| | [Mg] 0.012M | |
|---|---|---|
| | Value | Error |
| $m_1$ | 0.179299 | 0.024145 |
| $m_2$ | 0.000892 | 0.000049 |
| Chisq | 0.072735 | n/a |
| $R^2$ | 0.959934 | n/a |

| | [Mg] 0.040M | |
|---|---|---|
| | Value | Error |
| $m_1$ | 0.137358 | 0.024792 |
| $m_2$ | 0.001540 | 0.000050 |
| Chisq | 0.006875 | n/a |
| $R^2$ | 0.985440 | n/a |

| | [Mg] 0.048M | |
|---|---|---|
| | Value | Error |
| $m_1$ | 0.068124 | 0.014779 |
| $m_2$ | 0.002520 | 0.000048 |
| Chisq | 0.027985 | n/a |
| $R^2$ | 0.995610 | n/a |

| | [Mg] 0.064M | |
|---|---|---|
| | Value | Error |
| $m_1$ | 0.059523 | 0.036864 |
| $m_2$ | 0.004084 | 0.000220 |
| Chisq | 0.024854 | n/a |
| $R^2$ | 0.982841 | n/a |

| | [Mg] 0.068M | |
|---|---|---|
| | Value | Error |
| $m_1$ | -0.020818 | 0.028766 |
| $m_2$ | 0.005130 | 0.000172 |
| Chisq | 0.001947 | n/a |
| $R^2$ | 0.993308 | n/a |

**Figure S91.** 1/[ *m*-$MeOC_6H_4CN$] vs time; non-linear kinetics

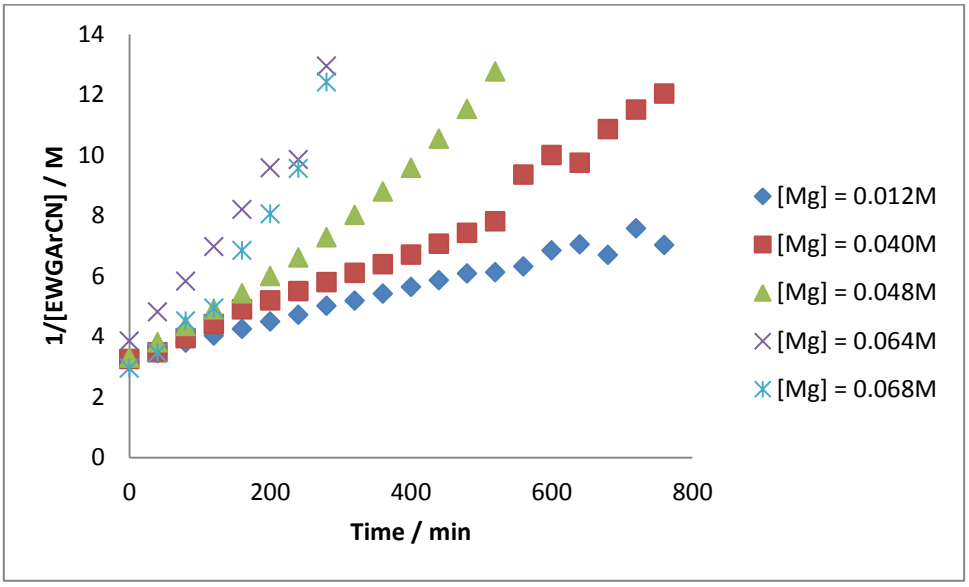


**Figure S92.** [Mg] vs $k_{obs}$; non-linear fit

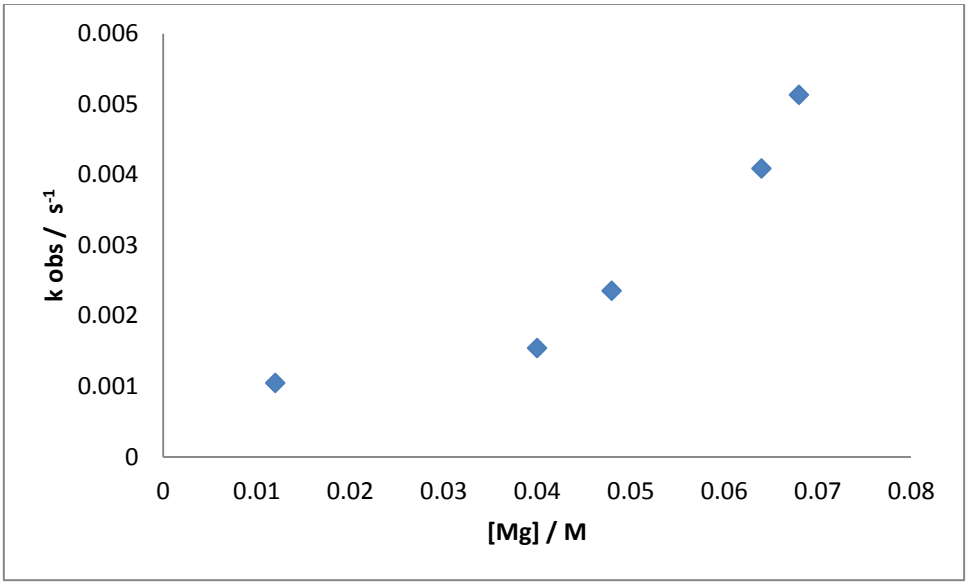

**Figure S93.** $[Mg]^2$ vs $k_{obs}$; non-linear fit

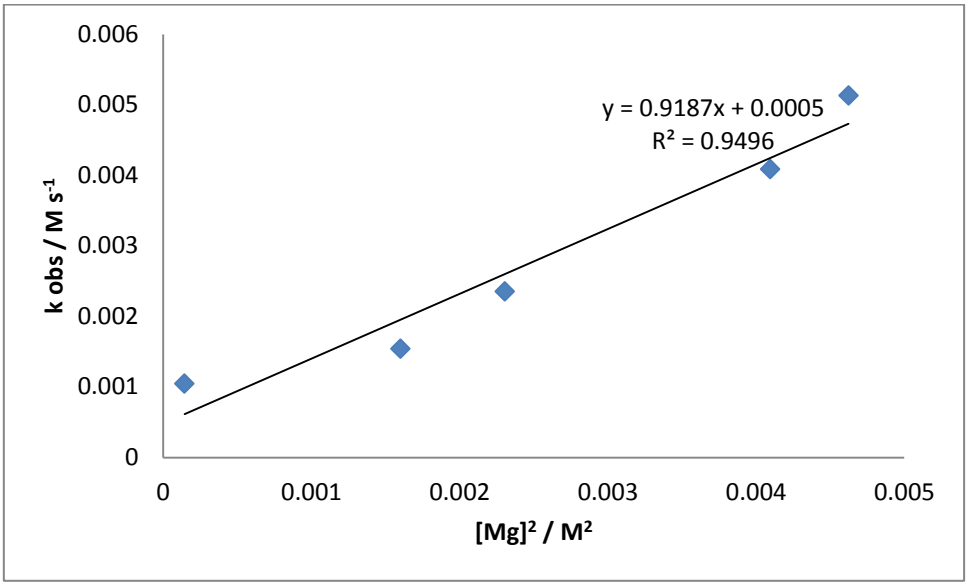


**Figure S94.** $[Mg]^3$ vs $k_{obs}$; indicated 3rd order dependence upon [Mg] under *pseudo*-first order conditions in [HBpin]

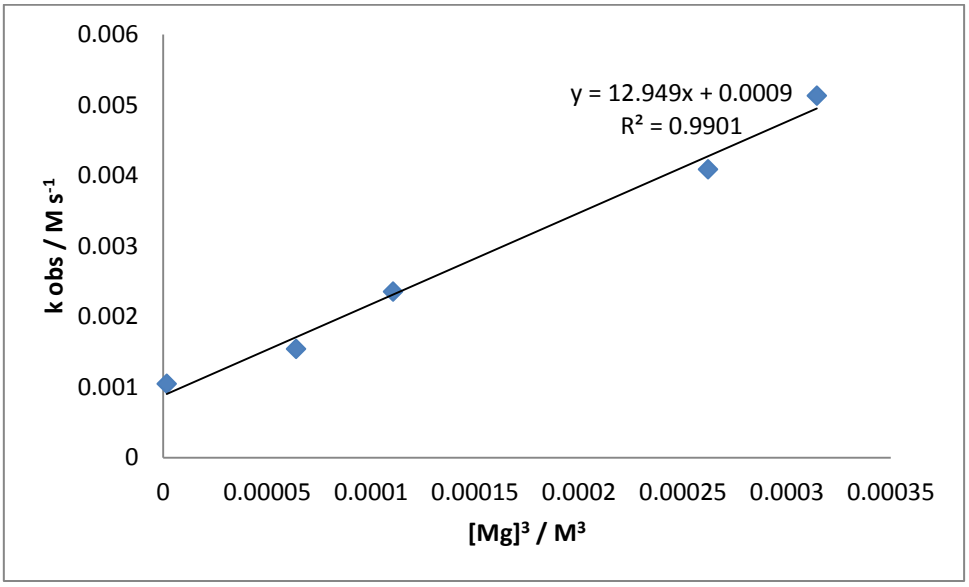


| | Value | Error |
|---|---|---|
| $m_1$ | 0.000879 | 0.000143 |
| $m_2$ | 12.949454 | 0.746753 |
| Chisq | 0.008512641 | n/a |
| $R^2$ | 0.990122 | n/a |

## Variable [Mg] under *pseudo*-first order in [*m*-$MeOC_6H_4CN$]

**Figure S95.** [*m*-$MeOC_6H_4CH_2N(Bpin)_2$] vs time; non-linear kinetics

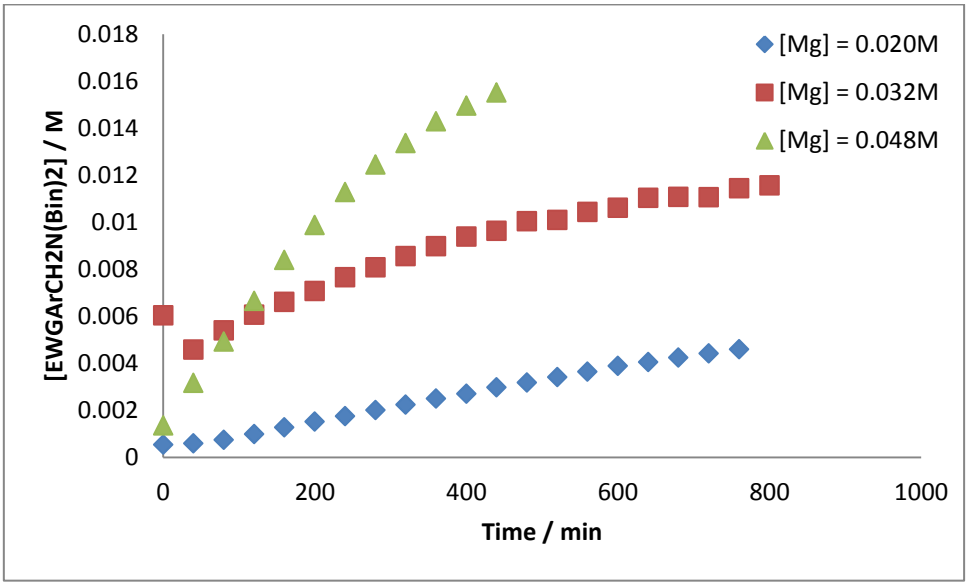


**Figure S96.** ln([*m*-$MeOC_6H_4CH_2N(Bpin)_2]_0$/[ *m*-$MeOC_6H_4CH_2N(Bpin)_2]_t$) vs time; non-linear kinetics

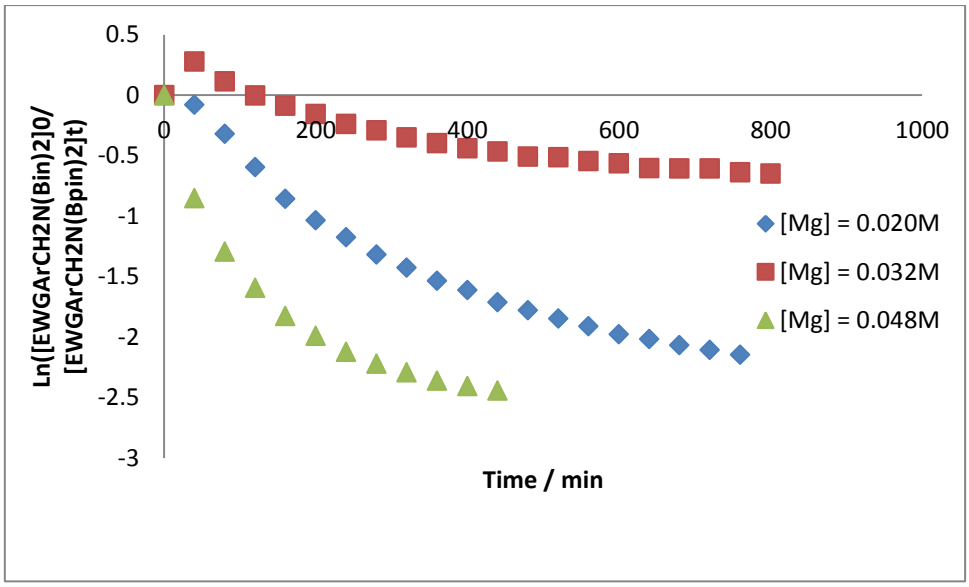

**Figure S97.** 1/[ *m*-$MeOC_6H_4CH_2N(Bpin)_2$] vs time; non-linear kinetics

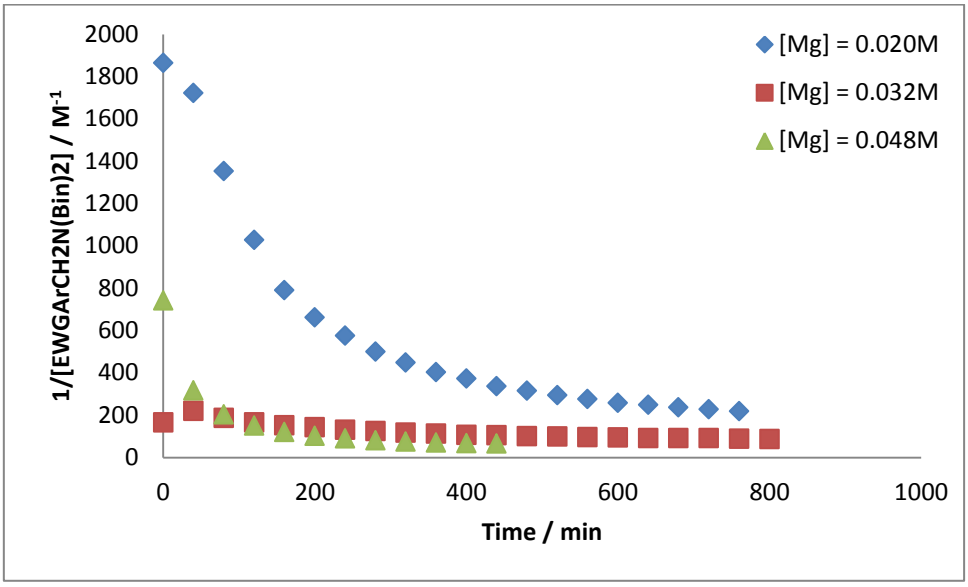


**Figure S98.** [*m*-$MeOC_6H_4CH_2N(Bpin)_2$]$^2$ vs time; variable [Mg] under *pseudo*-first order conditions in [*m*-$MeOC_6H_4CN$] (4.0M) whilst keeping [HBpin] (0.8M) invariant

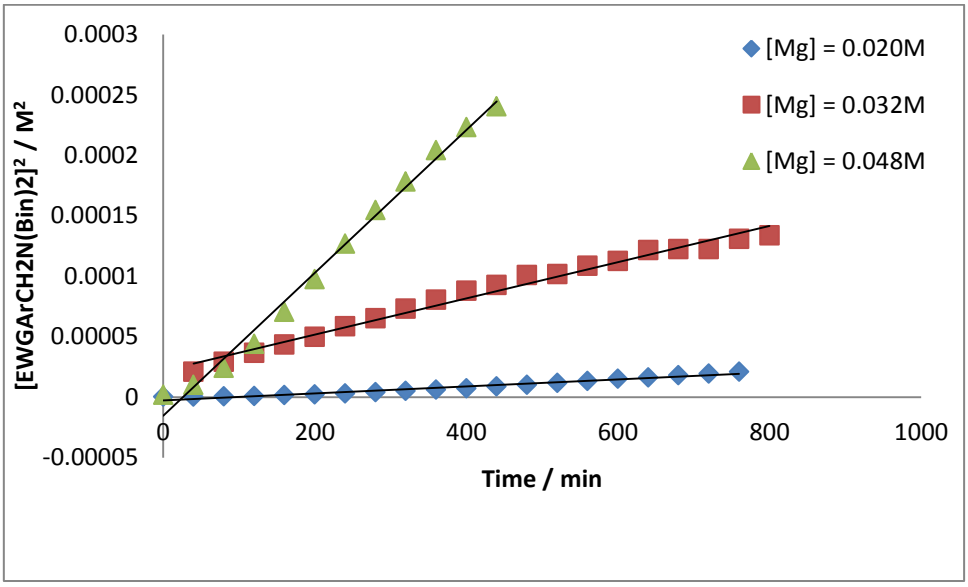


| | [Mg] 0.020M | |
|---|---|---|
| | Value | Error |
| $m_1$ | -2.68E-06 | 5.97E-07 |
| $m_2$ | 2.90E-08 | 1.34E-09 |
| Chisq | 0.192125 | n/a |
| $R^2$ | 0.962262 | n/a |

| | [Mg] 0.032M | |
|---|---|---|
| | Value | Error |
| $m_1$ | 2.17E-05 | 2.23E-06 |
| $m_2$ | 1.50E-07 | 4.64E-09 |
| Chisq | 0.038156 | n/a |
| $R^2$ | 0.983011 | n/a |

| | [Mg] 0.048M | |
|---|---|---|
| | Value | Error |
| $m_1$ | -1.53E-05 | 4.56E-06 |
| $m_2$ | 5.90E-07 | 1.75E-08 |
| Chisq | 0.04374 | n/a |
| $R^2$ | 0.991255 | n/a |

**Figure S99.** [Mg] vs $k_{obs}$; non-linear fit

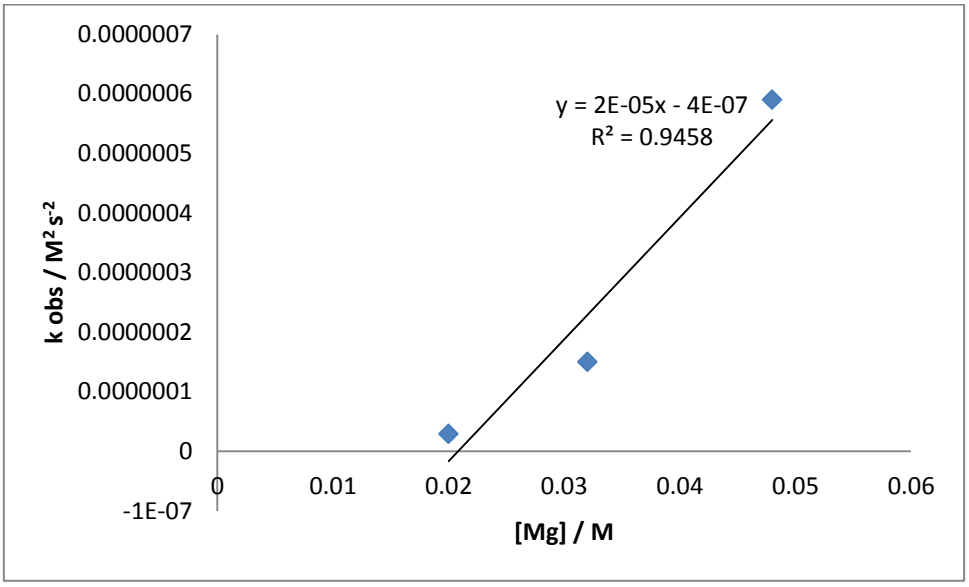


**Figure S100.** $[Mg]^2$ vs $k_{obs}$; non-linear fit

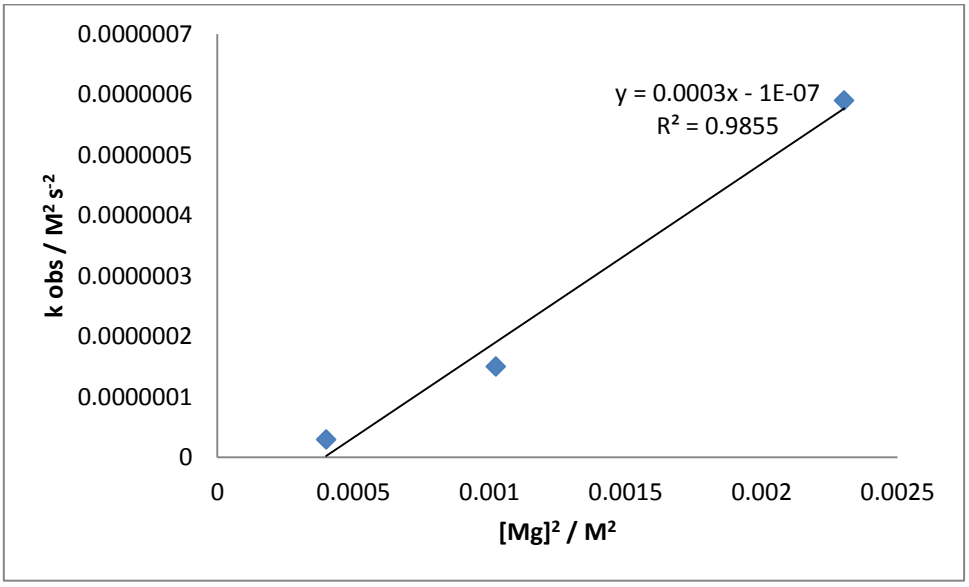

**Figure S101.** $[Mg]^3$ vs $k_{obs}$; indicating 3rd order dependence on [Mg] under *pseudo*-first order conditions in [*m*-$MeOC_6H_4CN$]

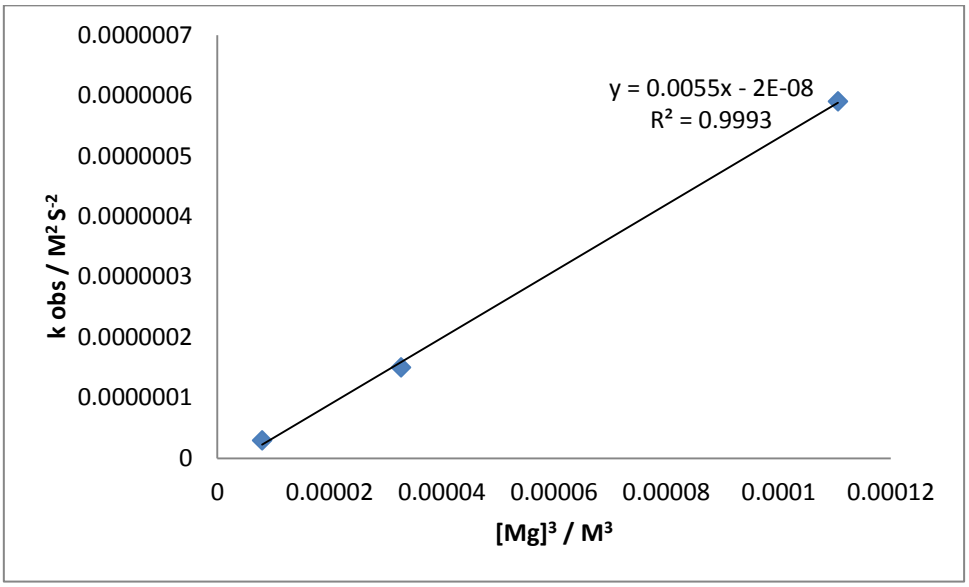


| | Value | Error |
|---|---|---|
| $m_1$ | -2.20E-08 | 9.96E-09 |
| $m_2$ | 0.005513 | 0.000149 |
| Chisq | 0.000819 | n/a |
| $R^2$ | 0.999268 | n/a |

## Variable Temperature Studies

**Figure S102.** [*m*-$MeOC_6H_4CN$] vs time; non-linear kinetics

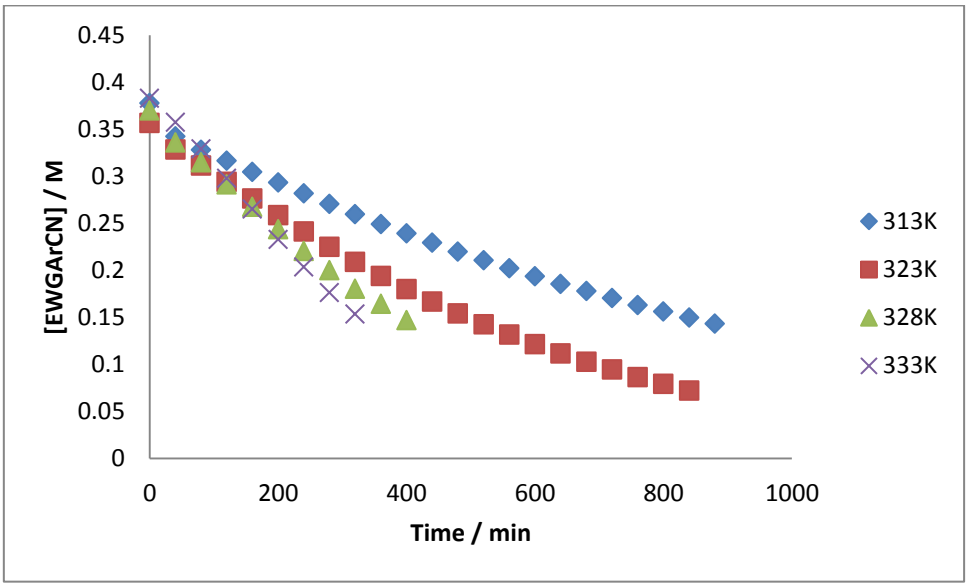


**Figure S103.** ln([*m*-$MeOC_6H_4CN$]$_0$/[ *m*-$MeOC_6H_4CN$]$_t$) vs time; variable temperature under standard reaction conditions

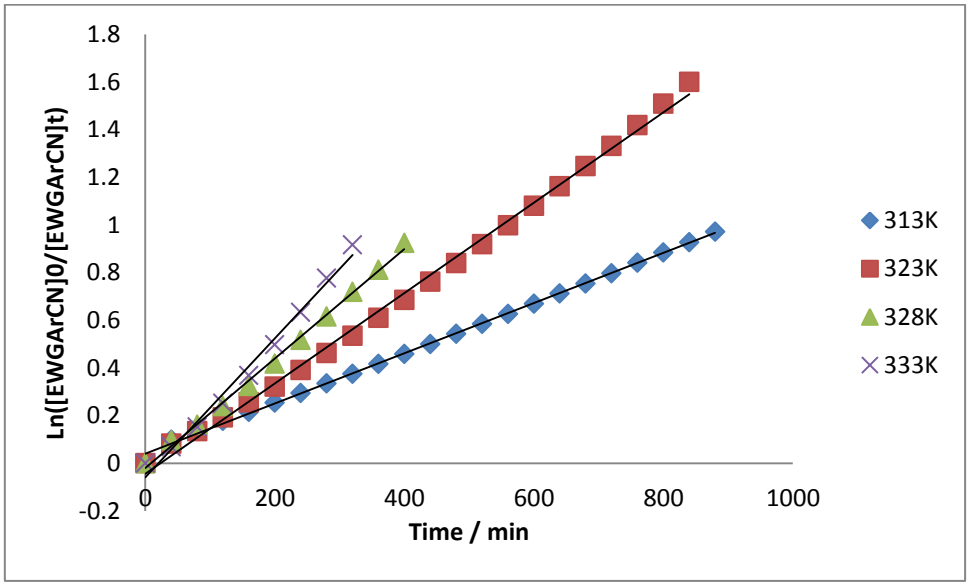


| | 313 K | |
|---|---|---|
| | Value | Error |
| $m_1$ | 0.039620 | 0.004333 |
| $m_2$ | 0.001050 | 0.000008 |
| Chisq | 0.02007 | n/a |
| $R^2$ | 0.99866 | n/a |

| | 323 K | |
|---|---|---|
| | Value | Error |
| $m_1$ | -0.040080 | 0.011011 |
| $m_2$ | 0.001880 | 0.000024 |
| Chisq | 0.00774 | n/a |
| $R^2$ | 0.99702 | n/a |

| | 328 K | |
|---|---|---|
| | Value | Error |
| $m_1$ | -0.020310 | 0.010620 |
| $m_2$ | 0.002300 | 0.000045 |
| Chisq | 0.004877 | n/a |
| $R^2$ | 0.9966 | n/a |

| | 333 K | |
|---|---|---|
| | Value | Error |
| $m_1$ | -0.059510 | 0.023468 |
| $m_2$ | 0.002920 | 0.000123 |
| Chisq | 0.038538 | n/a |
| $R^2$ | 0.98766 | n/a |

**Figure S104.** 1/ *m*-$MeOC_6H_4CN$] vs time; non-linear kinetics

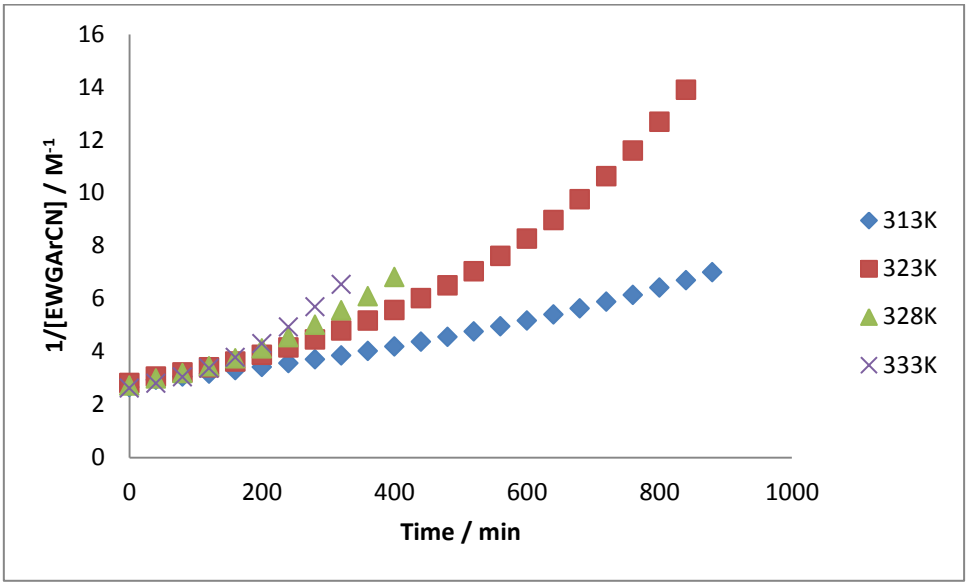


**Figure S105.** Eyring Plot; 1/T vs Ln(k/T)

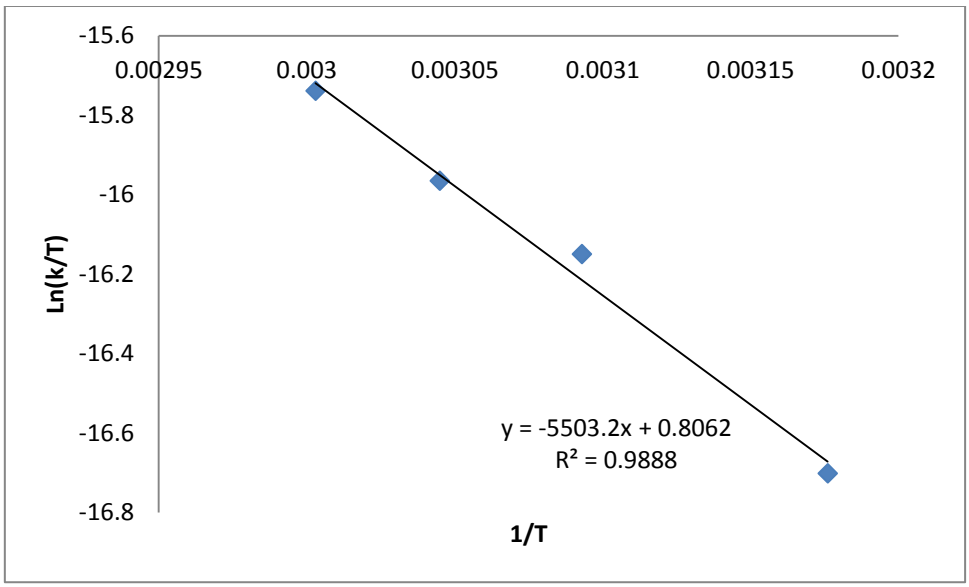


| | Value | Error |
|---|---|---|
| $m_1$ | 0.806183 | 1.277090 |
| $m_2$ | -5503.171097 | 414.646769 |
| Chisq | 0.007110758 | n/a |
| $R^2$ | 0.988773 | n/a |

This graph was used to calculate the following Activation Energy Parameters, least square error analysis was also carried to provide accurate error information.

| | Value | Error |
|---|---|---|
| ΔH | 45.75 kJ $mol^{-1}$ | ± 3.44 |
| ΔS | -190.84 J $k^{-1}$ $mol^{-1}$ | ± 10.61 |

**Figure S106.** Arrhenius Plot; 1/T vs Ln(k)

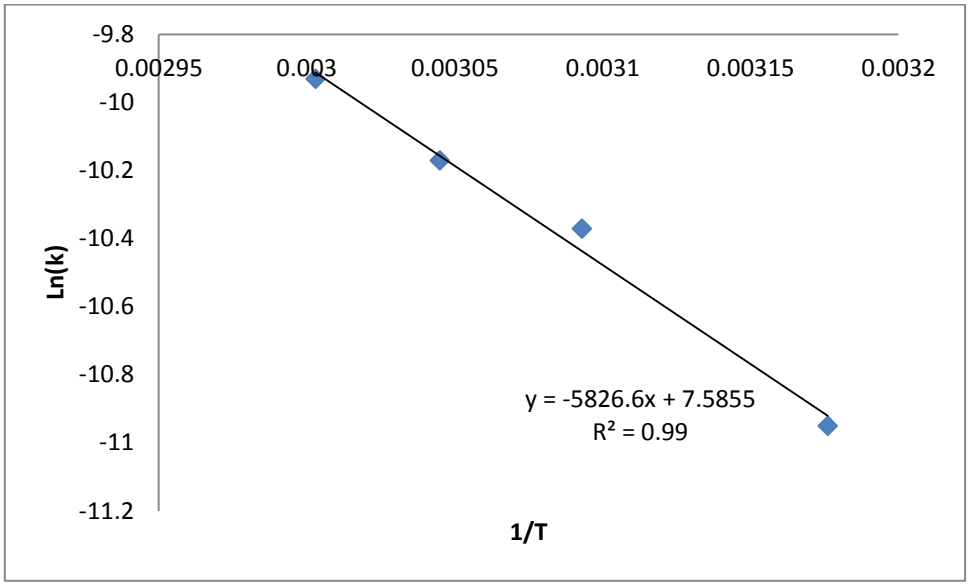


| | Value | Error |
|---|---|---|
| $m_1$ | 7.585536 | 1.272382 |
| $m_2$ | -5826.648141 | 413.118121 |
| Chisq | 0.006290611 | n/a |
| $R^2$ | 0.990046 | n/a |

This graph was used to calculate the following Activation Energy Parameter; least square error analysis was also carried to provide accurate error information.

| | Value | Error |
|---|---|---|
| Ea | 48.44 kJ $mol^{-1}$ | ± 3.43 |

*Kinetic Isotope Effect - EtCN*

Using the standard reaction: LMgBu (10 mg, 0.02 mmol ie. 10 mol%) was dissolved in 0.5 ml of $C_6D_6$, 110.5 µL (0.42 mmol) of deuterated pinacolborane was then added followed by 0.2 mmol of propionitrile. $^1$H NMR spectra were collected at consistent intervals until the reaction reached the desired 3 half-lives (80 % product conversion). All reactions were carried out at 323 K.

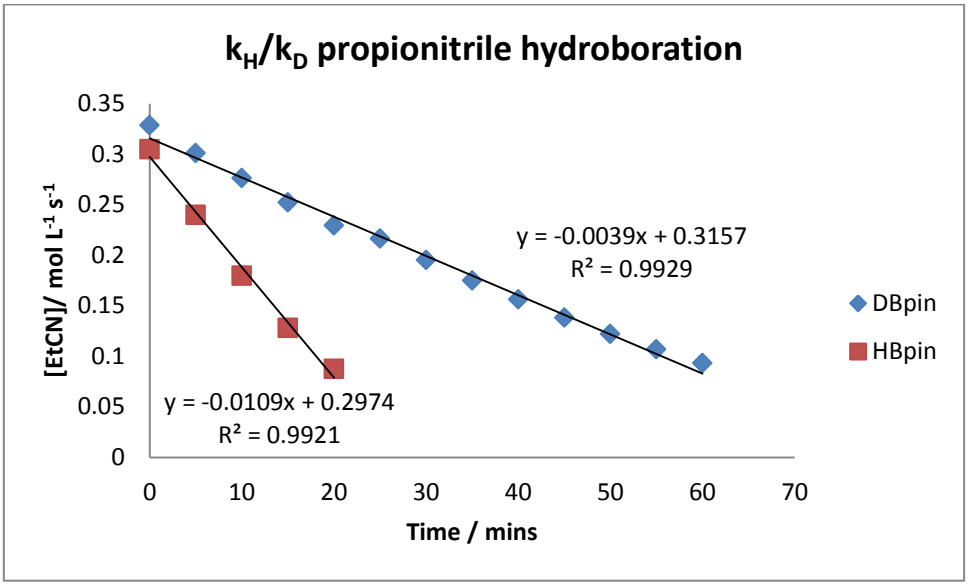


**Figure S107:** Determination of KIE for propionitrile dihydroboration

$K_H/k_D$ = 0.0109/0.0039 = 2.79

*Kinetic Isotope Effect – p-*$MeOC_6H_4$*CN*

Using the standard reaction: LMgBu (10 mg, 0.02 mmol ie. 10 mol%) was dissolved in 0.5 ml of $C_6D_6$, 110.5 µL (0.42 mmol) of deuterated pinacolborane was then added followed by 0.2 mmol of 4-methoxybenzonitrile. $^1$H NMR spectra were collected at consistent intervals until the reaction reached the desired 3 half-lives (80 % product conversion). All reactions were carried out at 323 K.

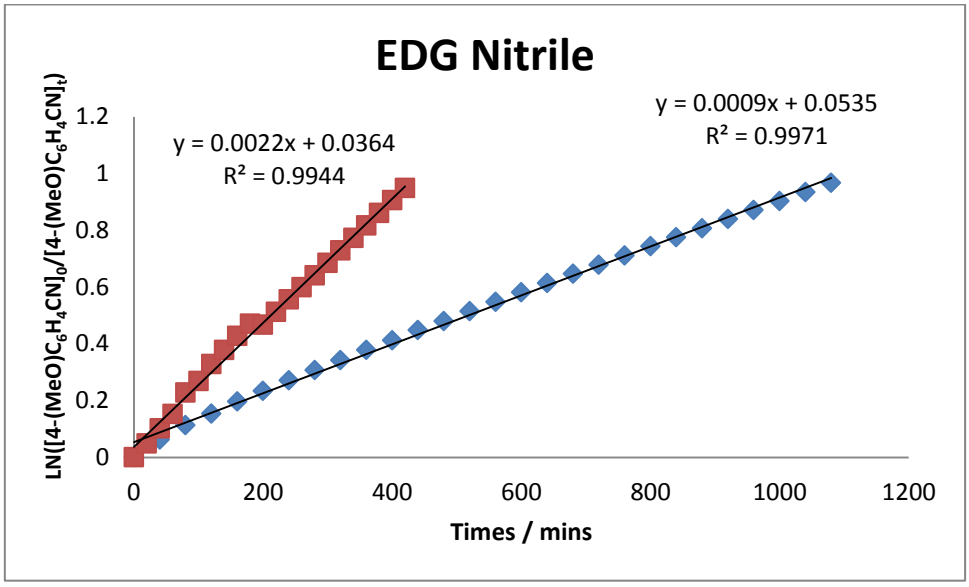


**Figure S108:** Determination of KIE for (4-methoxy)benzonitrile dihydroboration.

*Kinetic Isotope Effect - m-*$MeOC_6H_4CN$

Using the standard reaction: LMgBu (10 mg, 0.02 mmol ie. 10 mol%) was dissolved in 0.5 ml of $C_6D_6$, 110.5 µL (0.42 mmol) of deuterated pinacolborane was then added followed by 0.2 mmol of 3-methoxybenzonitrile. $^1$H NMR spectra were collected at consistent intervals until the reaction reached the desired 3 half-lives (80 % product conversion). All reactions were carried out at 323 K.

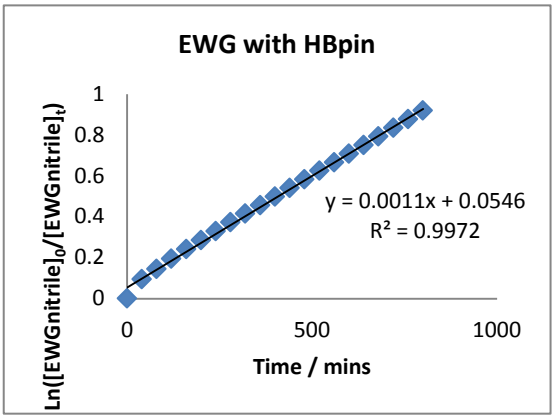


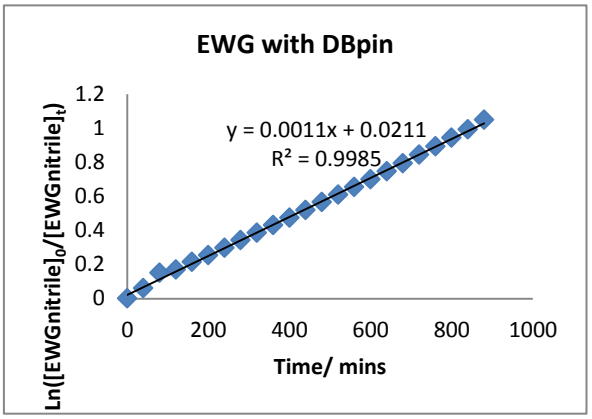


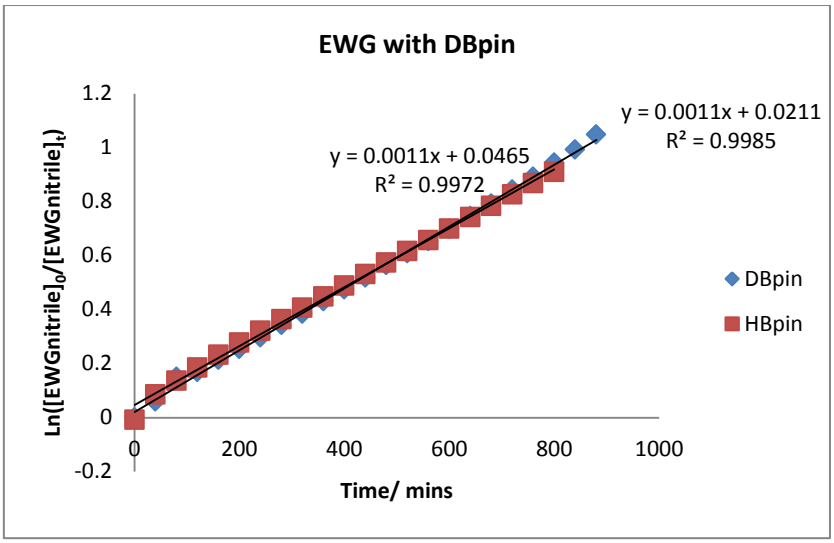


**Figure S109:** Determination of KIE for (3-methoxy)benzonitrile dihydroboration.

KIE = 1